Removal of Cesium from Aqueous Solution by Using Newly Developed Adsorbents and Comparative Study

April 2014

Dahu DING

Removal of Cesium from Aqueous Solution by Using Newly Developed

Adsorbents and Comparative Study

A Dissertation Submitted to

the Graduate School of Life Environmental Sciences,

the University of Tsukuba

in Partial Fulfillment of the Requirements

for the Degree of Doctor of Philosophy in Environmental Studies

(Doctoral Program in Sustainable Environmental Studies)

Dahu DING

Abstract

Removal of pollutants from industrial wastewater has become one of the most important issues recently for the increase in industrial activities, especially for heavy metals and radionuclides. Since the big nuclear accident at Fukushima, Japan in 2011, a large amount of radionuclides were released into water, soil and air, and the hazardous influence of radioactive wastewater has drawn much attention all over the world. Among radionuclides, ^{137}Cs is considered the most abundant and hazardous due to diverse sources and relatively long half-life. Furthermore, it can be easily incorporated into terrestrial and aquatic organisms because of its similar chemical characteristics with potassium. As a result, numerous efforts have been undertaken to find effective and low cost methods to separate and remove cesium (Cs) from waste solutions.

In this study, walnut shell (WS, biosorbent), akadama clay (AC, clay material) and ammonium molybdophosphate − polyacrylonitrile (AMP-PAN) beads (synthetic material) were used as adsorption materials for cesium removal from aqueous solution. The comprehensive comparison was carried out and the best application scopes of these materials were determined.

For the WS experiments, the rapid adsorption process was fitted well with the pseudo second-order kinetic model. The good correlation coefficient (R^2=0.93), low χ^2 and normalized standard deviation (NSD) values suggest that cesium adsorption on nickel hexacyanoferrate modified walnut shell (NiHCF-WS) could be best described by the Freundlich adsorption isotherm. The maximum adsorption capacity (Q_{max}) could reach about 4.94±0.5 mg g^{-1} for the NiHCF-WS. Results showed that, in comparison with other adsorbents, cesium adsorption onto NiHCF-WS was enhanced under acidic (80% removal at pH of 2) and suppressed under alkaline (40% removal at pH of 11) conditions, which makes it especially appropriate in treating acidic radioactive liquid waste. Cesium loaded NiHCF-WS could be reduced significantly through incineration at 500°C for 2 h and the total reduction (in volume) from liquid waste to slag residue was up to 99.9%, leading to a considerable

space and cost reduction in disposing the spent adsorption material.

For the AC experiments, AC was transferred into a typical mesoporous material and adsorption performance was greatly enhanced. The newly developed material had a much wider applicable pH range (5~12) than pristine one. The Q_{max} could reach about 16 mg g^{-1} for the modified AC, much higher than pristine one (4.5 mg g^{-1}). The distribution coefficient was strongly affected (negatively) by K$^+$ rather than Na$^+$ for both pristine and modified AC. Finally, modified AC was testified as a potential efficient adsorbent material for Cs$^+$ in the treatment of lake water. Above 80% of adsorbed Cs$^+$ could be desorbed in 0.1 M HCl and KCl, while relatively stable in synthetic groundwater.

AMP-PAN bead was synthesized in this study. Effect of different compositions on adsorption capacity was investigated through batch adsorption experiments. The prepared AMP-PAN beads were thermal stable under 300°C and chemical stable in acidic solution but unstable in alkaline solution. Multilayer chemical adsorption process was testified through kinetic and isotherm studies. The estimated Q_{max} for 2#, 3# and 4# beads were 138.9±21.3, 95.4±11.7 and 71.6±8.5 mg g^{-1}, respectively. The adsorption behavior could not be inhibited at acidic conditions until the pH was as low as 2.5. Competitive ions (Na$^+$, K$^+$ and Ca^{2+}) had little negative effect on the removal efficiencies, indicating a high selectivity for Cs$^+$ adsorption on AMP-PAN beads. A close relationship between the amounts of adsorbed Cs$^+$ and released NH$_4^+$ was demonstrated. Spent AMP-PAN beads were stable in DW and acidic solutions and relatively unstable in 0.1 M NH$_4$Cl solution, indicating a recycle capability.

The results of this thesis would provide useful information for applying these kinds of materials into Cs$^+$ wastewater treatment. Also, the results indicate a bright future for adopting these materials into treating nuclear wastewater from Fukushima nuclear plant, which would make this study more meaningful.

Contents

Chapter 1 Introduction

Removal of pollutants from industrial wastewaters has become one of the most important issues recently for the increase of industrial activities, especially for heavy metals and radionuclides. For example, chormium and arsenic in groundwater had led to serious problems for human health all over the world. Many countries have set rigorous concentration limits for drinking water and these standards will be much more severe in the future. This calls for much more efforts in controlling the release of these hazardous heavy metals into water environment. Fortunately, for the heavy metals' removal, there have been extensive researches, while for the radionucildes' removal, there is not yet enough research. It is worth noting that the negative impact brought by the radionuclides would be much more serious than common heavy metals because of the impact range and relatively long impact time. As the big nuclear accident occurred in Fukushima, Japan 2011 led a large amount of radionuclides released into water, soil and air, the hazardous influences of radioactive wastewater draw much attentions all over the world. Not only from the routine operation of nuclear power station, but also from the accident caused by unpredictable natural disasters such as earthquake and tsunami, liquid and solid wastes containing radionuclides are produced. Cesium is a commonly used radionuclide during the nuclear power generation and therefore a most important pollutant through the radioactive wastes. For instance, the great east Japan disaster of March 11, 2011 crippled the Fukushima Daiichi Nuclear Power Plant (NPP) leading to a long-term radiation contamination issue. The radioisotopes on the order of 630,000-770,000 terabecquerel (TBq) were released into the environment and left the region with contaminated soil, air and water [1, 2]. Cesium, including ^{134}Cs (approximately 2.15×10^{16} Bq) and ^{137}Cs (approximately 1.86×10^{16} Bq), has been released into the air and sea in the disaster affected areas [3]. Among radionuclides, ^{137}Cs is considered the most abundant

and hazardous due to diverse sources and relatively long half-life (approximately 30.5 years). Furthermore, it can be easily incorporated into terrestrial and aquatic organisms because of its similar chemical characteristics with potassium [4, 5].

1.1 Cesium species

Cesium has many kinds of isotopes and ^{133}Cs, ^{134}Cs and ^{137}Cs are most common used ones. It is worth noting that the first isotope is nonradioactive and the latter two are radioactive.

1.2 Treatment technologies

Generally speaking, the investigated physical-chemical methods for separation and removal of Cs are precipitation, solvent extraction, adsorption, ion exchange, electrochemical and membrane processes [6-11]. Among them, solvent extraction, ion exchange and adsorption methods are most widely used. However, due to the high cost of materials, large-scale application of solvent extraction is limited. In the case of ion exchange process, inorganic ion exchangers are found to be superior over organic ion exchangers due to their thermal stability, resistance to ionizing radiation and good compatibility with final waste forms [5, 12]. Natural occurring clay minerals such as zeolite, bentonite and montmorillonite are usually used as low cost adsorption materials for Cs^+ removal from aqueous solution [5, 13-16]. As for most clay materials, the main mechanism occurring in the adsorption process is known as ion exchange. According to the special cubic structure and driving force caused by concentration gradients, ion exchange can be accomplished by releasing metal ions existing in clay materials into solutions (such as Na^+, K^+, Ca^{2+} and etc.) and adsorbing cesium ions simultaneously. Though the adsorption capacity is high, the disadvantage is low/no selectivity for ion exchange during the adsorption process. This means, not only the target metal ion but also other metal ions can be exchanged during the process, which undoubtedly leads to a waste of adsorption

capacity, especially under high ionic strength conditions such as sea water. For clay materials, it is comparatively much more difficult to improve the selectivity of the ion exchange process than it is to increase adsorption capacity due to their complex compositions. As a result, much more attention from researchers has been paid to the improvement of adsorption capacity of clay material [11, 17]. Transition metals are known to undergo complexation with compounds containing aromatic groups based on an electron donation and back donation process [18]. In addition, modification with transition metals could result in a pillared material with microporosity and mesoporosity in layered crystalline inorganic compounds [19]. ZSM-5 zeolite [20] and kaolin [21] has been successfully modified with transition metal in previous studies. Still, it is unknown whether transition metals could be modified into other kinds of clay materials and whether the modification is positive for increasing adsorption capacity or not.

1.3 Objective, originality and structure of the dissertation

As mentioned above, each method has its own advantages and disadvantages. The most concerned topic is to find much proper material for each method. In addition, until now there is no study conducting on the comparison of different kinds of materials, which is relatively important when treating with different kinds of liquid wastes. As a result, the objective of this study is to find different kinds of materials for Cs^+ removal from different kinds of liquid wastes.

Several kinds of low cost biosorbent have been investigated for the removal of heavy metals recently. Walnut shell, an abundant agricultural residue with good stability has been successfully used in removing heavy metals by adsorption. To the best of our knowledge, however, few of them focused on equilibrium, kinetic and thermodynamic modeling studies of Cs^+ adsorption by walnut shell. In addition, transition metal hexacyanoferrates, especially nickel hexacyanoferrate (NiHCF) is known as a highly selective agent for Cs^+ adsorption. It possesses a special cubic structure with

channel diameter of about 3.2Å, through which only small hydrated ions like Cs^+ can permeate. And larger hydrated ions like Na^+ get blocked. However, very fine particle size of NiHCF restricts its direct use in practice, thus proper support materials are necessary. This study presents a low cost biosorbent derived from walnut shell incorporated with NiHCF (NiHCF-WS), firstly fabricated for Cs^+ adsorption. Also, a special kind of clay material, akadama clay was firstly used for this purpose. This low cost clay material comes from the volcanic ash and generally used for culturing plants. In order to improve its application in removing Cs^+, nickel oxide was introduced into akadama clay through modification. Finally, a synthetic compound, ammonium molybdophosphate – polyacrylonitrile was developed for removing Cs^+ from aquous solution. Different kinds of this material with different compositions were developed to find a best composition.

The contents of this thesis are divided into the following three parts so as to comprehensively evaluate the adsorption performance of Cs^+ onto different kinds of materials.

The first study focused on the removal of cesium from aqueous solution using agricultural residue – walnut shell (Chapter 2). Through various kinds of characterization, adsorption isotherms and kinetics insight and removal performance evaluation, Cs^+ removal mechanism was investigated.

The second part is the removal of cesium from aqueous solution using modified clay material (Chapter 3). A common and inexpensive andic soil in Japan, akadama clay (AC), was utilized in lab-scale experiments and its application in Cs^+ removal was evaluated. In order to improve its adsorption efficiency and widen adsorption conditions, a special modification process was adopted and the positive results indicated its success. Also, except the effects of pH, contact time, initial concentration, dosage, and coexisting ions, the adsorption isotherms and kinetics were also investigated. Based on the experimental results, removal mechanism was finally discussed.

The third part was the removal of cesium from aqueous solution using ammonium

molybdophosphate - polyacrylonitrile (AMP-PAN) beads (Chapter 4). As a synthetic compound with

high capacity, its stable characteristics and the effect of coexisting ions were especially investigated.

The removal mechanism was also disclosed and discussed.

Chapter 2 Removal of cesium from aqueous solution using agricultural residue –

Walnut shell

2.1 Introduction

Removal of pollutants from industrial wastewater has become one of the most important issues recently for the increase in industrial activities, especially for heavy metals and radionuclides. Since the big nuclear accident at Fukushima, Japan in 2011, a large amount of radionuclides were released into water, soil and air, and the hazardous influence of radioactive wastewater has drawn much attention all over the world. Among radionuclides, ^{137}Cs is considered the most abundant and hazardous due to diverse sources and relatively long half-life. Furthermore, it can be easily incorporated into terrestrial and aquatic organisms because of its similar chemical characteristics with potassium [4, 5]. As a result, numerous efforts have been undertaken to find effective and low cost methods to separate and remove Cs^+ from waste solutions [4, 7, 11, 22, 23].

Generally speaking, the investigated physical-chemical methods for separation and removal of Cs^+ are precipitation, solvent extraction, adsorption, ion exchange, electrochemical and membrane processes [6-11]. Among them, solvent extraction, ion exchange and adsorption methods are most widely used. However, due to the high cost of materials, large-scale application of solvent extraction is limited. In the case of ion exchange process, inorganic ion exchangers are found to be superior over organic ion exchangers due to their thermal stability, resistance to ionizing radiation and good compatibility with final waste forms [5, 12]. Natural occurring clay minerals such as zeolite, bentonite and montmorillonite are usually used as low cost adsorption materials for Cs^+ removal from aqueous solution, however the main disadvantage is the competitive interactions of other monovalent cations, in particular Na^+ and K^+ that can considerably block Cs^+ adsorption [5, 13-16].

Transition metal hexacyanoferrates, especially nickel hexacyanoferrate (NiHCF) is known as a highly selective agent for Cs^+ adsorption [5, 6]. It possesses a special cubic structure with a channel diameter of about 3.2 Å, through which only small hydrated ions like Cs^+ can permeate. Larger hydrated ions like Na^+ get blocked [5, 24]. However, the very fine particle size of NiHCF restricts its direct use in practice, thus proper support materials are necessary.

Recently, several kinds of low cost biosorbents have been investigated for the removal of heavy metals [5, 25, 26]. Walnut shell, an abundant agricultural residue with good stability has been successfully used in removing heavy metals by adsorption [27-29]. However, previous studies mainly focused on the determination of the adsorption mechanisms and improvement of adsorption capacity. To the best of our knowledge, the report about treating the spent adsorption material in order to obtain waste reduction before final disposal (deep landfill) is sparse. According to the IAEA guidelines, thermal treatment is the most suitable option for the volume reduction, especially of the organics-rich waste [30]. The main components in WS including lignin, cellulose and hemicellulose could be burned after incineration and the end result of the treatment process is the volume reduction from a huge amount of radioactive wastewater to a small volume of char or slag residue that can be converted to a stable form suitable for ultimate disposal, which makes it a particularly attractive adsorption/support material.

Therefore, as a first attempt to fill the knowledge gap, the removal behaviors of Cs^+ by the resulting functionalized biomass material – NiHCF-WS were investigated under different experimental conditions such as the contact time, initial pH, adsorbent dosage, initial Cs^+ concentration and competitive ions in detail. Adsorption kinetic, equilibrium and thermodynamic studies were also investigated. To highlight the economical advantage during the final disposal, the volume reduction of spent material (Cs-NiHCF-WS) after thermal treatment was analyzed. The aim

of this work is to obtain a functionalized biomass material that can be reduced effectively by thermal treatment. The results of this study are expected to shed light on the understanding of the underlying removal behavior of Cs^+ on NiHCF-WS. In addition, they are also of great significance for achieving a low cost treatment for the large quantity of radioactive liquid waste.

2.2 Materials and methods

2.2.1 Materials

Walnut shell used in this study was obtained from Shandong province, China and was immersed and washed with deionized water (DW) to remove soluble impurities until the water turned clear. The clean WS was completely dried in an oven (EYELA WFO-700, Japan) at $105^{o}C$ for more than 24 h, ground and sieved through No. 8 and 16 size meshes. The granules with diameter between 1~2.36 mm were selected and stored in a desiccator for further use or modification.

2.2.2 Reagents

The chemicals nickel chloride ($NiCl_2$ $6H_2O$) and potassium hexacyanoferrate ($K_3[Fe(CN)_6]$ · $3H_2O$) of A.R. grade were purchased from Wako Pure Chemical Industries Ltd., Japan. Non-radioactive cesium chloride (CsCl) purchased from Tokyo Chemical Industry Co. Ltd., Japan was used as a surrogate for ^{137}Cs because of its same chemical characteristics. All the other reagents used in this study were purchased from Wako Pure Chemical Industries Ltd., Japan with no purification before use. DW generated from a Millipore Elix 3 water purification system (Millipore, USA) equipped with a Progard 2 pre-treatment pack was used throughout the experiments except for ICP-MS analysis.

1.26 g CsCl was weighed exactly and dissolved into 1 L DW as standard stock Cs^+ solution (~1000 mg L^{-1}), which could be diluted to desired concentrations of Cs^+ solution for further

experiments.

2.2.3 Modification of walnut shell

The modification of walnut shell contains the following steps. 10 g of clean WS granules were immersed in 100 mL of 50% (v/v%) hydrochloric acid (HCl) for 10 h at a temperature of 50^oC. Then, the WS was dried in an oven at 105^oC overnight after being washed until the eluent pH was almost neutral. The loading of $NiCl_2$ onto WS and the treatment of $K_3[Fe(CN)_6]$ $3H_2O$ with $NiCl_2$ loaded WS was carried out according to the method reported by Parab and Sudersanan [22]. In brief, 5 g of WS was immersed in 20 mL of 0.5 M $NiCl_2$ $6H_2O$ solution and placed in a double shaker (Taitec NR-30, Japan) at 200 rpm and room temperature (25 ± 1^oC) for 24 h followed by filtration and washing with DW to remove excess $NiCl_2$ $6H_2O$. Next, the $NiCl_2$ loaded WS was added to 10 mL of 5% (wt%) $K_3[Fe(CN)_6]$ $3H_2O$ solution and placed into a water bath (SANSYO SWR-281D, Japan) at 30^oC for 24 h. The resultant NiHCF loaded WS was separated by filtration, washed with DW and dried at 60^oC. The entire procedure was repeated three times to ensure the incorporation of NiHCF onto the WS. This NiHCF-WS material was used for further characterization as well as Cs^+ adsorption studies.

2.2.4 Removal behavior and adsorption stability studies

Batch experiments were conducted to investigate the removal behavior of Cs^+ on NiHCF-WS. Much attention was paid to the effects of influencing factors such as contact time, initial pH, adsorbent dosage, initial Cs^+ concentration and competitive ions on the removal process. Desired concentrations of Cs^+ solutions including standards were prepared by diluting known volumes of the standard Cs^+ stock solution with DW. The solution pH was adjusted by 0.1 M HCl and NaOH solutions and measured by a pH meter (Mettler Toledo SG8, Switzerland).

To determine the effect of contact time, 4 g of NiHCF-WS was mixed with 200 mL of 10 mg L^{-1} Cs^+ solution in a 250 mL-glass flask (AS ONE, Japan). Supernatants (about 1 mL for each) were withdrawn at predetermined time intervals along with the initial solution (zero min point). For the effect of initial pH, 0.2 g of NiHCF-WS was mixed with 20 mL of 10 mg L^{-1} Cs^+ solutions with initial pH value of 2, 4, 7, 10 and 11, respectively. To determine the effect of adsorbent dosage, 0.1, 0.2, 0.3 or 0.4 g of NiHCF-WS was mixed with 20 mL of 10 mg L^{-1} Cs^+ solution respectively. To determine the effect of initial Cs^+ concentration, 0.4 g of NiHCF-WS was mixed with 20 mL of Cs^+ solutions of 1, 5, 10, 20, 50, 75 and 100 mg L^{-1}, respectively. To determine the effect of competitive ions, the initial Cs^+ concentrations of 1, 5, 10 mg L^{-1} and 100, 1000 mg L^{-1} of Na^+ or K^+ were adopted.

Adsorption stability studies were conducted after the removal behavior studies with synthetic groundwater (GW) and tap water (TW). Cs^+ loaded NiHCF-WS was collected from the contact time effect experiment. The amount of released Cs^+ and percentage was deemed as indicators of adsorption stability. The amount of released Cs^+ (μg) was calculated from the Cs^+ concentration and volume of the GW or TW. Chemical compositions of the GW was as follows (in 1 L of DW): 23 mg $MgSO_4 \cdot 7H_2O$, 73.9 mg $MgCl_2$, 131 mg $NaHCO_3$, 13 mg $KHCO_3$, 8.5 mg $K_2HPO_4 \cdot 3H_2O$ and 128 mg $NaNO_3$ (Table 2-1). A trace element stock solution was also prepared by adding 13.4 mg $MnCl_2 \cdot 6H_2O$ and 5.0 mg $FeCl_2 \cdot 4H_2O$ to 1 L of DW. Before the test, trace element solution was diluted in the synthetic solution by a factor of 100:1 [31]. TW was obtained from University of Tsukuba, Japan and used without any purification.

All the experiments were conducted in 50 mL-polypropylene tubes (Violamo, Japan) vigorously shaken (200 rpm) and at room temperature ($25 \pm 1^o C$) for 24 h (except contact time experiments). All the samples including initial solutions were collected by filtering the supernatants through 0.22 μm

mixed cellulose ester membrane (Millipore, Ireland) and diluted with DW to a proper extent (less than 1 mg L^{-1}) into 15 mL-polypropylene tubes (Violamo, Japan) prior to inductively coupled plasma-mass spectrometry (ICP-MS) (Perkin Elmer Elan DRC-e, USA) analysis. Along with the batch adsorption experiments, blank and control tests were also carried out to observe any precipitation and to determine the extent of wall adsorption. The negligible differences between the initial and final concentrations indicated that no precipitation or wall adsorption occurred in this study.

2.2.5 Kinetic studies

4 g of NiHCF-WS was mixed with 200 mL Cs$^+$ solution (adsorbent dosage of 20 g L^{-1}) in a 250 mL-glass flask (AS ONE, Japan) under initial Cs$^+$ concentration of 10 mg L^{-1}, and the flask was shaken by a double shaker (TAITEC NR-30, Japan) at 200 rpm for 48 h. Supernatants (about 1 mL for each) including the initial solution (as the zero min point) were withdrawn at predetermined time intervals prior to the Cs$^+$ concentration determination.

In order to investigate the mechanism of adsorption, non-linearized Lagergren pseudo first-order kinetic model [11] and pseudo second-order kinetic model [22] were applied to analyze the adsorption process, which were expressed as follows:

Lagergren pseudo first-order kinetic model:

$$q_t = q_e(1 - e^{-k_1 t}) \qquad \text{(2-1)}$$

pseudo second-order kinetic model:

$$q_t = \frac{k_2 q_e^2 t}{1 + k_2 q_e t} \qquad \text{(2-2)}$$

where t (min) is the contact time, k_1 (min^{-1}) and k_2 (g mg^{-1} min^{-1}) are the adsorption rate constants; q_e and q_t (mg g^{-1}) represent the uptake amount of ion by the adsorbent at equilibrium and time t, respectively.

In addition, the determination of the limiting step of the adsorption process is necessary by predicting the diffusion coefficient using a diffusion based model. The possibility of intra-particle diffusion resistance affecting the adsorption was explored in this study by using the intra-particle diffusion equation [10] as follows:

$$q_t = k_p t^{1/2} + C \qquad\qquad (2\text{-}3)$$

where t (min) is the contact time, q_t (mg g^{-1}) is the Cs$^+$ uptake amount at time t, k_p (mg g^{-1} min$^{-1/2}$) is the intra-particle diffusion rate constant determined from the slopes of the linear plots. C is the constant, which indicates the thickness of the boundary layer, i.e., the larger the value of C the greater is the boundary layer effect.

2.2.6 Equilibrium studies

A fixed amount of NiHCF-WS was mixed with 20 mL Cs$^+$ solution in a 50 mL-polypropylene tube (VIOLAMO, Japan) at a shaking speed of 200 rpm. Resultant supernatants were withdrawn after 24 h prior to the Cs$^+$ concentration determination.

(1) Adsorption isotherms

To optimize the design of a adsorption system, it is important to establish the most appropriate correlation for equilibrium conditions [22]. According to different adsorption mechanisms, there are currently several different adsorption isotherms used for fitting experimental adsorption results. Among these, Langmuir [32], Freundlich [33] and Dubinin-Radushkevich (D-R) [34] isotherms are widely used and therefore are applied in this study. The nonlinear forms of these isotherms are given

as follows:

$$\text{Langmuir isotherm: } q_e = \frac{q_m b C_e}{1 + b C_e} \qquad (2\text{-}4)$$

$$\text{Freundlich isotherm: } q_e = k_f C_e{}^n \qquad (2\text{-}5)$$

$$\text{D-R isotherm: } q_e = q_m \exp(-\beta \varepsilon^2) \qquad (2\text{-}6)$$

$$\varepsilon = RT \ln(1 + \frac{1}{C_e}) \qquad (2\text{-}7)$$

where, q_e (mg g^{-1}) is the amount of Cs$^+$ adsorbed at equilibrium, C_e (mg L^{-1}) is the equilibrium concentration of Cs$^+$. b (L mg^{-1}) is a constant related to the free energy or net enthalpy of adsorption ($b \propto e^{-\Delta G/RT}$) [35], and q_m (mg g^{-1}) is the adsorption capacity at the isotherm temperature. k_f and n are equilibrium constants indicative of adsorption capacity and adsorption intensity respectively. β (mol^2/kJ^2) is the constant related to the adsorption energy, R (8.314 J mol^{-1} K^{-1}) is the gas constant and T (K) is the absolute temperature of the aqueous solution.

(2) Role of ion exchange

In the case of anionic metal hexacyanoferrate complexes, it is assumed that there is a true exchange between K$^+$ and Cs$^+$ [13, 36]. Therefore, an attempt was made to link the Cs$^+$ adsorption to its likely ion exchange reaction with K$^+$ through equilibrium studies. In addition to the batch experiments, a blank experiment was carried out by adding a corresponding amount of adsorbent into the same volume of DW instead of Cs$^+$ solutions. The Cs$^+$ adsorbed and K$^+$ released was calculated according to mass balance using the equations below:

$$A_{Cs^+} = \frac{(C_0 - C_e)V}{133} \times 1000 \qquad (2\text{-}8)$$

where A_{Cs+} (μmol) is the amount of Cs$^+$ adsorbed by NiHCF-WS, C_0 (mg L^{-1}) is the initial

concentration of Cs$^+$, C_e (mg L^{-1}) is the equilibrium concentration of Cs$^+$, V (L) is the volume of

solution and 133 is the molar mass of Cs.

$$R_{K^+} = \frac{(C_e - C_b)V}{39} \times 1000 \qquad (2\text{-}9)$$

where R_{K+} (μmol) is the amount of K$^+$ released into solution, C_e (mg L^{-1}) is the equilibrium

concentration of K$^+$, C_b (mg L^{-1}) is the concentration of K$^+$ in the blank solution, V (L) is the volume

of solution and 39 is the molar mass of K.

2.2.7 Thermodynamic studies

In order to obtain the thermodynamic nature of the adsorption process, 0.2 g NiHCF-WS was

added into 20 mL Cs$^+$ solutions with an initial concentration of 10 mg L^{-1} (adsorbent dosage of 10 g

L^{-1}) at different temperatures (298, 308 and 318 K) for 24 h. Thermodynamic parameters, namely,

standard Gibbs free energy ($\Delta G°$), standard enthalpy ($\Delta H°$) and standard entropy ($\Delta S°$) changes were

also determined in order to obtain the thermodynamic nature of the adsorption process. The amounts

of $\Delta H°$ and $\Delta S°$ could be calculated from the slope and intercept of the straight line obtained from

plotting lnK_d versus $1/T$, respectively using the following equation [4, 37]:

$$\ln K_d = \frac{\Delta S°}{R} - \frac{\Delta H°}{RT} \qquad (2\text{-}10)$$

where K_d (mL g^{-1}) is the distribution coefficient, R (8.314 J mol^{-1} K^{-1}) is the gas constant and T (K) is

the absolute temperature of the aqueous solution.

After obtaining $\Delta H°$ and $\Delta S°$ values of the adsorption, $\Delta G°$ of each temperature was calculated

by the well-known equation as follows:

$$\Delta G° = \Delta H° - T\Delta S° \qquad\qquad\qquad (2\text{-}11)$$

2.2.8 Incineration of Cs-NiHCF-WS

The incineration experiment was conducted in triplicate in a muffle furnace (TGK F-1404, Japan) and the Cs-NiHCF-WS used in this experiment was obtained as described in Section 2.2.4. The Cs-NiHCF-WS (0.2 g for each) was completely dried and the volume was measured in a 1mL-syringe based on the Archimedes drainage method. A temperature higher than the calculated cesium dew point of 1000 K is generally not suggested for avoiding cesium volatilization during incineration [38]. In addition, according to the thermal analysis of NiHCF-WS, the decomposing temperature was approximately 450°C. Therefore, the Cs-NiHCF-WS was placed into a crucible (with a cover) and incinerated at 500°C for 2 h in this study in order to ensure a complete decomposition of walnut shell and no volatilization of cesium. Similarly, the volume of slag residue was thereafter determined as described previously.

2.2.9 Analysis

All of the samples were collected by filtering supernatants through 0.22 μm mixed cellulose ester membrane (Millipore, Ireland) and diluted with pure water to a proper extent (below 1 mg L^{-1}) into 15 mL-polypropylene tubes (VIOLAMO, Japan) prior to inductively coupled plasma-mass spectrometry (ICP-MS) (Perkin Elmer ELAN DRC-e, USA) analysis.

In order to evaluate the probable differences in structure between raw and modified walnut shell, field emission scanning electron microscope (FE-SEM) analysis was performed using a JEOL JSM-6330F type microscope. A thermogravimetric and differential thermal analysis (TG-DTA) of WS and NiHCF-WS was carried out using a thermal analyzer (EXSTAR TG/DTA 7300, Japan) equipped with an AS-3 auto sampler. About 7.5 mg of each sample was prepared into an

aluminum-PAN, heated up to 500°C at a constant rate of 10°C min^{-1} in normal atmosphere for thermal analysis using an open-Al-pan as reference.

The concentrations of Cs$^+$ and K$^+$ in aqueous samples were analyzed by a fully quantitative analytical method on a Perkin Elmer ELAN DRC-e ICP-MS in standard mode. Each sample was analyzed 5 times and the average was taken. The relative standard deviation (RSD) of multiple measurements was less than 2% and in most cases, less than 1.5%.

2.2.10 Calculation

The Cs$^+$ adsorption results are given as uptake amount (q) and distribution coefficient (K_d). The Cs$^+$ uptake amount q (mg g^{-1}) was calculated from the mass balance as follows:

$$q = \frac{(C_0 - C_t)V}{1000M}$$ (2-12)

Distribution coefficient K_d (mL g^{-1}), which is mass-weighted partition coefficient between solid phase and liquid supernatant phase reflecting the selectivity for objective metal ions, was calculated according to the formula:

$$K_d = \frac{C_0 - C_t}{C_t} \times \frac{V}{M}$$ (2-13)

where, C_0 and C_t (mg L^{-1}) are the concentrations of Cs$^+$ at contact time of 0 (initial concentration) and t determined by ICP-MS, V (mL) is the volume of Cs$^+$ solution and M (g) is the mass of adsorbent used.

2.2.11 Quality assurance and quality control

In order to ensure reliability and improve accuracy of the experimental data in this study, kinetic

and equilibrium studies on Cs^+ adsorption were conducted in duplicate with a mean ± SD being reported. All of the figures and the kinetic fitting displayed in this paper were accomplished using the Origin 7.5 program (OriginLab, USA).

2.3 Results and discussion

2.3.1 Characterization of biosorbent

(1) Field emission scanning electron microscope (FE-SEM)

The FE-SEM images of walnut shell before and after modification are shown in Fig.2-1. It can be seen that the raw walnut shell has a complex and multilayer structure including the obvious fibrous lignocellulosic (Fig.2-1a). After modification, there is a remarkable difference in the surface structure of walnut shell with NiHCF particles attached on the surface of walnut shell, as depicted by the arrows in Fig.2-1b.

(2) Thermogravimetric and differential thermal analysis (TG-DTA)

A large number of reactions occur during the thermal degradation of lignocellulosic materials. Therefore, a thermal degradation pre-study conducted on the biomass material, is very important in terms of the efficient design of thermochemical processes for the conversion of biomass into energy and products [39]. The TG-DTA curves, which display the thermal degradation characteristics for the WS and NiHCF-WS, were recorded as a function of time (Fig.2-2). Based on the TG curves, it can be said that the major mass loss occurred in the thermal degradation of WS (98.2%) and NiHCF-WS (96.4%), respectively. Their TG curves can be divided into three parts, representing loss of water, volatilation of hemicellulose like contents, and decomposition of celloluse and lignin components [40]. Compared with WS, the second and last parts of the TG curves obtained from the NiHCF-WS were obviously different with shorter time needed. It can be seen that approximately 37.4% of TG

loss occurred during the second part and finished at a time of about 28 minute for the NiHCF-WS. However, the positive peak of the DTA curve was more obvious than that of WS, which might be due to the loss of impurities with lower calorific value than hemicellulose during the modification. Another great difference, the third part began at time of 30 minutes and temperature of about $350^{o}C$, much lower than WS, indicating the decomposition temperature greatly decreased after modification. During this step, approximately 52.3% of TG was lost, higher than that of WS.

Through comparing the TG-DTA results of WS and NiHCF-WS, it can be concluded that the modification process didn't alter the thermal stability of WS and therefore NiHCF-WS can be used as a thermally stable adsorbent.

2.3.2 Removal behavior studies

(1) Effect of contact time

Besides the concentration of Cs^+, the variation in concentration of Ni^{2+} released into solution versus contact time was also measured and the results are presented in Fig.2-3. Significant difference between the Cs^+ adsorption performances of the WS and NiHCF-WS was observed: slow and unstable for WS while high and stable for NiHCF-WS.

From the WS curve in Fig.2-3, during the first 3 h, the Cs^+ concentration in solution basically decreased slowly and gradually, probably due to the physical adsorption by the irregular surface of WS. However, the Cs^+ concentration increased after 5 h, demonstrating that Cs^+ sorption onto WS was unstable. On the other hand, an obviously rapid uptake of Cs^+ was observed at first by the NiHCF-WS, possibly due to the easy availability of spare adsorbent surface compared to the Cs^+ concentration applied. The equilibrium could be attained within about 2 h (0.27 mg L^{-1}) with an adsorption percentage of nearly 100%, and its equilibrium uptake amount was calculated to be 0.52 mg g^{-1}. Rapid adsorption kinetics is a very important feature of adsorption materials for their

application in wastewater treatment, resulting in a short operation cycle, small reactor volume and low investment and operation cost. As a heavy metal, which may be hazardous to human health, the concentration of Ni^{2+} released into solution was also detected. From the results, it can be seen that the concentration of Ni^{2+} gradually increased with the contact time and was 0.38 mg L^{-1} at the contact time of 2 h, which is lower than the short-term effluent reuse limit of 2.0 mg L^{-1} set by U.S. Environmental Protection Agency (USEPA) [41].

(2) Effect of initial pH

Metal adsorption from aqueous solutions can be greatly affected by solution pH, which impacts not only the binding sites (e.g., degree of protonation) but also the metal chemistry (e.g., speciation and precipitation) [42, 43]. Therefore the influence of pH on the removal of Cs^+ was examined in the pH range from 2.0 to 11.0 and the results are shown in Fig.2-4. It can be seen that, the adsorption percentage of Cs^+ gradually decreased with increasing pH from 2.0 to 10.0 and dramatically from 10.0 to 11.0, which was different from other researches [4, 11, 43] in which the sorption of Cs^+ was mostly reported to be suppressed under acidic conditions due to the competition of H_3O^+. However, the results of this study indicated that the sorption of Cs^+ was not suppressed but enhanced under acidic conditions, demonstrating that H_3O^+ was preferred for Cs^+ sorption on NiHCF-WS. These special characteristics might be meaningful in expanding the application scope of adsorption methods in treating acidic radioactive liquid waste. In addition, there was no significant difference between the pH values of the initial solution and final solution, indicating no competition sorption occurred between H_3O^+ and Cs^+ under acidic conditions. On the other hand, Cs^+ sorption was significantly affected under the alkaline conditions, probably due to the formation of cesium hydroxides, especially at the initial pH of 11.0. The negatively charged $Cs(OH)_2^-$ might lead to the decrease of Cs^+ adsorption due to electrostatic repulsion [6, 44]. This observation is in accordance with the

phenomenon reported by Lilga et al. [45] who observed a similar decreased Cs^+ adsorption on hexacyanoferrates film in basic waste solutions. In addition, it can be seen from Fig.2-4 that all of the pH values of the final solutions decreased under initial neutral and alkaline conditions, indicating the decrease in OH^-. This phenomenon denotes that the suppress of Cs^+ sorption under neutral and alkaline conditions was mainly attributed to the formation of $Cs(OH)_2^-$.

(3) Effect of adsorbent dosage

In order to evaluate the effect of adsorbent dosage on Cs^+ adsorption, 0.1, 0.2, 0.3 and 0.4 g NiHCF-WS were added into 20 mL of Cs^+ solutions with initial Cs^+ concentration of 10 mg L^{-1}, corresponding to the dosage of 5, 10, 15 and 20 g L^{-1} respectively. As shown in Fig.2-5, with the increase of adsorbent dosage from 5 to 15 g L^{-1}, the adsorption percentage increased gradually due to the greater availability of the sorption sites. Further increase in adsorption percentage was not observed when the dosage increased to 20 g L^{-1}, possibly due to the relatively low equilibrium concentration of Cs^+ (data not shown) resulting in a low driving force. The Cs^+ uptake amount, however, was relatively stable compared to the variation of adsorption percentage, about 0.53-0.62 mg g^{-1} when NiHCF-WS dosage varied from 5-15 g L^{-1}. 15 g L^{-1} of NiHCF-WS dosed into 10 mg L^{-1} of initial Cs^+ solution could achieve the highest Cs^+ uptake amount (0.62±0 mg g^{-1}) and adsorption percentage (93.6±0.08 %).

On the other hand, the equilibrium adsorption capacity of the newly developed NiHCF-WS was found to be lower than that reported in other literature [4, 22]. However, this result is still promising when considering that the amount of NiHCF particles introduced into WS by surface modification were very little. In addition, the adsorption capacity had a close relationship with the pattern and characteristics of adsorbent such as the size (*i.e.* particle and pore size) and density.

(4) Effect of initial Cs^+ concentration

   Cs^+ solutions of desired concentrations were prepared by diluting known volumes of the standard Cs^+ stock solution with DW. As stated, the pH values of solutions with different initial Cs^+ concentration were all about 7 and unadjusted.

   As shown in Fig.2-6, the Cs^+ adsorption percentage decreased significantly with the increase in initial Cs^+ concentration, especially when initial Cs^+ concentration higher than 50 mg L^{-1}. When initial Cs^+ concentration was lower than 20 mg L^{-1}, above 90% of adsorption percentages could be obtained, whereas it was only about 70% when initial Cs^+ concentration increased to 50 mg L^{-1}. This is because after consuming all of the higher energy sites, excess Cs^+ would then be adsorbed on the lower energy sites, resulting in loose binding of cesium and the decrease of removal efficiency [46]. On the other hand, the Cs^+ uptake amount increased with the increase of initial Cs^+ concentration, from 0.05 mg g^{-1} to 3.44 mg g^{-1} when initial Cs^+ concentration varied from 1 mg L^{-1} to 100 mg L^{-1}. The best Cs^+ adsorption percentage and uptake amount were 99.1±0.1% and 3.4±0.02 mg g^{-1}, which were obtained at the initial concentration of 20 mg L^{-1} and 100 mg L^{-1}, respectively.

(5) Effect of competitive ions

   As well known, selectivity is a very important factor for an adsorption material, as it will influence its application in real wastewater treatment, especially for Cs^+. Generally, the concentration of Cs^+ in wastewater is much lower than that of Na^+ or K^+, normally present in natural water bodies. Therefore, the selectivity of Cs^+ adsorption on NiHCF-WS was evaluated by using Na^+ and K^+ as competitive ions in this study.

   As a highly efficient adsorption material, NiHCF has a higher selectivity towards Cs^+ because of its cubic structure with a channel diameter of about 3.2 Å, which may permeate small hydrated ion such as Cs^+, whereas block larger hydrated ions like Na^+. Chen et al. [6] pointed out that similar and relatively high K_d values could be obtained by using NiHCF loaded electrode under both conditions

of with and without competitive ions.

In this study, as shown in Fig.2-7, when the initial Cs^+ concentration was 1 mg L^{-1}, the K_d value was higher than 10^4 under a non-competitive ion condition, which was relatively higher than previous researches [4, 47]. Under competitive ion conditions, however, the value of K_d decreased, demonstrating that the negative influence brought by competitive ions. The same negative influence was also observed in other research using copper hexacyanoferrrate–PAN composite as an ion exchanger for cesium removal [4]. In addition, as the concentration of competitive ions increased from 100 mg L^{-1} to 1000 mg L^{-1}, the K_d value decreased slightly in accordance with the results of Avramenko et al. [8]. The negative effect of competitive ions might be caused by a lesser amount of NiHCF loaded on the WS, which was difficult to resist the strong influence of relatively high concentration of competitive ions. This observation could be confirmed by the low uptake amount in Section 2.3.2. According to the results of Chen et al. [6], the Cs^+ uptake amount reached 250 mg g^{-1} and smaller differences existed between the K_d values with and without competitive ions addition. In this study, the Cs^+ uptake amount was not greater than 10 mg g^{-1} which may contribute to the varied K_d values under different conditions. On the other hand, the concentrations of competitive ions were much higher in this study compared with other literature (1 mg L^{-1}) [6], which might also explain the much stronger influence of competitive ions. However, from Fig.2-7 it can be seen that the differences in equilibrium concentration of Cs^+ brought by the competitive ions were not as significant as those in K_d values, especially for K^+. For example, when the initial Cs^+ concentration was 10 mg L^{-1}, the equilibrium Cs^+ concentration was 0.15 mg L^{-1} and 0.19 mg L^{-1}, respectively without and with K^+ (100 mg L^{-1}). This observation demonstrated that NiHCF-WS still had some selectivity for Cs^+ adsorption although the K_d values decreased. In addition, it can be concluded that under the initial Cs^+ concentration of 1 mg L^{-1}, K^+ was more competitive than Na^+ due to the fact that

the lower K_d value was obtained for K^+ addition at the same concentration with Na^+. This phenomenon might be attributed to the similar characteristics between Cs^+ and K^+, resulting in much easier sorption of K^+ rather than Na^+. When the initial Cs^+ concentration was increased to 5 mg L^{-1} and 10 mg L^{-1}, however, Na^+ ions seemed to be much more competitive than K^+. This observation implied that the effect of competitive ions on Cs^+ adsorption might depend on the concentration ratio of Cs^+ to the competitive ions. In addition, it is believed that the influence of competitive ions was much stronger with lower Cs^+ concentration.

2.3.3 Adsorption stability studies

As shown in Table 2-2, more Cs^+ was released in GW than TW probably due to higher ionic strength. It was well believed that ion exchange occurred between Cs^+ on Cs-NiHCF-WS and exchangeable metal ions in GW. Basing on this hypothesis, it was easy to understand the differences between amounts of Cs^+ released in GW and TW. On the other hand, low liquid/solid ratio seemed unfavorable for safety disposal of Cs-NiHCF-WS in this study because much more Cs^+ was released at lower liquid/solid ratio. This unusual phenomenon might be contradictive with the ion exchange hypothesis. Generally, more Cs^+ would be released because of the more exchangeable ions in higher liquid/solid ratio. However, the concentrations of Cs^+ in these solutions were very low (in ppb level) and therefore, experimental errors might lead to a contradictive result. In all these case, however, the amount of Cs^+ released was very little, indicating the stable adsorption of Cs^+ on NiHCF-WS.

2.3.4 Adsorption kinetic study

Fig.2-8 shows the effect of contact time on the Cs^+ adsorption and application of kinetic models to Cs^+ adsorption by WS and NiHCF-WS. Table 2-3 lists the sorption rate constants associated with pseudo first and second order kinetic models. It can be seen from Fig.2-8 that Cs^+ adsorption is a

rapid process, about 2 h is needed to reach equilibrium for the NiHCF-WS. The equilibrium uptake amount of Cs^+ was greater than 0.5 mg g^{-1}. In addition, the adsorption process on only-WS is complicated and not efficient with an equilibrium uptake amount of approximately 0.1 mg g^{-1}. It is clearly indicated that the NiHCF-WS has a much better adsorption performance for Cs^+ than only-WS.

Compared to the first-order model, the pseudo second-order kinetic model had a higher correlation coefficient (R^2) for NiHCF-WS, suggesting that the Cs^+ adsorption process is a chemisorption rather than physisorption.

Fig.2-9 shows the amount of adsorbed Cs^+, q_t (mg g^{-1}), versus the square root of time for NiHCF-WS. The presence of three linear regions on the curve is possibly due to the presence of three steps during the adsorption process [39]: An external mass transfer step such as the boundary layer diffusion occurred first, then an intra-particle diffusion step for the second and lastly a saturation step. In this study, the first linear region with a high slope signaled a rapid external diffusion stage depicting macro-pore or inter-particle diffusion, which is different from the second step, gradual adsorption stage controlled by intra-particle (micro-pore) diffusion, and the last step (saturation stage). This observation can also be linked with adsorption mechanisms mainly involving the surface layers of crystallites [48].

2.3.5 Equilibrium studies

(1) Cesium adsorption isotherms

In order to obtain the equilibrium isotherm, the initial Cs^+ concentration varied from 5-400 mg L^{-1} (5, 10, 20, 50, 75, 100, 200, 400) while maintaining an adsorbent dosage of 20 g L^{-1}, and the amount of adsorbed Cs^+ was investigated.

Fig.2-10 shows the application of nonlinear Langmuir, Freundlich and D-R isotherms to the Cs^+

adsorption on NiHCF-WS. In this study, chi-square analysis was applied to estimate the degree of difference (χ^2) between the experimental data and the isotherm data, which is calculated by the following equation [49]:

$$\chi^2 = \sum \frac{(q_e^{\,\exp} - q_e^{\,cal})^2}{q_e^{\,cal}} \qquad (2\text{-}14)$$

where $q_e^{\,cal}$ (mg g^{-1}) is the equilibrium uptake amount calculated from the isotherm and $q_e^{\,exp}$ (mg g^{-1}) is the experimental equilibrium uptake amount. A smaller χ^2 value indicates a better fitting isotherm.

In addition, the values of normalized standard deviation (NSD (%)) were also calculated to validate the fitness of isotherm to experimental data [11], which is defined as:

$$\text{NSD}(\%) = 100 \times \sqrt{\frac{\sum [(q_e^{\,\exp} - q_e^{\,cal})/q_e^{\,\exp}]^2}{N - 1}} \qquad (2\text{-}15)$$

where N is the number of measurements. Similarly, a smaller NSD (%) value indicates a better fitting isotherm.

The results of χ^2 and NSD (%) are given in Table 2-4 and indicate the three adsorption isotherms match the experimental data ($R^2 > 0.9$). Although the R^2 value of the Freundlich isotherm is similar with that of the Langmuir or D-R isotherm, the χ^2 and NSD (%) values of the Freundlich isotherm are much smaller, implying that the adsorption of Cs$^+$ on NiHCF-WS is a multilayer adsorption rather than monolayer adsorption. Furthermore, the value of n is less than 1, suggesting this adsorption process is favorable [22].

As another important function, the Langmuir isotherm could give us the estimated maximum adsorption capacity (q_m) of NiHCF-WS, 4.94±0.5 mg g^{-1}, which is similar to that provided by D-R isotherm. In conclusion, the adsorption isotherms demonstrated that the Cs$^+$ adsorption onto NiHCF-WS is a multilayer chemical ion exchange process.

(2) Role of ion exchange with K^+

It is hypothesized that if adsorption is mainly caused by ion exchange reaction, then the quantity of the released cations (in gram-equivalent) would be close to that of the adsorbed target ions. Table 2-5 shows the relationship between the Cs^+ adsorbed and K^+ released during the Cs^+ adsorption process and two significant phenomena are observed. With the increase in dosage (No.1-4) and initial Cs^+ concentration (No.4-7), both Cs^+ adsorbed and K^+ released increase, demonstrating affinity between them. On the other hand, the test results reveal that the amount of K^+ released into solutions are greater than that of Cs^+ adsorbed except for the dosage of 5 g L^{-1} (probably caused by experimental error). In other words, the released K^+ from the adsorbent is not completely exchanged by Cs^+ [8, 50], which is also in agreement with the relationship between Ca^{2+} released and Cs^+ adsorbed reported by Miah et al. [51]. This indicates that the amount of K^+ released into the solution is partly through dissolution other than ion exchange with Cs^+. However, it is not clearly demonstrated the existence of chemical ion exchange process between Cs^+ and K^+ from the data reported in this table. Basing on the above conclusion that the existence of dissolution of K^+, as a result, the variations between adsorbed Cs^+ and released K^+ at the same dosage (20 g L^{-1}) and different initial Cs^+ concentrations are compared in order to determine the possible equal relationship between them. As a comparison between No.4 and 5, the variation of adsorbed Cs^+ is 8.94±0.07 μmol, which is similar with the variation of released K^+ (8.72±0.03 μmol). In addition, the variation of adsorbed Cs^+ between No.5 and 6 is 2.01±0.08 μmol, which is also similar with the variation of released K^+ (3.31±0.17 μmol). When the initial Cs^+ concentration is increased from 200 to 400 mg L^{-1} (No.6 and 7), the variation of adsorbed Cs^+ (2.21±0.11 μmol) is similar with released K^+ (2.91±0.09 μmol). Through the above comparisons, it is consequently concluded that there is indeed an exchange process between Cs^+ and K^+. The K^+ in the NiHCF-WS plays an important role in the Cs^+ adsorption process as the ion exchanger.

2.3.6 Thermodynamic study

The distribution coefficient Kd was calculated using Eq. (2-13). The plotting of $\ln K_d$ versus $1/T$ gave a straight line with a R^2 of 0.99, from which the $\Delta H°$ and $\Delta S°$ was determined using Eq. (2-10). Furthermore, the standard Gibbs free energy at each temperature was calculated using Eq. (2-11) and the results are listed in Table 2-6.

As shown in Table 2-6, the distribution coefficient of Cs^+ adsorption by NiHCF-WS increased remarkably with the increase in temperature, implying that high temperature was favorable for Cs^+ adsorption. The same phenomenon was observed by Nilchi et al. [4], who used copper hexacyanoferrate to adsorb Cs^+ from aqueous solution. The negative amounts of $\Delta G°$ at different temperatures and the positive amount of $\Delta H°$ revealed that the chemical ion exchange process was a spontaneous and endothermic adsorption reaction in this study.

2.3.7 Reduction of Cs-NiHCF-WS after incineration

Variations of weight and volume of Cs-NiHCF-WS before and after incineration are listed in Table 2-7. It can be seen that 10 mL of 10 mg L^{-1} Cs^+ solution was reduced to 0.17 mL Cs-NiHCF-WS after adsorption process. Approximately 97.9% (in weight) and 91.9% (in volume) of Cs-NiHCF-WS was reduced after incineration ($500°C$ for 2 h), probably due to the loss of water content, lignin, cellulose and hemicellulose. This result was in agreement with the TG-DTA analysis. Generally speaking, the waste volume is of more concern during the final disposal of radioactive wastes than weight (in deep landfill). Therefore, as shown in Table 2-7, the total reduction (from liquid waste to slag residue) was given in volume, which was as high as 99.9%. This will be much more attractive option when the volume of radioactive liquid waste is very large. The results show that the NiHCF-WS has great potential for reduction of radioactive liquid waste to a small volume of

slag residue, making it suitable for ultimate disposal. As discussed in Section 2.2.8, volatilization of cesium is not anticipated during the incineration process in this study.

In order to obtain a better understanding of the changes in the structure of Cs-NiHCF-WS during the incineration process, the photographs and SEM images of Cs-NiHCF-WS before and after incineration are presented in Fig.2-11. As shown in Fig.2-11a, the Cs-NiHCF-WS has a diameter of approximately 2 mm, making it easy separated from wastewater. After incineration, as shown in Fig.2-11b, obvious color change was observed (from caesious to brown). Though the visual shape was still particulate, the incinerated Cs-NiHCF-WS could be easily transferred into powder form, indicating the main organic components (lignin, cellulose and hemicellulose) might have decomposed and the structure was destructed. In addition, it was found that the particulate form of incinerated Cs-NiHCF-WS could be immediately dispersed in water and transferred into powder form again after evaporation of water (Fig.2-11c). The surface morphology of the powder was observed by SEM and is depicted in Fig.2-11d ($2500\times$) and Fig.2-11e ($10000\times$). It can be seen that most of the components of WS have been burned to slag residue (Fig.2-11d). In addition, there were still some crystal-like structures observed in the incinerated Cs-NiHCF-WS (as shown in the circles in Fig.2-11e), probably the incineration product of NiHCF.

2.3.8 Comparison of Cs$^+$ adsorption performance

For the sake of practical application of the newly developed NiHCF-WS, a comparison of Cs$^+$ removal performance was made with other available adsorbents in this study. In general, distribution coefficient, K_d is always taken as an important parameter in the comparison study. Table 2-8 shows the comparison results of K_d value of Cs$^+$ adsorption using different adsorbents reported in other literature. Because the K_d value has a close relationship with experimental conditions, the information was listed with as much detail as possible, including initial Cs$^+$ concentration, adsorbent dosage and

other important conditions. In comparison, it can be concluded that the K_d value of NiHCF-WS is higher than most clay mineral materials and lower than FC-Cu-EDA-SAMMS [43], demonstrating the NiHCF-WS is a potential efficient adsorbent for Cs^+ adsorption when taking cost and volume reduction into consideration. WS is a renewable resource and can be reduced remarkably after incineration as described in Section 2.3.7 when compared with clay materials. The total volume reduction rate during the treatment process was up to 99.9%, which will result in a considerable space and cost reduction in disposing the spent adsorption materials. Furthermore, NiHCF-WS needs a simple modification process and is low cost, which makes it a competitive adsorption material in practical application.

2.4 Summary

NiHCF was incorporated with walnut shell for cesium removal. The equilibrium of removal process was attained within 2 h and the cesium uptake amount was 0.52 mg g^{-1}. The adsorption process well fitted to the pseudo second-order kinetic model, suggesting chemisorption was the main rate-controlling step. In addition, in comparison with other adsorbents, cesium removal by NiHCF-WS was enhanced under acidic and suppressed under alkaline conditions, which makes it especially appropriate for treating acidic radioactive liquid wastes. Formation of $Cs(OH)_2^-$ during alkaline conditions might suppress the sorption of Cs^+. NiHCF-WS had some selectivity to cesium adsorption and the adsorption was stable. The good correlation coefficient ($R^2 = 0.93$), low χ^2 and NSD values suggest that cesium adsorption on NiHCF-WS could be best described by the Freundlich adsorption isotherm. Results showed that the NiHCF-WS was an effective adsorbent for cesium adsorption and the adsorption process was endothermic and spontaneous. Spent NiHCF-WS could be reduced significantly through incineration at 500^oC for 2 h and the total reduction (in volume) from liquid waste to slag residue was up to 99.9%, leading to a considerable space and cost reduction in

disposing of the spent adsorption material. Finally, compared with other adsorption materials, NiHCF-WS is a renewable resource and needs a simple modification process and is low cost, making it a competitive adsorption material in practice.

Table 2-1 Chemical composition of synthetic groundwater.

Ion	Concentration (mmol L^{-1})
Cl^-	1.72
HCO_3^-	1.69
SO_4^{2-}	0.09
PO_4^{3-}	0.04
NO_3^-	1.51
Na^+	1.56
K^+	0.2
Mg^{2+}	0.87
Mn^{2+}	0.06
Fe^{2+}	0.03
Ca^{2+}	0.762

Table 2-2 Cesium sorption stability of NiHCF-WS in synthetic groundwater and tap water. [*]

M (g)	Q (mg g^{-1})	Solution type	V (mL)	Cs$^+$ released (μg)		
				1 day	10 days	15 days
0.1	0.52±0.02	GW	10	2.65±1.83 (5.0±4.7%)	ND	ND
			20	0.23±0.11 (0.43±0.27%)	0.52±0.25 (1.0±0.68%)	0.11±0.02 (0.21±0.05%)
			40	0.12±0.07 (0.23±0.18%)	ND	ND
		TW	20	0.05±0.02 (0.09±0.05%)	ND	ND

[*]Adsorption stability study was conducted in room temperature without any shake to simulate the real environment. The values represented in the brackets means the percentage of released Cs$^+$ accounts for the adsorbed Cs$^+$. ND means not detected.

Table 2-3 Kinetic parameters of Cs^+ adsorption on WS and NiHCF-WS.

Pseudo first-order kinetic model			Pseudo second-order kinetic model		
	WS	NiHCF-WS		WS	NiHCF-WS
q_{eexp} [a] (mg g^{-1})	0.11±0.04	0.52±0.004	q_{eexp} (mg g^{-1})	0.11±0.04	0.52±0.004
k_1 (min^{-1})	0.37±0.39	0.071±0.006	k_2 (g mg^{-1} min^{-1})	(-3.8±4.0)×10^{45}	0.23±0.03
q_{ecal} [b] (mg g^{-1})	0.10±0.01	0.52±0.009	q_{ecal} (mg g^{-1})	0.099±0.01	0.54±0.01
R^2	0.492	0.946	R^2	0.483	0.981

[a] means the equilibrium sorption capacity estimated from the experimental data.

[b] means the equilibrium sorption capacity calculated from the kinetic model.

Table 2-4 Adsorption isotherm parameters of Cs^+ on NiHCF-WS.

Langmuir isotherm		Freundlich isotherm		D-R isotherm	
q_m (mg g^{-1})	4.94 ± 0.5	k_f (mg g^{-1} L$^{1/n}$ mg$^{-1/n}$)	1.12 ± 0.2	q_m (mg g^{-1})	4.43 ± 0.4
b (L mg^{-1})	0.06 ± 0.02	n	0.27 ± 0.04	β (mol^2/kJ^2)	$(3 \pm 0.8) \times 10^{-5}$
R^2	0.93	R^2	0.93	R^2	0.92
χ^2	21.1	χ^2	0.96	χ^2	1.3×10^{281}
NSD (%)	57.3	NSD (%)	60.7	NSD (%)	310.2

Table 2-5 Relationship between Cs^+ adsorbed and K^+ released during the adsorption process of Cs^+

on NiHCF-WS.[a]

No.	Dosage $(g\ L^{-1})$	Initial Cs^+ concentration $(mg\ L^{-1})$	Cs^+ adsorbed (μmol)	K^+ released (μmol)
1	5	10	0.5±0.02	0.1±0.0
2	10	10	0.9±0.002	1.5±0.06
3	15	10	1.4±0.001	4.6±0.3
4	20	10	1.4±0.001	4.7±0.2
5	20	100	10.3±0.07	13.4±0.2
6	20	200	12.3±0.01	16.7±0.02
7	20	400	14.6±0.1	19.6±0.1

[a] Samples were tested in 50 mL polypropylene tubes with 20 mL Cs^+ solutions at room temperature and 200 rpm for 24 h.

Table 2-6 Thermodynamic parameters of Cs^+ adsorption on NiHCF-WS.

Temp. (K)	K_d (mL g^{-1})	$\Delta G°$ (kJ mol^{-1})	$\Delta H°$ (kJ mol^{-1})	$\Delta S°$ (kJ K^{-1} mol^{-1})
298	171.4	−12.9		
308	757.1	−16.8	101.8	0.385
318	2264.3	−20.6		

Table 2-7 Variation of weight and volume of cesium loaded NiHCF-WS before and after incineration.

Items concerned			Values
Liquid waste	Initial Cs^+ concentration (mg L^{-1})		10.7 (0.3)
	Final Cs^+ concentration (mg L^{-1})		0.26 (0.0)
	Volume (mL)		10
Cs-NiHCF-WS	Before incineration	Weight (g)	0.198 (0.01)
		Volume (mL)	0.17 (0.01)
	After incineration	Weight (g)	0.004 (0.00)
		Volume (mL)	0.014 (0.00)
	Reduction	Weight (%)	97.9 (0.3)
		Volume (%)	91.9 (0.9)
Total reduction		Volume (%)	99.9 (0.02)

The results are expressed as Means (Standard Deviations).

Table 2-8 Comparison of distribution coefficients between NiHCF-WS and other adsorbents.

Adsorbent	Initial Cs^+ concentration $(mg\ L^{-1})$	Dosage $(g\ L^{-1})$	Solution condition or competitive ions	Distribution coefficient, K_d $(L\ g^{-1})$	References
A-X zeolite	50	1	-	0.19	[16]
Natural zeolite, Turkey	$8.45 \times 10^5\ Bq\ L^{-1\ a}$	10	-	3.75-4.45	[52]
Ain Oussera soil	1	2	-	0.37	[53]
Antimony silicate	-	5	$0.23\ g\ L^{-1}\ Na^+$	1	[54]
Antimony silicate	-	5	$3.9\ g\ L^{-1}\ K^+$	1	[54]
Copper hexacyanoferrate -PAN	13.3	-	-	1.67	[4]
Copper hexacyanoferrate -PAN	13.3	-	$10^{-4}\ M\ K^+$	0.17	[4]
NaSM zeolite	$2.280 \times 10^4\ Bq\ L^{-1}$	10	$0.0119\ M\ K^+$	4.65	[15]
ISM-25mg Calix[4] arene	$2.280 \times 10^4\ Bq\ L^{-1}$	10	$0.0119\ M\ K^+$	27.63	[15]
Aluminum-pillared montmorillonite	0.133	-	$1.95\ g\ L^{-1}\ K^+$	0.4	[11]
CoFC@Silica-Py	10	-	$9.6\ g\ L^{-1}\ Na^+$	>10	[10]
CoFC@Glass-Py	10	-	$9.6\ g\ L^{-1}\ Na^+$	1	[10]
FC-Cu-EDA-SA MMS	0.5	1	Sequim Bay seawater	240	[43]
FC-Cu-EDA-SA MMS	0.5	1	Hanford groundwater	1400	[43]
Raw bentonite	0.133	66.7	Synthetic groundwater	1.9	[55]
Activated bentonite	0.133	66.7	Synthetic groundwater	8.9	[55]
GE clay	0.133	66.7	Synthetic groundwater	3.1	[55]
Local Taiwan laterite	1.33	33.3	-	0.025	[56]
Bure mudrock	-	-	-	0.1-0.6	[57]
NiHCF-WS	1	5	0	10.8	This study
NiHCF-WS	1	5	$1\ g\ L^{-1}\ K^+$	3.5	This study
NiHCF-WS	1	5	$0.1\ g\ L^{-1}\ Na^+$	4.7	This study

[a] $1M\ Bq\ L^{-1}\ {}^{137}Cs$ is equivalent to $9.044 \times 10^{-4}\ mg\ L^{-1}$.

- No data in the literature.
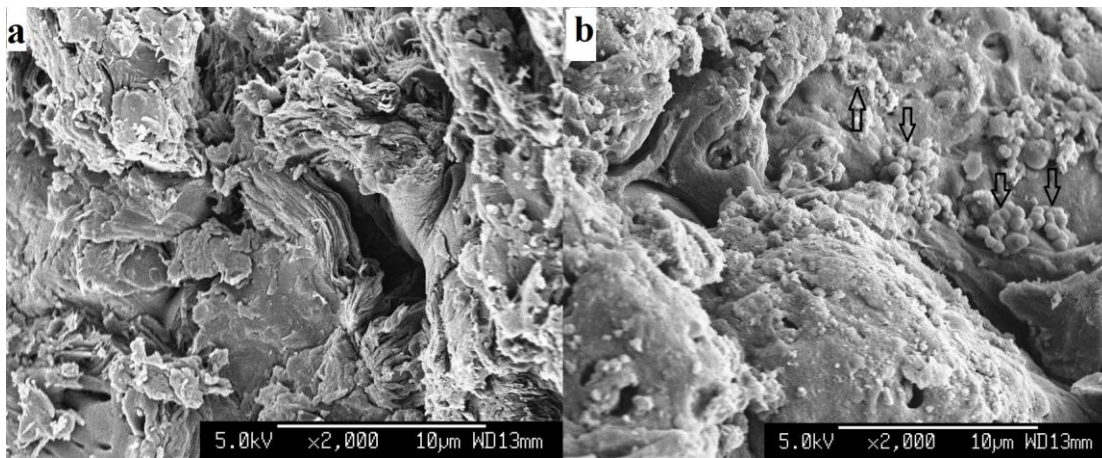
Fig.2-1 Typical scanning electron microscope images of walnut shell before (a) and after (b) modification. (Acceleration voltage of 5.0 kV and 2000 × magnification, arrows show the nickel hexacyanoferrate particles)
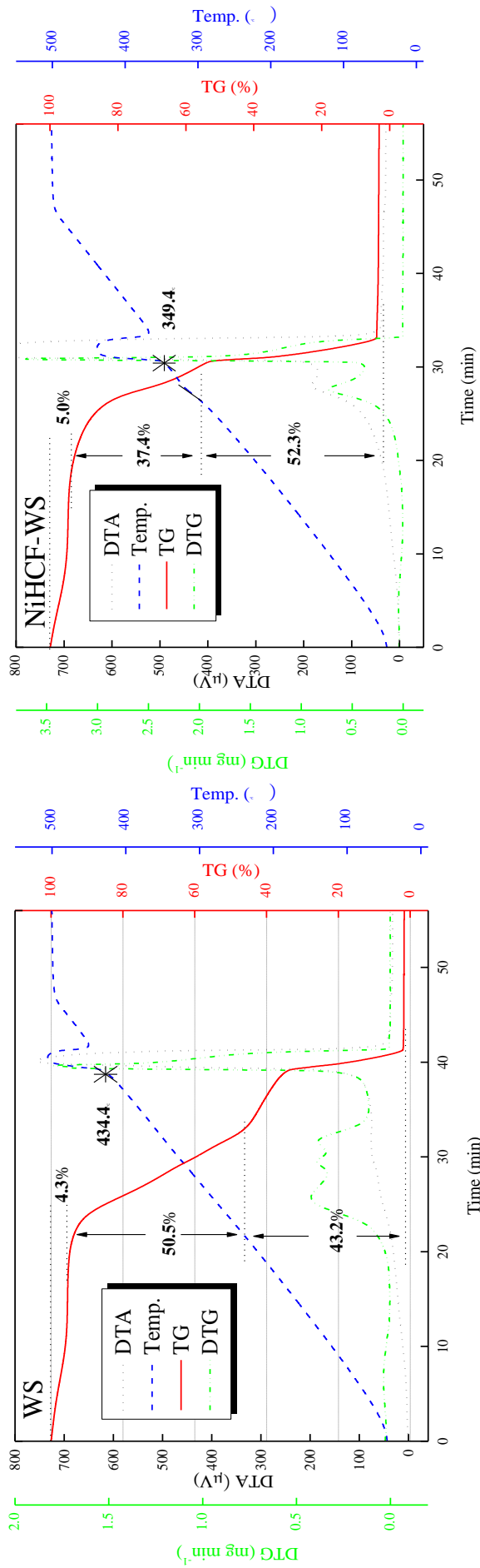
Fig.2-2 TG-DTA results of walnut shell and nickel hexacyanoferrate incorporated walnut shell obtained at the heating rate of 10°C

min^{-1} in air atmosphere. (Pan: Al-Pan; Reference: Open-Al-Pan; Upper limit temperature: 550°C; Gas flow rate: 200 mL min^{-1})
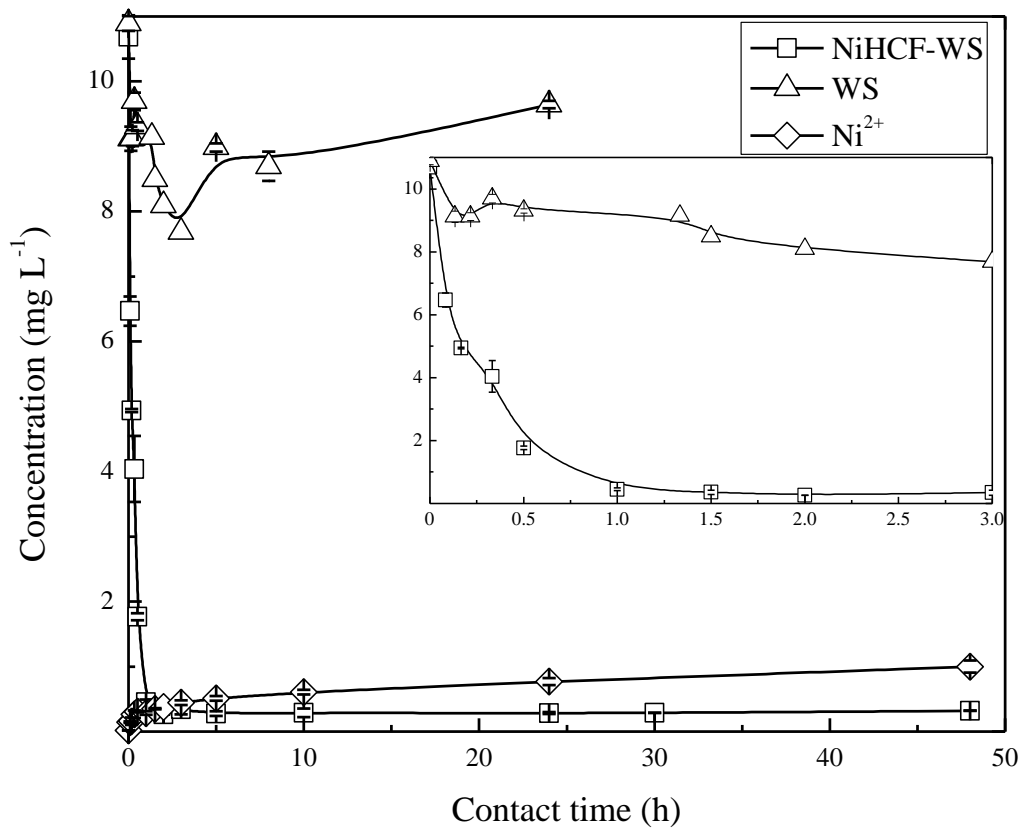
Fig.2-3 Effect of contact time on adsorption of cesium (C_0=10 mg L^{-1}) with the dosage of 20 g L^{-1}

and shaking speed of 200 rpm.
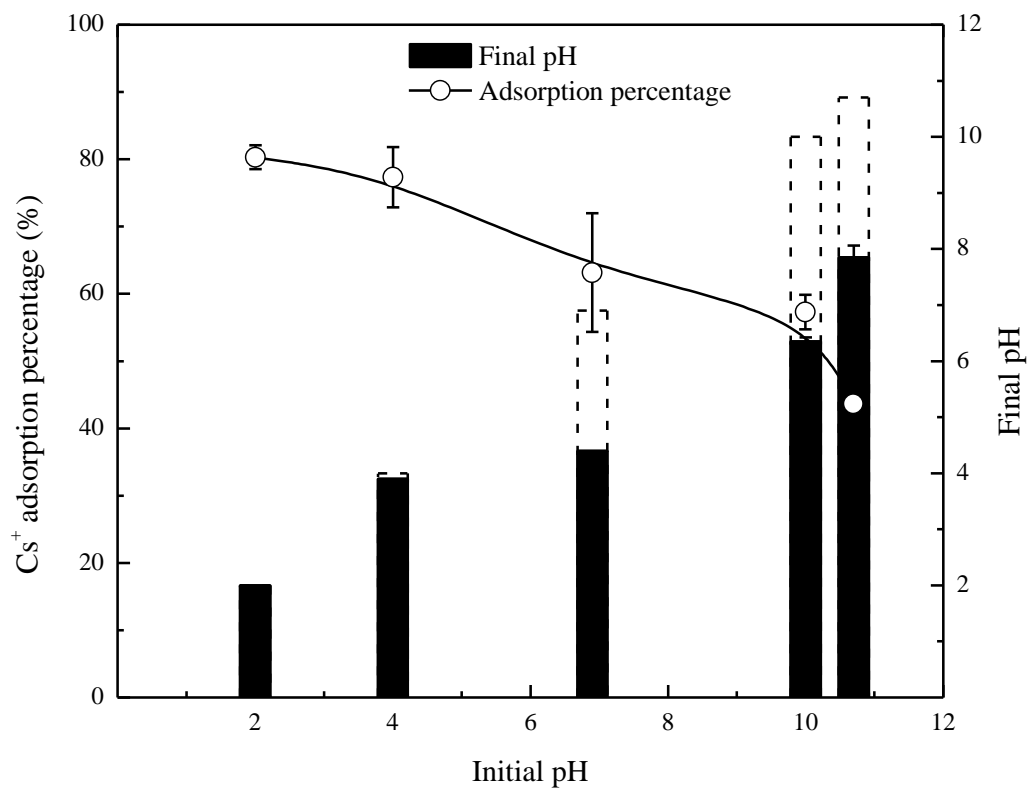
Fig.2-4 Effect of initial pH on the cesium (C_0=10 mg L^{-1}) adsorption by NiHCF-WS (10 g L^{-1}) with

the shaking (200 rpm) time of 24 h at 25°C.
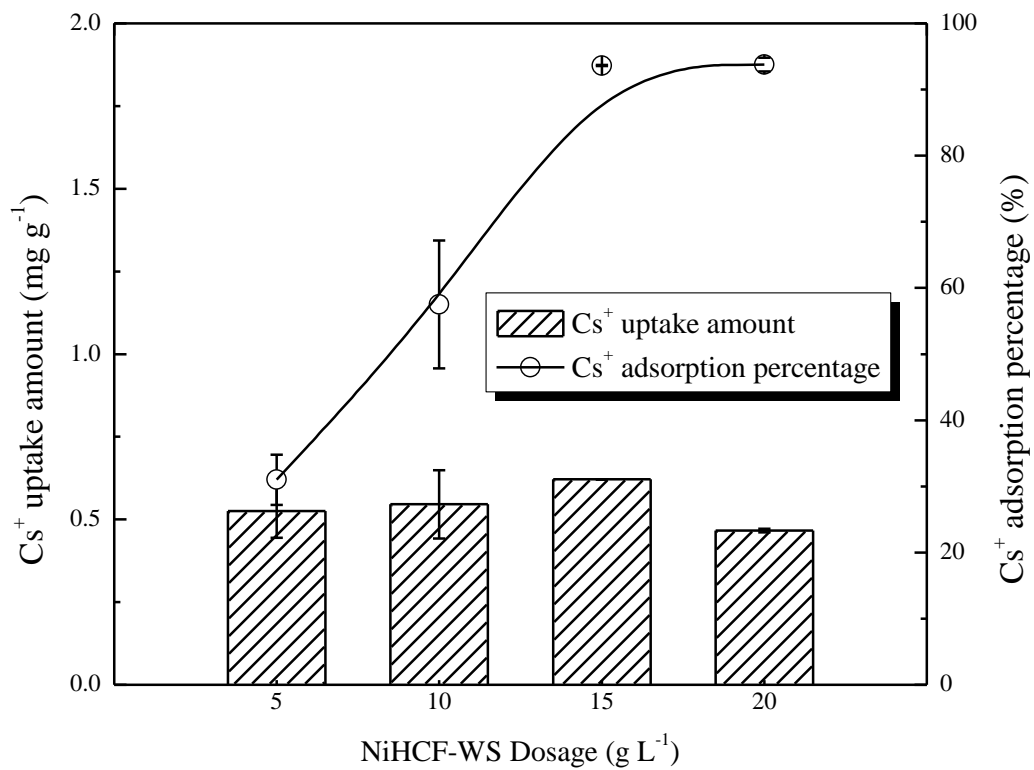
Fig.2-5 Effect of sorbent dosage on the cesium (C_0=10 mg L^{-1}; V=20 mL) adsorption by NiHCF-WS

with shaking (200 rpm) time of 24 h at 25°C.
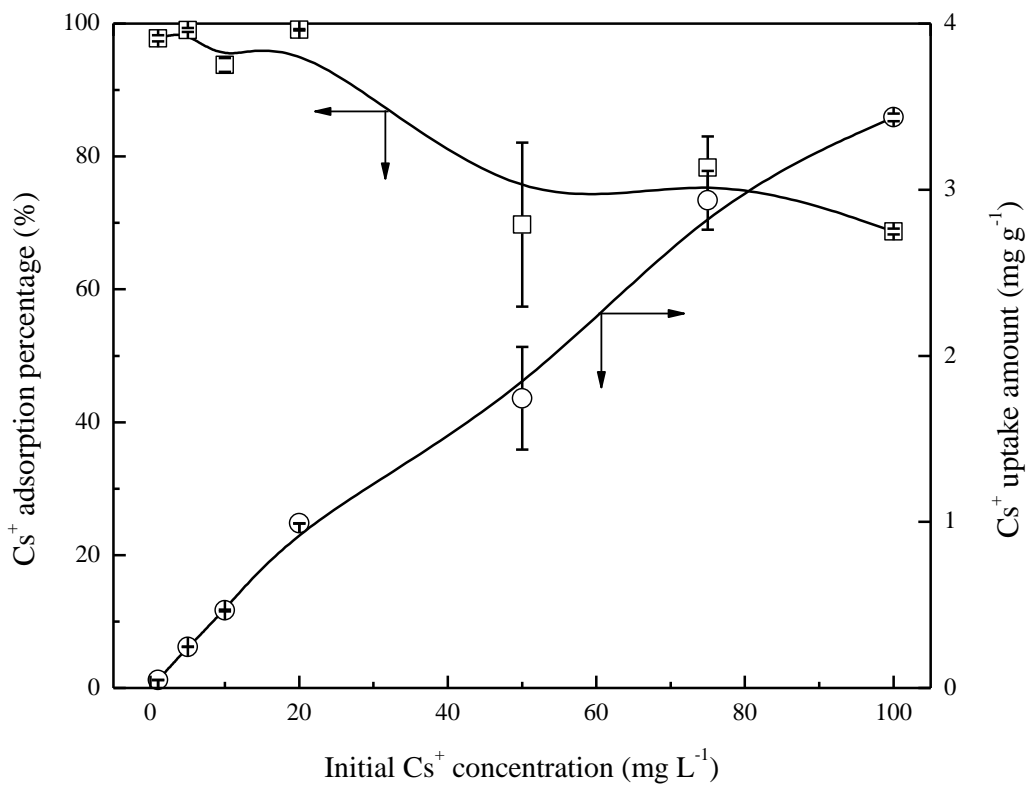
Fig.2-6 Effect of initial concentration on the cesium adsorption on NiHCF-WS (20 g L^{-1}) with the

shaking (200 rpm) time of 24 h at 25°C.
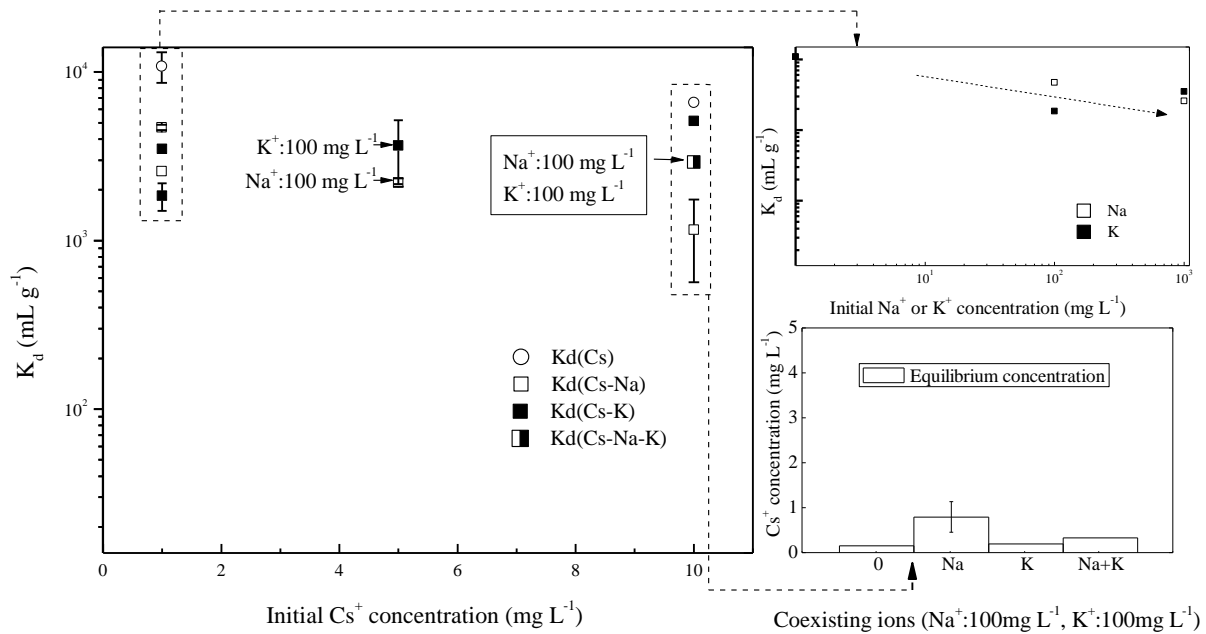
Fig.2-7 Selectivity for cesium sorption by NiHCF-WS with shaking (200 rpm) time of 24 h at 25°C.

(When the initial Cs$^+$ concentration was 1 mg L^{-1}, the sorbent dosage was 5 g L^{-1}; when 5 mg L^{-1} and

10 mg L^{-1}, the dosage was 10 g L^{-1})
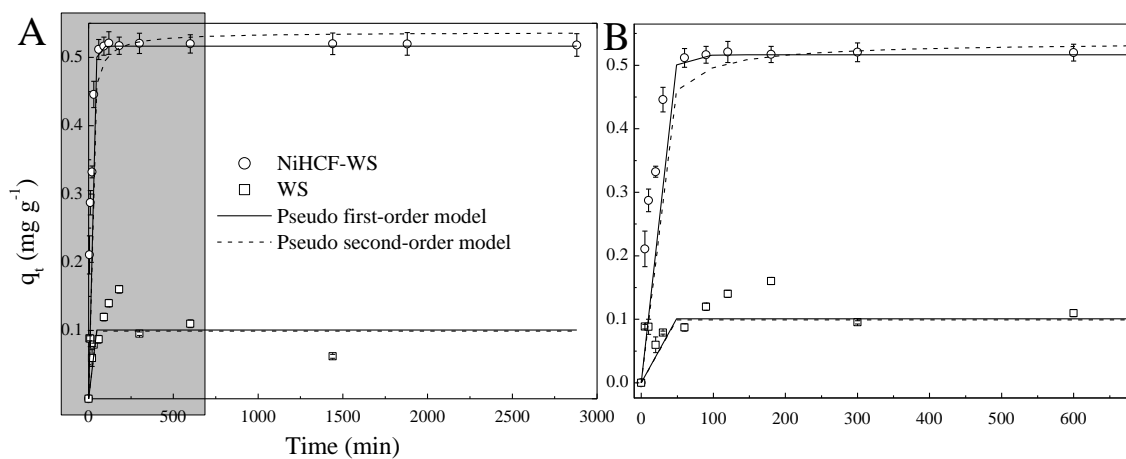
Fig.2-8 Application of non-linearized pseudo first (solid line) and second (dash line) order kinetic

models for cesium (10 mg L^{-1}) adsorption by walnut shell (square) and nickel hexacyanoferrate

incorporated walnut shell (circle) at 25°C (20 g L^{-1}). (B shows the enlarged dark part in A)
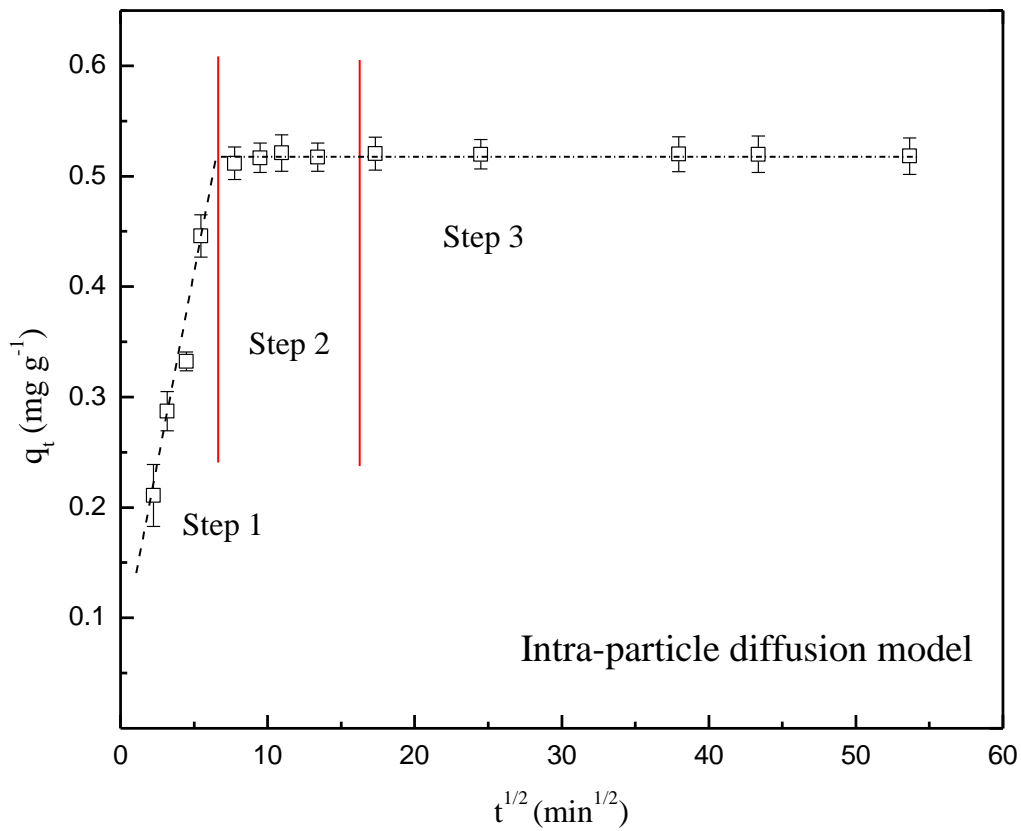
Fig.2-9 Intra-particle diffusion model of cesium (10 mg L^{-1}) adsorption by nickel hexacyanoferrate

incorporated walnut shell (20 g L^{-1}) at 25°C. (Symbols represent the experimental data.)
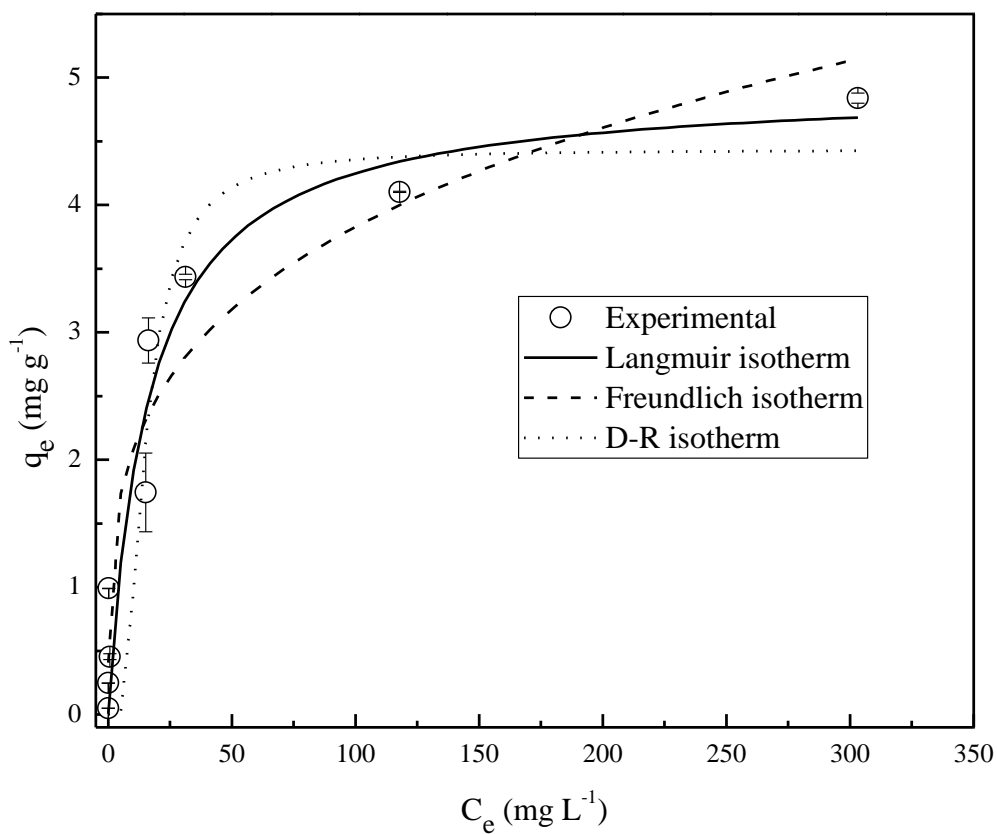
Fig.2-10 Nonlinear Langmuir (solid line), Freundlich (dash line) and D-R (dot line) isotherms of cesium adsorption on nickel hexacyanoferrate incorporated walnut shell at 25°C. (Symbols represent the experimental data, whereas the lines represent the simulated data fitted using the adsorption isotherms.)
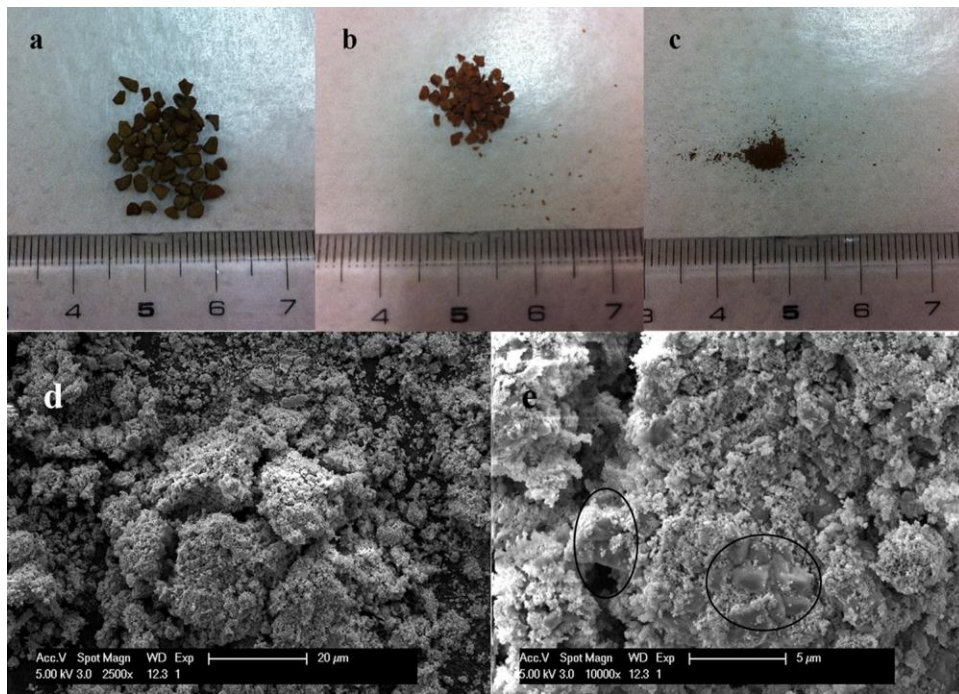
Fig.2-11 Photographs of Cs-NiHCF-WS before (a) and after (b and c) incineration process (500°C for

2 h) and surface morphology images of incinerated Cs-NiHCF-WS (d and e). (b is the particulate

form of incinerated Cs-NiHCF-WS, c is the powder form of incinerated Cs-NiHCF-WS, d is the

SEM image with 2,500 $\times$ magnification and e is the SEM image with 10,000 $\times$ magnification)

Chapter 3 Removal of cesium from aqueous solution using modified Akadama clay

3.1 Introduction

As a new clean energy, nuclear power has drawn much attention throughout the world, especially since the application of nuclear enrichment technology. However, during the operation of nuclear power stations, some radioactive nuclides are released into the surrounding environment (air, water and soil) which inevitably, are a potential danger to human health. The most abundant and important radioactive waste, namely low-level liquid radioactive waste (LLRW), comes from the operation, repair and disposal of facilities in nuclear power stations. Moreover, cost-effective volume reduction of LLRW has become of great concern in recent decades [47].

Among various radioactive nuclides, 137-cesium (^{137}Cs) is considered to be the most hazardous because of its large quantity and relatively long half-life (approximately 30.5 years) [51]. Accordingly, extensive research has been carried out with respect to the adsorption of cesium on various materials [7, 8, 11, 15, 16, 22, 23, 53, 58]. Among these developed materials, most attention has been paid to clay materials because of their structural and economic advantages, such as large quantity, low cost, physical stability and high adsorption capacity [11, 15, 16]. As for most clay materials, the main mechanism occurring in the adsorption process is known as ion exchange. According to the special cubic structure and driving force caused by concentration gradients, ion exchange can be accomplished by releasing metal ions existing in clay materials into solutions (such as Na^+, K^+, Ca^{2+} and etc.) and adsorbing cesium ions simultaneously. Though the adsorption capacity is high, the disadvantage is low/no selectivity for ion exchange during the adsorption process. This means, not only the target metal ion but also other metal ions can be exchanged during the process,

which undoubtedly leads to a waste of adsorption capacity, especially under high ionic strength conditions such as sea water. For clay materials, it is comparatively much more difficult to improve the selectivity of the ion exchange process than it is to increase adsorption capacity due to their complex compositions. As a result, much more attention from researchers has been paid to the improvement of adsorption capacity of clay material [11, 17].

Transition metals are known to undergo complexation with compounds containing aromatic groups based on an electron donation and back donation process [18]. In addition, modification with transition metals could result in a pillared material with microporosity and mesoporosity in layered crystalline inorganic compounds [19]. ZSM-5 zeolite [20] and kaolin [21] has been successfully modified with transition metal in previous studies. Still, it is unknown whether transition metals could be modified into other kinds of clay materials and whether the modification is positive for increasing adsorption capacity or not.

On the other hand, it is necessary to find alternative ways to resolve environmental pollution, especially for resources limited countries like Japan. Through our laboratory's efforts, akadama clay (AC), a common and inexpensive andic soil in Japan has been utilized in lab-scale experiments, demonstrating its use as a potential adsorbent material for hazardous pollutants (like arsenate) [59, 60] and odorous compounds (like geosimin [61] and 2-methylisoborneol [62]). Up to now, however, little information could be found on cesium adsorption by AC. The aim of this work is to develop an efficient adsorption material for cesium removal from AC through transition metal modification. The adsorption kinetics and capacity of pristine and modified AC were determined in relation to the effect of factors such as contact time, initial pH of the solution, adsorbent dosage, initial concentration and the presence of competitive cations. In addition, in order to evaluate the feasibility of the modified AC in practice, fresh lake water was chosen as the background water in this study due to its

importance in natural waterbodies in Japan and the probable contamination of many lakes and pools resulting from the Fukushima nuclear accident [63].

3.2 Materials and methods

3.2.1 Materials

Akadama clay used in this study was provided by Makino Store, Kiyosu, Japan. pH_{pzc} and electrical conductivity of akadama clay were 6.9 and 0.052 mS cm^{-1}, respectively. The akadama clay was ground and sieved through a No. 150 mesh. Particles with a diameter below 105 µm were dried in an oven (EYELA WFO-700, Japan) at 105°C and further used for modification. Synthetic zeolite A-4 and bentonite powder were purchased from Wako Pure Chemical Industries Ltd., Japan.

The chemicals, nickel chloride (NiCl$_2$•6H$_2$O) and sodium hydroxide (NaOH), were of A.R. grade and purchased from Wako Pure Chemical Industries Ltd., Japan. Non-radioactive cesium chloride (CsCl) purchased from Tokyo Chemical Industry Co. Ltd., Japan was used as a surrogate for ^{137}Cs as it has the same chemical characteristics. All the other reagents used in this study were purchased from Wako Pure Chemical Industries Ltd., Japan and used without any purification. Deionized water (DW) generated from a Millipore Elix 3 water purification system (Millipore, USA) equipped with a Progard 2 pre-treatment pack was used throughout this study.

3.2.2 Modification process

Briefly, the modification process included overall two steps. Firstly, 10 g of dried akadama clay was added to a mixed solution (100 mL 0.5 M NiCl$_2$ solution with 100 mL 1 M NaOH solution) with a ratio of 5 mmol Ni per gram of clay and left to react for 1 h during vigorous stirring at 70°C in a thermostated shaking machine (IKA RET basic, Germany). Once the first step was completed, the

precipitate was repeatedly washed, centrifuged and finally dried at 105°C. During the second step, the dried precipitate was ground into powder form and heated in air at 600°C for 1 h using a muffle furnace (TGK F-1404, Japan) in order to create a rigid, non-swelling, three dimensional zeolite-like structure [64]. Finally, the resultant modified AC was stored in an oven at 105°C prior to the Cs$^+$ removal experiments.

3.2.3 Cs$^+$ removal studies

For the Cs$^+$ removal experiments in DW, a stock Cs$^+$ solution (~1000 mg L^{-1}) was prepared by dissolving 1.26 g CsCl accurately into 1 L DW. Cs$^+$ solutions of desired concentrations were prepared by diluting known volumes of the standard Cs$^+$ stock solution in DW. The solution pH was adjusted by 0.1 M HCl and NaOH solutions and measured by a pH meter (Mettler Toledo SG8, Switzerland). To determine contact time and kinetic properties, 1 g of pristine and modified AC were mixed with 200 mL 10 mg L^{-1} Cs$^+$ solution in 250 mL-glass flasks, and the flasks were shaken by a double shaker (TAITEC NR-30, Japan). Supernatants (about 1 mL for each) were retrieved at predetermined time intervals along with the initial solution (zero min point). In order to ensure reliability and improve accuracy of the kinetic data in this study, the kinetic studies were carried out in duplicate and the results reported in this paper are average values with standard deviations. For the other experiments, clay sample was added to 20 mL Cs$^+$ solution in a 50 mL-polypropylene tube and placed in a double shaker for 2 h till equilibrium was reached. The contact time of 2 h is much longer than the equilibrium times determined from typical kinetic experiments. In order to compare the adsorption capacities of modified AC, zeolite and bentonite, namely commercial synthetic zeolite A-4 and bentonite powder were also utilized for Cs$^+$ adsorption isotherm experiments. During the competitive ion experiments, two competitive ions (Na$^+$ and K$^+$) and three ratio levels of Na$^+$/ K$^+$: Cs$^+$ (10, 100 and 1000) with a constant Cs$^+$ concentration (1 mg L^{-1}) were utilized in this study.

For Cs$^+$ removal experiments in lake water, considering the extremely low concentration of Cs$^+$ in surface water (less than 1 ppb even in the case of a nuclear accident) [11] and the detection limit of ICP-MS, two low initial Cs$^+$ concentrations were used in this experiment, which were 10 and 100 μg L^{-1}, respectively. The experimental conditions were similar to those in the DW tests with the pH unadjusted. Lake water used in this study was collected from Matsumi lake (36 ˚30 ´´N, 140 ˚15 ´´ E) located in the University of Tsukuba, Japan, which mainly receives stormwater. The lake water was filtrated with a glass microfiber (Whatman, England) prior to the experiments. The naturally existing metal ions in the lake water were determined by ICP-MS and are given in Table 3-1.

The whole study was conducted at room temperature (25 ±1°C) with a shaking speed of 200 rpm to obtain vigorous contact between solution and solid adsorbent. All of the solution samples were collected by filtering supernatants with 0.22 μm mixed cellulose ester membrane (Millipore, Ireland), diluted with DW to a proper extent (less than 1 mg L^{-1}) into 15 mL-polypropylene tubes and finally stored at 4°C in a refrigerator prior to concentration determination. Along with the removal studies, blank control tests were also carried out to observe any precipitation and to determine the extent of adsorption on the wall of tubes, and the negligible differences between the initial and final concentrations indicated no precipitation or adsorption on wall of tubes in this study.

3.2.4 Desorption tests

In order to evaluate the recycle performance and adsorption stability of modified AC, desorption tests were carried out using three kinds of desorption solutions: 0.1 M HCl (acidic solution), 0.1 M KCl (high strength ion exchange solution) and synthetic groundwater (GW). The chemical compositions of synthetic groundwater were listed in Table 2-1. The former two solutions were used to evaluate recycling capability and the last one was to investigate the adsorption stability when the

final disposal of spent adsorbents was supposed to utilize deep landfill. DW was adopted in this study as the reference. 0.2 g of modified AC was firstly contacted with 40 mL 10 mg L^{-1} Cs^+ solution for 1 d under vigorous shaking and separated by centrifugation. The resultant Cs^+ adsorbed clay sample was then resuspended into a 50 mL desorption solution with no shaking. The supernatant was collected at predetermined time intervals, filtered and analyzed in a similar way as described previously. The quantity of Cs^+ desorbed was determined by the amount of Cs^+ in solution after the desorption experiment. All the experiments were conducted at room temperature $(25\pm1^{o}C)$ and without pH adjustment.

3.2.5 Analysis and characterization

(1) Elemental analysis

Coarse elemental analysis is performed with an energy dispersive X-ray spectroscopy (EDS) equipped on a JSM 7000F field emission scanning electron microscope (FE-SEM) operated at an acceleration voltage of 20.0 kV. In addition, elemental mapping technology was applied to determine the distribution of elements on the surface of samples.

(2) Scanning electron microscope (SEM)

The surface morphology of the pristine and modified akadama clay was observed by a JSM 6330F SEM. The samples were put onto a conductive carbon tape above the metal stub and coated with a thin layer of platinum for charge dissipation during SEM imaging. Acceleration voltage of 5.0 kV and magnification of 5000 $\times$ were applied.

(3) Powder X-ray diffraction (XRD)

The XRD patterns were recorded on a computer controlled Rigaku X-ray diffractometer with CuKα radiation source (λ=1.540562 Å) at operation conditions of 40 kV and 150 mA. A step of

$0.02°$ and a scan speed of $10 °\ min^{-1}$ were selected.

(4) Fourier transform infrared spectroscopy (FT-IR)

Fourier transform infrared spectroscopy was recorded in the region of 4000-400 cm^{-1} by a JASCO 300E FT-IR spectrophotometer (JASCO, Japan) using KBr pellet at a resolution of 4 cm^{-1}.

(5) Surface area and pore size distribution

The specific surface area and pore size distributions were measured by N_2 adsorption-desorption isotherms at $-196°C$ (77 K) after out-gassing the powder clay samples for 90 min at $120°C$ with a Coulter SA3100 specific surface area analysis device. The Brunauer–Emmett–Teller (BET) equation was used for the determination of the specific surface area (S_{BET}) while the Kelvin equation was used to determine the Barrett-Joyner-Halenda (BJH) pore size distribution and pore volume. The total pore volume (V_t) was calculated from the volume adsorbed at $Ps/Po=0.98$ in the desorption branch of the isotherm and the micropore volume (V_{mic}) was calculated by means of the t-plot method.

(6) Thermogravimetric-differential thermal analysis (TG-DTA)

Simultaneous thermogravimetric and differential thermal analysis of pristine and modified akadama clay was carried out using an Exstar TG/DTA 7300 thermal analyzer (Japan). About 7 mg of each sample was placed into a Pt pan and heated up to $1000°C$ in air (carrier gas, 200 mL min^{-1}) atmosphere at a rate of $20°C\ min^{-1}$ for thermal analysis.

(7) Cation exchange capacity (CEC) determination

The CEC of pristine and modified akadama clay was determined according to the sodium acetate method (EPA method 9081, USA).

(8) Surface charge (SC) determination

The SC of pristine and modified akadama clay was determined according to the colloid titration

technique described by Kawamura and Tanaka [65]. Polybren and potassium polyvinyl sulfate (PVSK) were used as the standard cationic and anionic colloids [66]. A known weight (0.05 g) of the sample was suspended in DW (20 mL) and mixed with excess 0.001 M Polybren then titrated against 0.001 M PVSK until electrical neutrality was reached. Equal volumes of Polybren in distilled water were used as blanks. The colloid charge expressed as milliequivalents per gram of positive or negative colloid charge can then be determined from the expression given below.

$$SC \text{ (meq/g)} = \frac{(A - B) \times N}{M} \qquad (3\text{-}1)$$

where A (mL) and B (mL) represents the volumes of PVSK added to the sample and blank respectively, N represents the normality of PVSK (0.001 M), M (g) represents the mass of sample used.

(9) Zeta potential determination

Samples for zeta potential determination were prepared by suspending 0.01 g of clay in 40 mL of DW containing 1.0 mM $NaNO_3$. The suspensions were shaken at a speed of 200 rpm for 2 h to be dispersed completely. Suspension pH was adjusted to 2.0-12.0 using 0.1 M HNO_3 or NaOH solutions. After equilibrating for 24 h, the zeta potential was measured using a Malvern zetasizer (Malvern, England).

(10) Inductively coupled plasma mass spectrometer (ICP-MS)

The concentration of metal ions was analyzed by using a fully quantitative analytical method on an ICP-MS (Perkin Elmer Elan DRC-e, USA) in standard mode throughout this study. ICP-MS tuning solution (1 ppb) was used as the calibration solution to monitor the quality of the ICP. Each sample was set to be analyzed 5 times with average being used. The relative standard deviation of multiple measurements was less than 2% and in most cases, less than 1.5%.

3.2.6 Experimental calculation

Two main factors should be taken into account to evaluate the efficiency of an adsorbent: (*i*) the maximum adsorption capacity, Q_{max} (mg g^{-1}), which indicates the efficiency of the material to uptake target ions at (or near) saturation. It can be estimated from the adsorption isotherm's plateau; (*ii*) distribution coefficient, K_d (mL g^{-1}), evaluates the selectivity of the adsorbent to extract the target ions at very low concentrations in the presence of other competitive ions such as Na$^+$ and K$^+$ at high concentrations [7]. Therefore, the Cs$^+$ removal results were given as both adsorption amount (*q*) and distribution coefficient (K_d) in this study, where the adsorption amount could reflect the adsorption capacity in most cases.

3.3 Results and discussion

3.3.1 Characterization of pristine and modified AC samples

For the coarse chemical compositions of clay samples, duplicate tests were conducted and the average was finally taken. As shown in Table 3-2, the atom percentage of nickel was greatly increased after modification, indicating the successful modification process. Almost all of other elements were decreased due to the introduction of nickel other than sodium.

In order to observe the change of surface morphology after the modification process, the SEM images of pristine and modified AC samples were obtained and presented in Fig. 3-1A and B.

SEM images showed that obvious crystals were developed after modification, which was believed as nickel oxide. In addition, the EDS elemental analysis demonstrated that nickel has been introduced into clay samples successfully and accordingly, the content of silicon decreases significantly. Perhaps due to the dose of NiCl$_2$ during the modification, the peak of chlorine appeared in Fig.3-1E.

TG/DTA curves indicated that the modified AC samples had a better thermal stability compared with pristine ones. There was only 5% of weight lost until the temperature increased to 700°C. The first sharp weight loss at around 100°C in pristine AC samples was probably attributed to the evaporation of water content.

According to the XRD patterns, obvious peaks of quartz (JCPDS 65-0466) were detected in all the three samples, indicating the main composition of pristine AC is quartz. And nickel oxide (JCPDS 44-1159), sodium hydride (JCPDS 65-9247) and iron silicon (JCPDS 65-0994) were clearly detected in the modified AC (before adsorption, red pattern in Fig.3-2A). Also, after the adsorption of cesium, peaks of nickel oxide were still detected in the sample, whereas those of sodium hydride and iron silicon disappeared.

Similar absorption peaks were detected in the FTIR spectrums of both pristine and modified AC samples. As shown in Fig.3-2B, the broad absorption peaks observed at the range of 3300-3600 cm^{-1} are assigned to the stretching vibration of hydroxyl groups. The broad band is indicative of hydroxyl group stretching vibrations when the hydroxyl group is hydrogen bonded [67]. Those at 1570-1655 cm^{-1} are the C=O stretching mode of the functional groups on the surface of the clay samples [68]. Band at 462 cm^{-1} is assigned to a T–O bending mode (where T = Si or Al). The intensity of this band is independent on the degree of crystallinity [69]. It could be seen that the peak at 462 cm^{-1} is much more intensified after modification, indicating the degree of crystallinity in AC increased after the modification process. This result was in well agreement with the SEM results, where well grown crystals were observed.

Generally speaking, a higher S_{BET} would lead to a better contact between adsorbent and solution resulting in a higher adsorption capacity. However, the S_{BET} was decreased from 174.3 to 64.3 $m^2\,g^{-1}$ after modification in this study, probably due to the accumulation of clay particles and introduction

of transition metal oxides during the calcination. As described in the SEM images, the well grown crystals through modification process may be another explanation to the decreased surface area. In addition to the SSA, some more details about PSD could also give further knowledge on the structural changes.

According to the definitions of international union of pure and applied chemistry (IUPAC) [70], as shown in Fig.3-3 and Table 3-3, both macropores (diameter of larger than 50 nm) and mesopores (diameter of between 2 and 50 nm) were presented in the pristine and modified AC. And there was no micropore (with diameter < 2 nm) in either of them according to the V_{mic} of 0 (data not shown). In addition, an evident phenomenon was found that the PSD in the two samples were greatly different. As shown in Fig.3-3, the majority of pore volume (above 50% of total pore volume) is contributed by pores with diameter > 20 nm in the pristine AC, whereas < 8 nm in the modified AC. When further compared the PSD results, significant difference in pore volume could be found between the pores with diameter > 20 nm and < 12 nm. In the pristine AC, approximately 31.8% of total pore volume was contributed by pores with diameter of 20~80 nm and 22.4% by pores with diameter > 80 nm, indicating meso/macro pores with diameter > 20 nm played an important role. On the other hand, approximately 33.5% and 23.6% of total pore volume were contributed by pores with diameter < smaller than 6 nm and 6~8 nm in the modified AC, respectively. Taking into account of the above discussion, it can be concluded that the macropores and mesopores with diameter > 20 nm in the pristine AC were transformed into mesopores with diameter < 12 nm to a great extent through the modification process. Based on the fact that most pores (above 95% of the total pore volume) are mesopores, the modified AC can be defined as a typical mesoporous material. According to the previous studies, mesoporous materials should have better pollutants removal performance than macro-mesoporous materials due to their smaller pore size [71-73].

3.3.2 Cs$^+$ removal experiments in DW

(1) Effect of contact time and kinetic study

As an important characteristic of adsorbent material, adsorption rate could be a crucial factor that limits the application of a new adsorbent material. The most direct mean to evaluate the adsorption rate of an adsorbent material is to determine the equilibrium time of adsorption process. Generally speaking, different adsorbent materials have their own equilibrium times for adsorption process due to their different physical and chemical characteristics, such as adsorption mechanism, pore size and etc. Besides, the equilibrium time may also have some relationship with the adsorbent dosage and initial Cs$^+$ concentration. As reported in previous studies, around 10 d is needed for Cs$^+$ adsorption (0.114-23.9 mg L^{-1}) by ceiling tiles (about 8 g L^{-1}) to attain the adsorption equilibrium [51], 8 h for crushed granite (initial Cs$^+$ concentration of 1×10^{-3}-1×10^{-7} M and dosage of approximately 33.3 g L^{-1}) [37], 6 h for zeolite (initial Cs$^+$ concentration of 2.280×10^4 Bq L^{-1} and dosage of 10 g L^{-1}) [15], 280 min for copper hexacyanoferrate polyacrylonitrile (CHCF-PAN, initial Cs$^+$ concentration of 10^{-4} M and dosage of 10 g L^{-1}) [4], 30 min for coir pith (initial Cs$^+$ concentration of 200 mg L^{-1} and dosage of 2 g L^{-1}) [22], 30 min for aluminum-pillared montmorillonite (initial Cs$^+$ concentration of 1 mM and dosage of 0.5 g L^{-1}) [11] and synthesized A-X zeolite (initial Cs$^+$ concentration of 50 mg L^{-1} and dosage of 1 g L^{-1}) [16]. Consequently, in order to evaluate the equilibrium time of the adsorption of Cs$^+$ on the clay samples, 1 g of each adsorbent was added into 200 mL Cs$^+$ solution (dosage of 5 g L^{-1}) with the initial concentration of 10 mg L^{-1} and water samples were collected at determined time intervals. Relatively long adsorption duration (2 d) and time intervals (1 h at least) were applied during the preliminary experiment (data not shown). Depending on the preliminary results, much more detailed investigations with the time intervals of 0 (initial solution), 5, 10, 20, 30, 60, 90, 120, 210, 300 min and 24 h were carried out for the pristine AC and 0 (initial solution), 5, 10, 20, 30, 60,

90, 120 and 180 min for the modified AC samples, respectively. The variation of C_t/C_0 as a function of time for the adsorption of Cs^+ on the clay samples were depicted in Fig.3-4.

It was clearly indicated that both clay samples exhibited rapid adsorption of Cs^+ with an equilibrium time of approximately 10 min, which was superior compared with previous adsorbents [4, 11, 15, 37, 51]. This might be a great advantage for AC in its future application in real pollution remediation because a more rapid process means a much smaller volume of reactor thus large decrease in investment. In order to observe the initial period of adsorption process more clearly, the experimental data of the first 1.5 h were enlarged. From the detailed figure, it could be seen that compared with the pristine AC samples, the modified ones had a much higher removal efficiency (approximately twice) and a shorter equilibrium time, demonstrating that the modification process improved the Cs^+ removal behavior of clay samples. According to the results, the contact time was determined as 2 h conservatively for the following experiments.

Kinetic study is one of the most important means for investigating adsorption process, through which the rate constants could be obtained. Pseudo first and second order kinetic models could generally simulate the most physical and chemical adsorption processes [11, 16, 22, 23, 26, 49, 51, 74, 75] and therefore were selected to fit the experimental results in this study. Fig.3-5 showed the comparison of pseudo first and second order kinetic models for the fitting of Cs^+ adsorption on pristine and modified AC samples. Besides, Table 3-4 listed the adsorption rate constants associated with pseudo first and second order kinetic model in this study. It could be seen that both pseudo first and second order kinetic models fitted very well with the experimental results, especially the second order model for the modified AC ($R^2 = 1$).

(2) Effect of solution pH value

It could be seen that both pristine and modified AC samples had a similar tendency that alkaline

rather than acidic condition was favorable for Cs^+ adsorption. The Cs^+ removal efficiency on pristine AC followed an order of acidic<neutral<alkaline, whereas the order was acidic<neutral≈alkaline for modified AC. When pH value < 5, significant decreases in Cs^+ removal efficiency were observed for both clay samples. This phenomenon had been reported previously during the Cs^+ adsorption on other clay materials [11, 16, 56, 76-78], probably attributable to the competition behavior between H_3O^+ and Cs^+ during the adsorption process under acidic condition. On the other hand, the negative charge on the surface of clay samples was preferentially compensated by H_3O^+ ions. The detailed competition process was noted by Avena et al. [79] who interpreted the process as $SO^- + H^+ \rightarrow SOH$ and $SOH + H^+ \rightarrow SOH^{+2}$ where S stands for any surface site. While when pH value > 5, even at extremely alkaline condition (pH approximately 12), no significant decrease in Cs^+ removal efficiency was observed, possibly due to the decrease of the competition of hydronium ions for modified AC's sites under alkaline condition [11]. In addition, it can also be found that the removal efficiency of pristine AC could be approximately 90% when pH > 11, similar with that of modified AC when pH = 8-12, indicating the potential feasibility of pristine AC in extremely alkaline conditions.

Compared with Cs^+ removal efficiency and adsorption amount, distribution coefficient could display their difference much more remarkably (Fig.3-6B). The variation of distribution coefficient as a function of pH value (Fig.3-6B) indicates that the best adsorption performance was obtained at pH about 10. Overall, it can be concluded that the applicable pH range for Cs^+ removal (>90%) was extended from extremely alkaline condition (>11) to neutral condition (≥ 5) after modification.

(3) Effect of adsorbent dosage

From the results of Section 3.3.2(1), it could be concluded that 5 g L^{-1} of the adsorbent dosage was not enough for effectively removing Cs^+ from solution under initial Cs^+ concentration of 10 mg

L^{-1}. Therefore, four adsorbent dosages, *i.e.* 2.5, 5, 7.5 and 10 g L^{-1} were adopted to the following adsorption experiments under initial Cs$^+$ concentration of 1 and 10 mg L^{-1}, respectively in order to evaluate the effect of adsorbent dosage on the Cs$^+$ adsorption on modified AC.

It can be seen from Fig.3-7 that, under relatively higher Cs$^+$ concentration (10 mg L^{-1}), the Cs$^+$ removal efficiency increased with the increase of adsorbent dosage. This observation was in good agreement with the previous study [78], indicating that the more adsorption sites available, the better Cs$^+$ adsorption can be achieved. However, the Cs$^+$ adsorption amount had a symmetrical variation, which can be explained as the increase rate of (C_0-C_t) was lower than adsorbent dosage. The phenomenon implied that larger adsorbent dosage favored the increase of adsorption efficiency while lowered the adsorbent utilization rate.

(4) Effect of initial concentration

Fig.3-8 showed that the Cs$^+$ adsorption amount increased with the initial Cs$^+$ concentration, whereas the removal efficiency did not. This might be due to the fact that after all the higher energy sites being occupied, excess Cs$^+$ would then be adsorbed on the lower energy sites, resulting in loose binding of Cs$^+$ and the decrease of removal efficiency [80]. The modified AC had a much higher Cs$^+$ adsorption amount than pristine ones, which became much remarkable with the increase of initial Cs$^+$ concentration.

(5) Effect of competitive ions

According to previous studies [7], it was well believed that the abundant metal ions in natural waters (sea, surface and ground waters) such as Na$^+$ and K$^+$ had great negative effects on adsorption of target species through competing for the binding sites [43], especially for Cs$^+$, which was much less than Na$^+$ or K$^+$ even in the radioactive contaminated wastewater. Table 3-5 showed the effect of Na$^+$ and K$^+$ on the removal efficiency and distribution coefficient of Cs$^+$ adsorption on pristine and

modified AC. It was found that the removal efficiency and distribution coefficient was highly affected (negative) by K^+ rather than Na^+ no matter for the pristine or modified AC, similar with the observations by Borai et al. [15, 53]. This could be attributed to the closer similarity in Pauling's ionic radii between Cs^+ (1.69 Å) and K^+ (1.33 Å) rather than Cs^+ and Na^+ (0.95 Å). This phenomenon also indicated that Cs^+ adsorption was the result of ion exchange reaction, in which cations, with similar radius and hydration energy, could compete more effectively against Cs^+ on the mineral surface [53, 81]. In addition, it can be seen that the distribution coefficient of modified AC was much higher than that of pristine AC when no competitive ions existed in the solution, indicating a better adsorption behavior after modification. However, the difference became insignificant when large amount of competitive ions were existed in the solution, especially K^+. This observation could be attributed to that the concentration of K^+ was much higher than the adsorption capacity of AC in the experiment. Detailed mechanism is still under investigation.

3.3.3 Adsorption isotherms

All the non-linear fittings and the statistical analysis were performed with Origin 7.5 software. The estimated model parameters with the R^2 and χ^2/DoF for the different isotherms are calculated by the software and given in Table 3-6. Basing on the physical meanings of these two parameters, a higher R^2 and lower χ^2/DoF values usually mean a better isotherm fit. It is shown that the experimental data of Cs^+ adsorption on modified akadama clay could be well fitted by these isotherms except Temkin isotherm, which provides the lowest R^2 and highest χ^2/DoF values. According to the assumption of Temkin isotherm, it is therefore deduced that the heat of adsorption of all the molecules in the layer did not decrease linearly with coverage. As shown in Fig.3-9, the isotherm curves of Langmuir, Redlich-Peterson and Langmuir-Freundlich almost coincide with each other. As a matter of fact, the three-parameter isotherms provided better fitting in terms of R^2 and

χ^2/DoF values than most of the two-parameter isotherms (except Langmuir isotherm), which agreed well with the conclusion from other study [82]. Among all the isotherms, Langmuir isotherm gave the highest R^2 and lowest χ^2/DoF values, meaning the adsorption of Cs$^+$ on modified akadama clay is probably a monolayer adsorption process.

Although the fits of adsorption data to these adsorption isotherms are more mathematically meaningful and don't reflect the actual adsorption process, some of the isotherm parameters could be helpful to determine the adsorption mechanism. The essential characteristic of the Langmuir isotherm may be expressed in terms of a dimensionless equilibrium parameter R_L, which is defined as [83]:

$$R_L = \frac{1}{1 + K_L C_0} \qquad (3\text{-}2)$$

where K_L is the Langmuir constant and C_0 is the initial solute concentration (initial Cs$^+$ concentration in this study). For the value of K_L in this study is 0.07, which is a positive value, the calculated R_L must be located between 0 and 1. Similarly, when using the constant of Langmuir-Freundlich isotherm, the expression for $R_{L\text{-}F}$ can be modified as [82]:

$$R_{L-F} = \frac{1}{1 + bC_0^{1/n}} \qquad (3\text{-}3)$$

where b and n are the Langmuir-Freundlich constants, and C_0 is the initial solute concentration. Given the fact that b is a positive value (0.08), the $R_{L\text{-}F}$ must be located between 0 and 1. In any case, the values of R_L and $R_{L\text{-}F}$ in this study fall between 0 and 1, indicating a favorable adsorption of Cs$^+$ on modified akadama clay. As another important parameter, Q_L or q_m in Langmuir or Langmuir-Freundlich isotherm, representing the maximum adsorption capacity of Cs$^+$ on modified akadama clay, were 16.1±0.85 and 16.6±2.5 mg g^{-1}, respectively. It is worth noting that the maximum adsorption capacity of clay material prepared in this study is comparatively lower than the other well-known clay materials such as zeolite [15] and montmorillonite [11], whose adsorption

capacities are approximately 100 mg g^{-1}. However, it is relatively higher than those of natural soils and rocks such as ceiling tiles (0.21 mg g^{-1}) [51], bure mudrock (13.3 mg g^{-1}) [57] and Ain Oussera soil (4.31 mg g^{-1}) [53]. In addition, the clay material used in this study has not been well explored for other applications except horticulture and it is widely distributed in Japan. Compared with zeolite and montmorillonite, it has much more meaning to expand the application of this clay material. Therefore, this study would contribute for its application in environmental remediation. On the other hand, this alternative clay material would also save zeolite and montmorillonite, which have much more other applications such as catalysis and medicine industries.

3.3.4 Desorption studies

It is well believed that the surface charge of clay material is positive at the acidic condition (pH<pH$_{pzc}$). As shown in Fig.3-10, a large portion (approximately 70%) of adsorbed Cs$^+$ was desorbed in 0.1 M HCl (acidic solution), indicating a reversible adsorption of Cs$^+$ on modified akadama clay. This phenomenon might be well explained by the electric repulsion between the positive charge and adsorbed positive charged Cs$^+$ on the surface of modified akadama clay. In addition, this phenomenon seems lead to a conclusion that there is electrostatic adsorption during the Cs$^+$ adsorption on modified akadama clay, which could well explain the relationship between the increase of negative charge (Table 3-3) on the surface of modified akadama clay and adsorption performance. On the other hand, approximately 40% of adsorbed Cs$^+$ was desorbed in the 0.1 M NaOH (alkaline solution), indicating there is other mechanism in the adsorption process of Cs$^+$ on modified akadama clay except the electrostatic adsorption. In addition, a similar phenomenon was also observed between 0.1 M HCl and 0.1 M KCl (Fig.3-10), a strong ion exchange solution, indicating the existence of exchange between Cs$^+$ and K$^+$. This phenomenon might demonstrate the existence of ion exchange during the Cs$^+$ adsorption on modified akadama clay. Finally, as shown in

Fig.3-10, there is almost no Cs^+ desorbed from modified akadama clay in DW, indicating a relatively stability of adsorption. Above all, the desorption results revealed that the adsorption of Cs^+ on modified akadama clay might include electrostatic adsorption and ion exchange process.

3.3.5 Adsorption mechanisms speculation

As a clay material with complex composition, there may be many different kinds of adsorption mechanisms during the Cs^+ adsorption on modified akadama clay. As deduced from the kinetic analysis, there might be both physical and chemical adsorption processes in the Cs^+ adsorption on modified akadama clay. Adsorption isotherm studies gave the conclusion that the adsorption process was probably a monolayer adsorption process and the isotherm parameters indicated a favorable adsorption of Cs^+ on modified akadama clay. Furthermore, desorption study provided a much more detailed description about the adsorption mechanisms, which might include electrostatic adsorption and ion exchange process.

Zeta potential, which is an important indicator for the stability of colloidal dispersions, indicates the potential difference between the dispersion medium and the stationary layer of fluid attached to the dispersed particle. In addition, surface charge is another important parameter for a clay material during the adsorption process. As well known, both of them have much relationship with the electrical characteristics on the surface of clay materials, and therefore, with the electrostatic adsorption. As shown in Fig.3-11, the zeta potential of akadama clay colloid decreased after the modification, which maybe contributed by the grafting of positive Ni^{2+} and loss of some alkali-earth metals. In addition, the change of clay surface properties could also reduce the zeta potential of modified clay. On the other hand, the differences of zeta potential between pristine and modified akadama clay decreased with the increase of pH. The similar phenomenon is observed for the Cs^+

removal efficiency, indicating there is a close relationship between zeta potential and Cs^+ removal efficiency. When the pH value is approximately 11.0, there is no obvious difference between the zeta potentials, and also between the removal efficiencies. Obviously, there is a good correspondence between the variation of zeta potential and Cs^+ adsorption performance, which is opposite. Besides, the adsorption performance is favored at alkaline conditions and suppressed at acidic conditions (Fig.3-11). The explanation for this phenomenon could be related with the surface charge. It is well believed that low pH value (pH<pH_{pzc}) could result in positive surface charge, which is not favorable for the adsorption of positive Cs^+ basing on the electrostatic adsorption theory. Whereas, high pH value (pH>pH_{pzc}) could result in negative surface charge, which benefits the adsorption of Cs^+. As shown in Fig.3-11, there is an obvious decrease of adsorption behavior at the pH < 5, which well agrees with the pH_{pzc} value of modified akadama clay (Table 3-3). As listed in Table 3-3, the surface charge of pristine and modified akadama clay is negative at neutral condition. In addition, the negative charge of akadama clay at neutral condition is greatly enhanced after modification, which well agrees with the decrease of pH_{pzc}. According to the electrostatic adsorption theory, the enhancement of negative charge on the surface of modified akadama clay at neutral condition might be the main reason why the adsorption performance was greatly enhanced. Above all, according to the desorption study and surface charge analysis, it could be deduced that there was a possible electrostatic adsorption during the Cs^+ adsorption on modified akadama clay. Probably due to the enhancement of negative charge on the surface of modified akadama clay, the Cs^+ adsorption performance was greatly enhanced.

As deduced from the desorption study, the ion exchange process might be existed in the Cs^+ adsorption on modified akadama clay. Ion exchange process is a common mechanism in metal ion adsorption process by using clay materials [15, 16, 84]. It was hypothesized that if adsorption is

mainly caused by ion exchange reaction, then the quantity of the released cations (in gram-equivalent) would be close to that of the adsorbed target ions. Unfortunately, the results show that there is not a good relationship between the quantities (in gram-equivalent) of adsorbed Cs^+ and released cations (Table 3-7). However, the increase of the initial concentration enhanced the release of cations, which might indicate that there was but not just ion exchange process during the Cs^+ adsorption on modified akadama clay. It was also observed that large amounts of Na^+ were released into DW without Cs^+ (Table 3-7), probably due to the dissolution of soluble sodium compounds. The similar phenomenon was also reported by Miah et al. [51], who used ceiling tiles as adsorbent for cesium removal. The author found the cations were released into solutions in much greater quantities compared to cesium. As an important indicator for the ion exchange process, CEC values of pristine and modified akadama clay were detected and listed in Table 3-3. The results showed that the CEC value of akadama clay decreased after modification, indicating that the ion exchange process is not the most important mechanism during the Cs^+ adsorption on modified akadama clay. Above all, it is concluded that there is ion exchange during the adsorption process but it is not the most important mechanism.

3.3.6 Cs^+ removal in treating lake water

It could be seen from Table 3-8 that high dosage resulted in high removal efficiency. On the other hand, higher removal efficiency was achieved at lower initial Cs^+ concentration. As in this case, the concentration ratio of competitive ions to Cs^+ was more than 3000, however, a satisfactory removal efficiency (about 85%) was obtained, implying the clay material developed in this study could be used as an efficient adsorption material for Cs^+ removal from natural water.

3.3.7 Comparison with other clay materials

According to the previous studies [7, 11, 15, 22, 43, 53], there are many adsorbent materials applied in Cs^+ adsorption from aqueous solution. In general, they can be divided into three categories based on their compositions, including natural and modified clay materials, synthetic compounds and modified biosorbents. Because of their significantly different physical and chemical characteristics, it is not comparable among the different kinds of adsorbent materials. However, for the same kind of adsorbent material, clay material in this study, it is meaningful to compare their adsorption performance so as to evaluate the potential of application. As described in Section 3.2.3, in order to make the comparison more valuable, commercial synthetic zeolite and bentonite were used to carry out the adsorption capacity determination under the same conditions in this study. The adsorption results of zeolite and bentonite fitted with Langmuir isotherm were listed in Table 3-9.

Distribution coefficient and adsorption capacity are usually used as two important indices when doing this kind of comparison [15]. As shown in Table 3-9, the modified AC developed in this study has a relatively higher K_d value compared with other reported clay minerals, indicating it is a potential efficient adsorbent material for Cs^+ removal. Although a lower adsorption capacity was obtained from the modified AC compared with zeolite or bentonite in this study, its adsorption capacity was relatively higher than other natural soils [53] or rocks [57]. Its applicability in wastewater with low Cs^+ concentration was still promising. In addition, different with zeolite and bentonite, which have been demonstrated as useful materials for many other applications such as catalyst and medicine industries, akadama clay, an andic soil widely distributed in Japan has not been well developed for other applications except as horticultural medium. The enhancement of adsorption capacity towards Cs^+ would be meaningful for exploring its application in environmental pollution

remediation. This work would also be helpful for its further investigation and improvement of its adsorption capacity of radionuclides towards practical application.

3.4 Summary

Novel transition metal modified akadama clay (AC) was prepared for cesium adsorption from aqueous solution. After modification, akadama clay was transferred into a typical mesoporous material and adsorption performance was greatly enhanced. The newly developed material had a much wider applicable pH range (5~12) than the pristine one. Removal efficiency increased with adsorbent dosage, while the uptake amount showed an opposite trend. The maximum adsorption capacity (Q_{max}) reached about 16mg g^{-1} for the modified AC, much higher than the pristine one. The distribution coefficient was strongly affected (negatively) by K^{+} rather than Na^{+} for both pristine and modified AC. Adsorption isotherms indicate the Cs^{+} adsorption on modified akadama clay is a monolayer adsorption process. Multiple adsorption interaction mechanisms including electrostatic adsorption and ion exchange are proved during the Cs^{+} adsorption on modified akadama clay. Modified AC is therefore regarded as a potential efficient adsorbent material for Cs^{+} in the treatment of lake water. Above 80% of adsorbed Cs^{+} could be desorbed in 0.1 M HCl and KCl, while relatively stable in synthetic groundwater. The modified AC developed in this study is more efficient than other natural soils and rocks. This study is meaningful and valuable for exploring the application of akadama clay in environmental remediation.

Table 3-1 Characteristics of lake water.*

Parameter	Value
pH	7.5 ±0
Na^+ (mg L^{-1})	12.6 ±0.7
K^+ (mg L^{-1})	2.8 ±0.3
Ca^{2+} (mg L^{-1})	16.7 ±0.9
Mg^{2+} (mg L^{-1})	4.6 ±0.05
Cs^+ (mg L^{-1})	0

Measurement was conducted in quadruplicates and the mean values ± standard deviations were undertaken.

Table 3-2 The results of coarse EDS element analysis on the surfaces of clay samples.

Element (at%[a])	O	Si	Al	Fe	Mg	K	Ca	Na	Ni
Pristine AC[b]	56.8±10.1	24.5±2.4	13.9±5.4	2.4±1.4	0.69 ±0.05	0.44±0.04	0.17±0.14	0.14±0.03	0.0
Modified AC	55.6±4.6	5.3±3.2	8.1±5.7	1.4±0.6	0.44±0.07	0.11±0.16	0.07±0.08	3.2±2.7	23.9±9.1

[a] means atom percentage.

[b] the pristine AC used for chemical element analysis is obtained after calcination pretreatment (600°C for 1h) and the effect of loss on ignition (LOI) has been neglected.

74

Table 3-3 Material properties of pristine and modified AC.

Samples	S_{BET} (m^2/g)	V_t (mL/g)	V_{mic} (%)	V_{mes} (%)	V_{mac} (%)	CEC (meq/g)	pH$_{pzc}$	SC (meq/g)
Pristine akadama clay	174.3	0.1920	4.08	58.7	37.2	6.97±0.35	6.9[a]	-0.018±0.001[c]
Modified akadama clay	64.3	0.1298	0	96.9	3.1	3.35±0.11	≈5[b]	-0.086±0.002[c]

[a] Data was provide by manufacturer

[b] Estimated from Fig.3-11.

[c] The minus sign means the surface charge is negative and the absolute value represents the amount of negative charge.

Table 3-4 Adsorption rate constants associated with pseudo first and second order kinetic models.

Pseudo first-order kinetic model				Pseudo second-order kinetic model		
	Pristine AC	Modified AC			Pristine AC	Modified AC
q_{eexp} (mg g^{-1})	0.83 ±0.01	1.76±0.007	q_{eexp} (mg g^{-1})		0.85 ±0.02	1.76±0.003
k_1 (h^{-1})	23.2 ±2.6	49.9±2.2	k_2 (g mg^{-1} h^{-1})		95.5 ±43.3	406.9±85.5
q_{ecal} (mg g^{-1})	0.83 ±0.01	1.76±0.002	q_{ecal} (mg g^{-1})		0.82	1.76
R^2	0.994	0.999	R^2		0.987	1.0

Table 3-5 Effect of Na^+ and K^+ on the removal efficiency and distribution coefficient of cesium adsorption on pristine and modified AC. (Initial Cs^+ concentration: 1 mg L^{-1}, dosage: 2.5 g L^{-1})

Na^+ (mg L^{-1})	K^+ (mg L^{-1})	Removal efficiency (%)		K_d (mL g^{-1})	
		Pristine	Modified	Pristine	Modified
0	0	71	90.5	979.3	3810.5
10	0	66.4	87.7	790.5	2852.0
100	0	62.7	78.5	672.4	1460.5
1000	0	37.3	69	237.9	890.3
0	10	44.2	86.5	316.8	2562.9
0	100	16.4	41.7	78.5	286.1
0	1000	21.5	24.6	109.5	130.5
50	50	34.5	67.7	210.7	838.4
500	500	26.1	24.7	141.3	131.2

Table 3-6 Estimated isotherm parameters for cesium adsorption on modified AC.*

Langmuir isotherm	Q_L (mg g^{-1})	K_L (L mg^{-1})		R^2	χ^2/DoF
($q=Q_LK_LC_e/(1+K_LC_e)$	16.1 ±0.85	0.07 ±0.01		0.988	0.336
Freundlich isotherm	K_f(mg g^{-1} L$^{1/n}$ mg$^{-1/n}$)	$1/n$		R^2	χ^2/DoF
($q=K_fC_e^{1/n}$)	2.19 ±0.4	0.45 ±0.05		0.965	1.00
Dubinin-Radushkevich isotherm	Q_m (mg g^{-1})	β (mol^2/J^2 ×10^{-6})	E (kJ mol^{-1})	R^2	χ^2/DoF
($q=Q_m$exp[$-\beta(RT\ln(1+1/C_e))^2$], $E=1/(2\beta)^{1/2}$)	12.04 ±1.04	6.68 ±2.3	0.27	0.901	2.88
Temkin isotherm	a	b		R^2	χ^2/DoF
($q=a+b\ln C_e$)	2.55 ±0.96	2.21 ±0.36		0.862	4.02
Redlich-Peterson isotherm	a	b	n	R^2	χ^2/DoF
($q=aC_e/(1+bC_e^n)$)	1.22 ±0.34	0.09 ±0.08	0.97 ±0.17	0.988	0.400
Langmuir-Freundlich isotherm	q_m (mg g^{-1})	b (L mg^{-1})	n	R^2	χ^2/DoF
($q=q_mbC_e^{1/n}/(1+bC_e^{1/n})$)	16.6 ±2.5	0.08 ±0.02	1.04 ±0.21	0.988	0.399

* Adsorbent dosage: 2.5 g L^{-1}.

Table 3-7 Comparison between amounts of adsorbed cesium and released ions during the

adsorption process of modified AC (5 g L^{-1}).

Background water	Adsorbed (μmol)	Released (μmol)				
	Cs$^+$	Na$^+$	K$^+$	Ca^{2+}	Mg^{2+}	Ni^{2+}
10 mg L^{-1} Cs$^+$ solution	1.4	26.6	0.47	0.16	0.21	0.01
100 mg L^{-1} Cs$^+$ solution	11.4	39.3	2.8	4.8	6.1	0.04
DW	0	34.7	0.55	0.15	0.18	0.01

Table 3-8 Efficiency of modified AC on removing cesium from lake water.

Initial Cs$^+$ concentration (μg L^{-1})	Dosage (g L^{-1})	Removal efficiency (%)
10	1	72.5±1.0
10	2.5	85.9±0.5
100	1	63.3±1.1
100	2.5	84.6±0.1

Table 3-9 Comparison between distribution coefficients and adsorption capacities of Cs^+ adsorption on various adsorbents.

Adsorbent	Distribution coefficient, K_d (L g^{-1})	Adsorption capacity (mg g^{-1})	References
A-X zeolite	0.19-0.39 (50, 1) [a]	30 (50) [c]	[16]
Natural zeolite	3.75-4.45 (8.45×10^{5}Bq L^{-1} [b], 10)	199-266 (app.) [d]	[52]
Ain Oussera soil	0.37 (1, 2)	4.31 (100) [c]	[53]
NaSM zeolite	3.8-4.9 (2.280×10^{4}Bq L^{-1}, 10)	159.7-248.0	[15]
Bentonite	1.4 (133, 50)	96.5	[77]
Local Taiwan laterite	0.025 (1.33, 33.3)	39.9	[56]
Bure mudrock	0.1-0.9 (0.12, 7-200)	13.3	[57]
Ceiling tiles	-	0.21	[51]
Synthetic zeolite A-4	38.5 (5, 2.5)	58.7	This work
Bentonite	10.2 (5, 2.5)	40.0	This work
Pristine AC	0.98 (1, 2.5)	4.5	This work
Modified AC	3.8 (1, 2.5)	16.1	This work

[a] The values in brackets were initial concentration of Cs^+ (mg L^{-1}, otherwise stated) and dosage (g L^{-1}), respectively.

[b] 1 MBq L^{-1} ^{137}Cs is equivalent to 9.044×10^{-4} mg L^{-1}.

[c] The adsorption capacity was not given directly in this literature and the capacity shown here was obtained at a certain initial concentration (given in the brackets, unit: mg L^{-1}).

[d] approximate value as no exact value was given in the literature, and the data obtained here were based on the figures in this literature.

- Not mentioned in the literature.
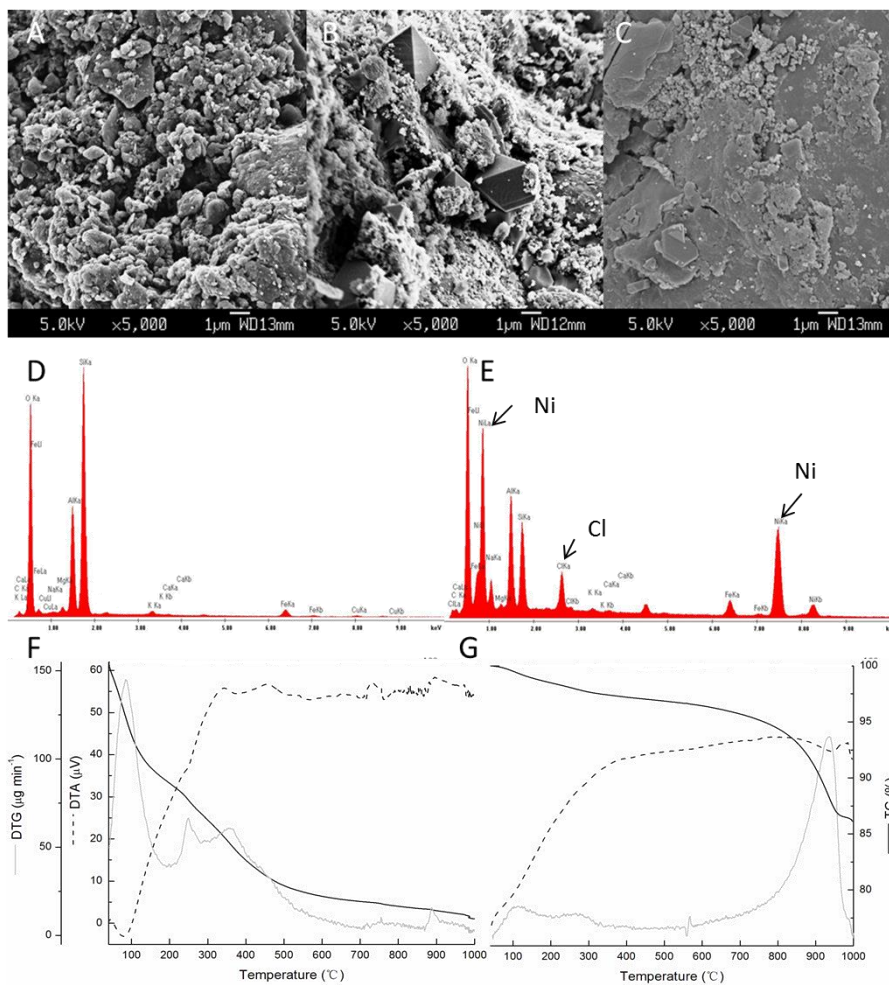
Fig.3-1 SEM images (acceleration voltage: 20.0 kV and 5000 ×magnification) of pristine (A) and

modified (B: before Cs$^+$ adsorption, C: after Cs$^+$ adsorption) AC, EDS spectrums and TG/DTA

curves of pristine (D, F) and modified AC powders (E, G) (particle size: approximately 100 μm).
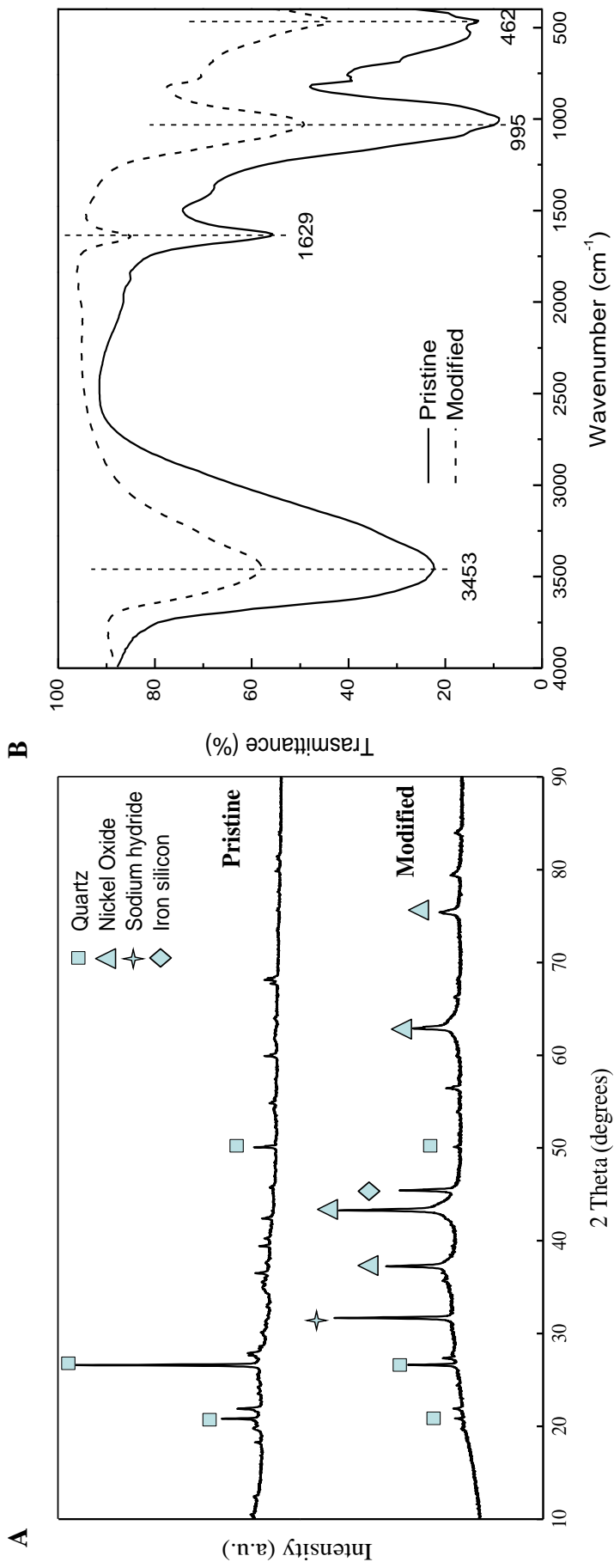
Fig.3-2 Typical X-ray diffraction patterns (A) and FTIR spectrums (B) of pristine and modified AC (a.u., arbitrary units).

83
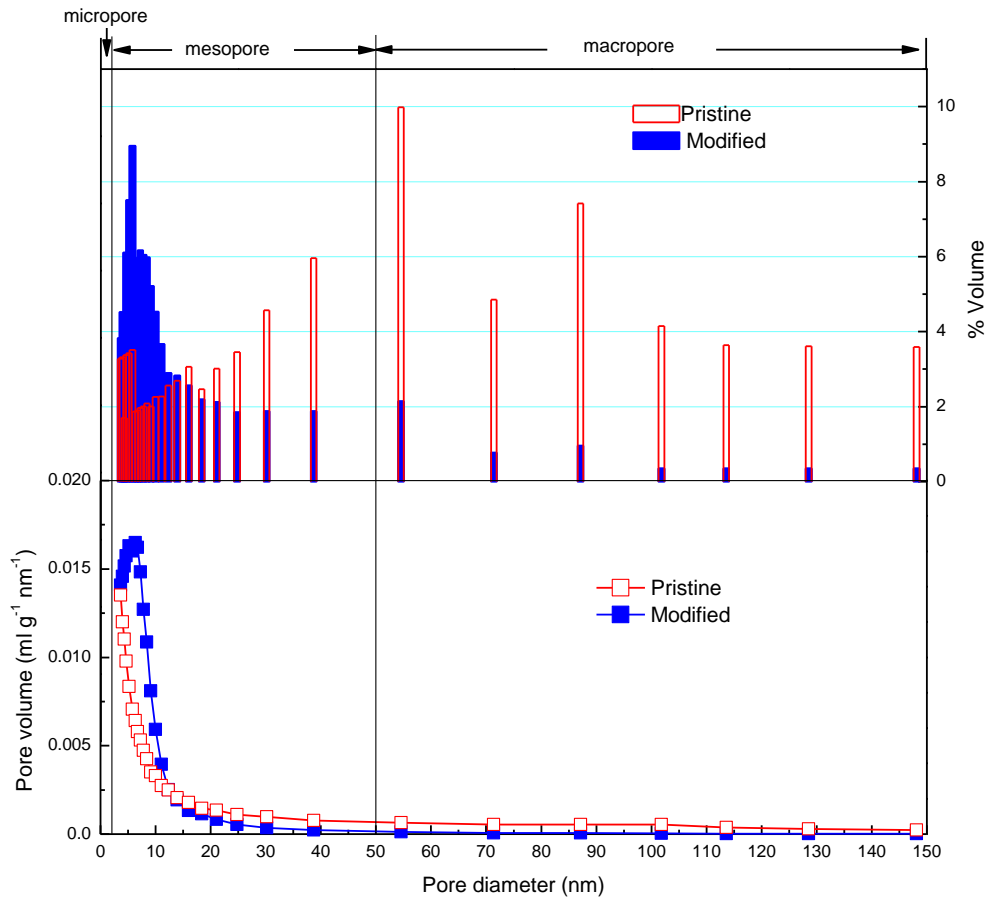
Fig.3-3 BJH pore size distribution in the pristine (red) and modified (blue) AC samples (particle size: approximately 100 μm).
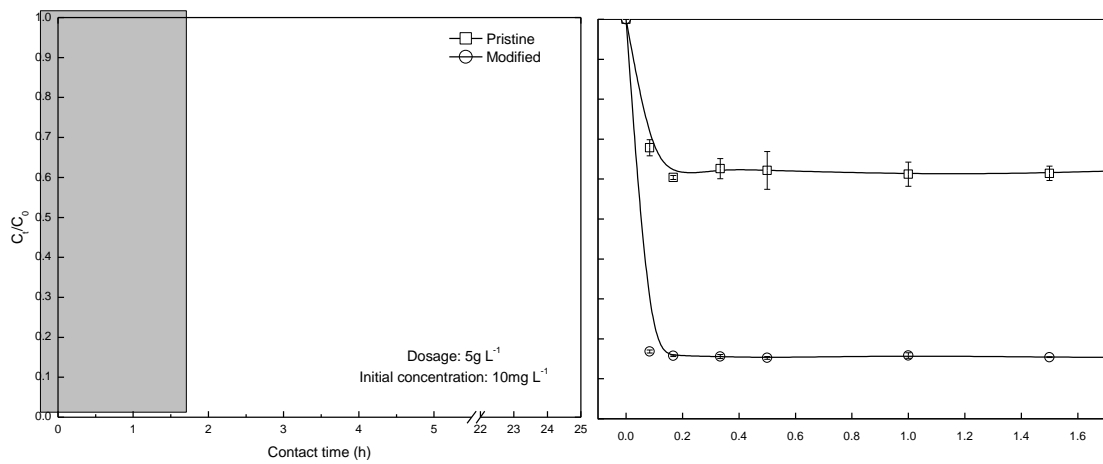
Fig.3-4 Variation of Cs$^+$ concentrations in solution, C_t/C_0, as a function of time, t, for adsorption

of Cs$^+$ on the pristine and modified AC samples at 25°C. (Initial Cs$^+$ concentration: 10 mg L^{-1},

sample dosage: 5 g L^{-1}, the right figure shows the enlarged dark part of the left figure)
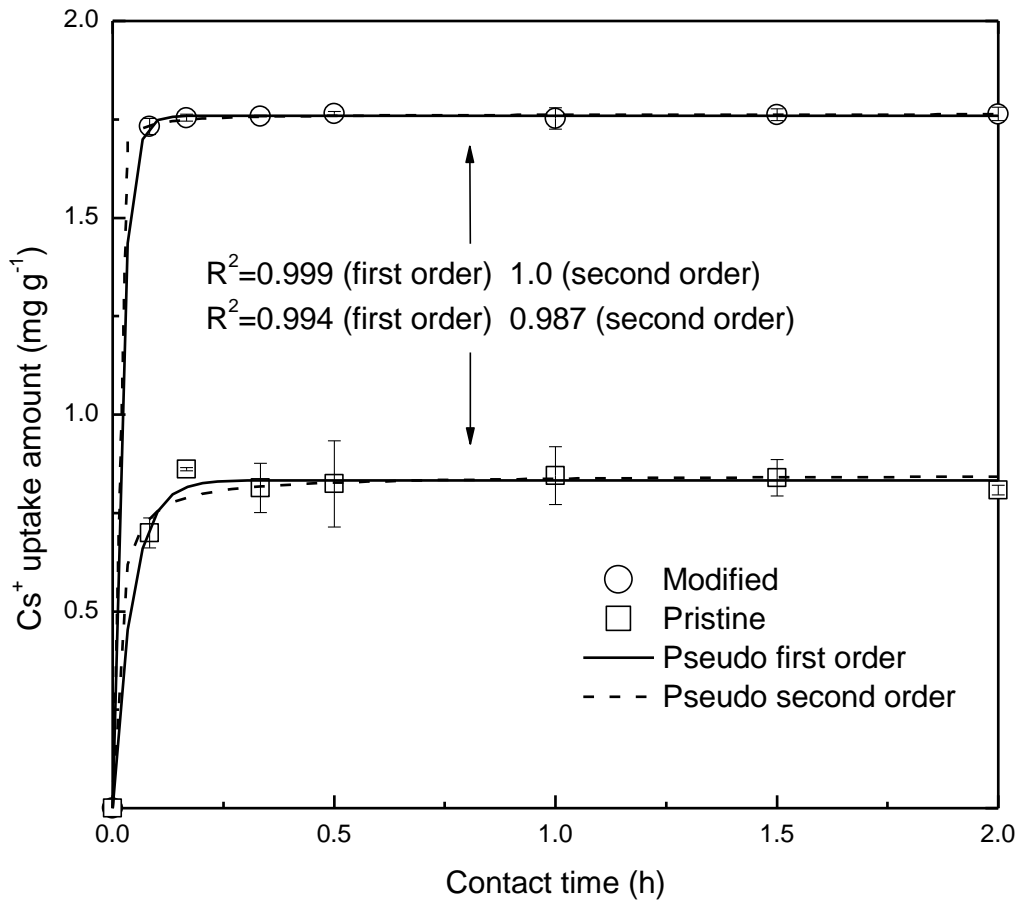
Fig.3-5 Comparison of pseudo first-order and second-order kinetic models for the fitting of

cesium adsorption on clay samples. (Initial Cs^+ concentration: 10 mg L^{-1}, adsorbent dosage: 5 g

L^{-1})
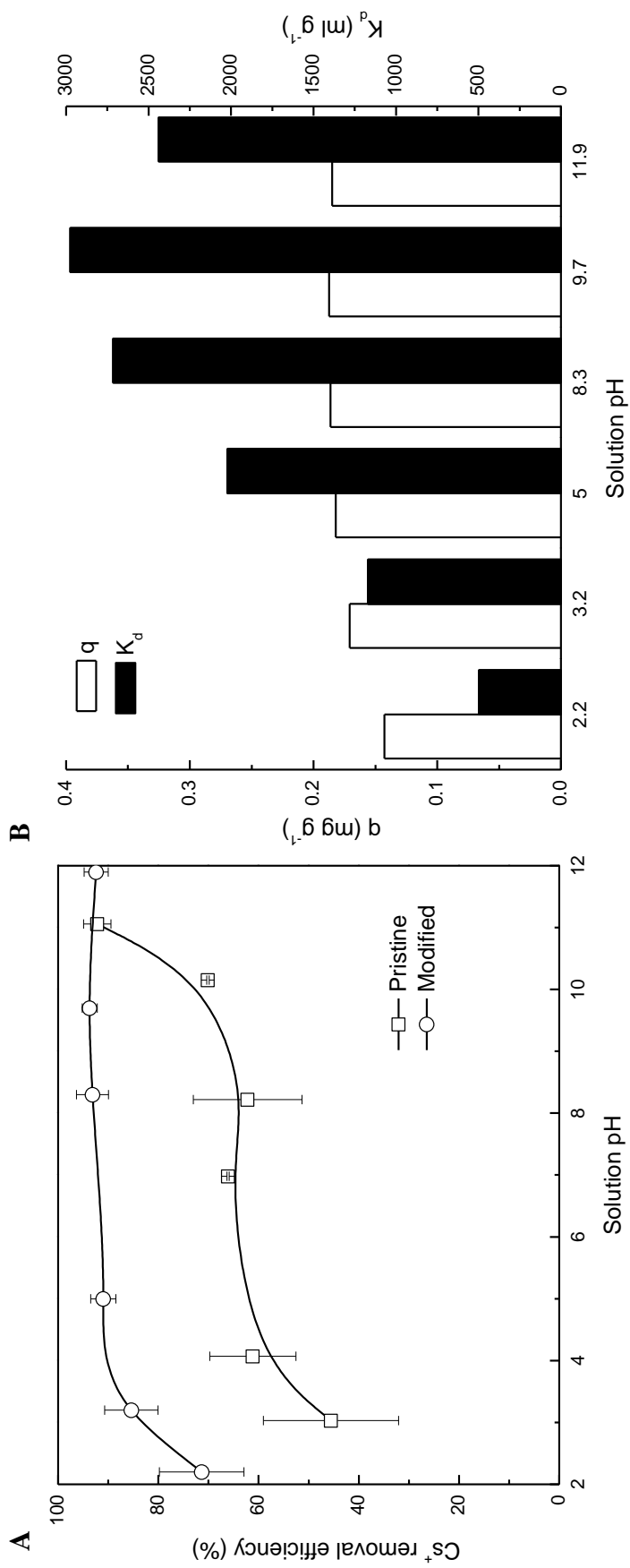
Fig.3-6 Effect of solution pH on cesium removal efficiency of clay samples (A) and variation of adsorption amount and distribution coefficient of cesium adsorption on modified AC as a function of solution pH (B). (Initial Cs^+ concentration: 1 mg L^{-1}, pristine or modified AC dosage: 5 g L^{-1})
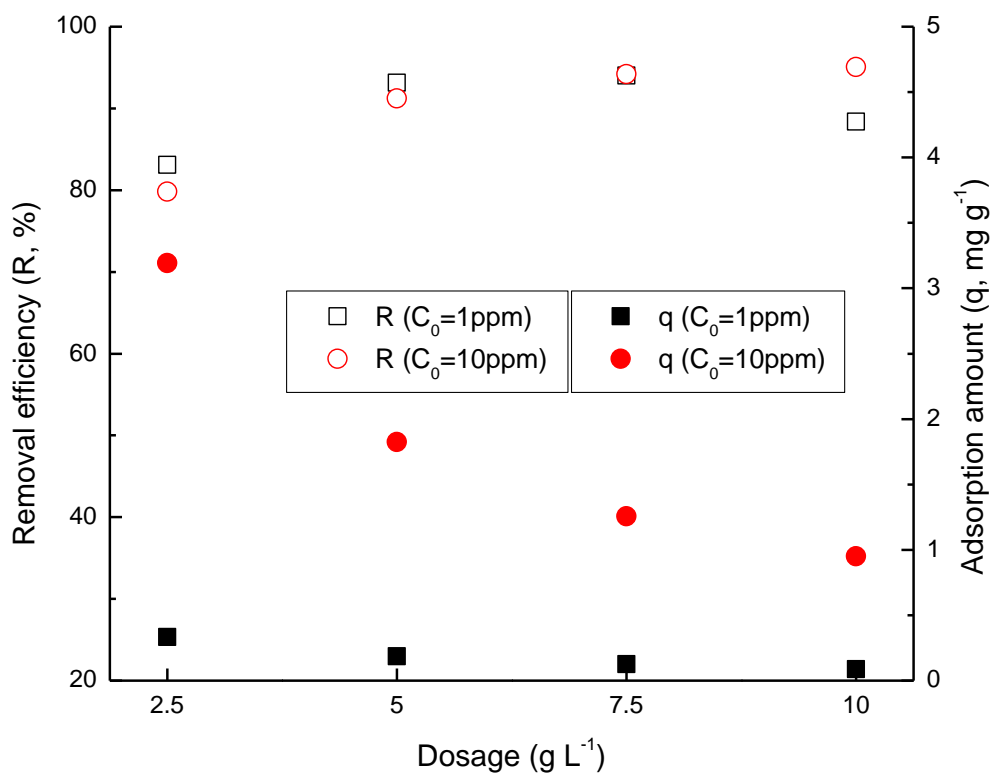
Fig.3-7 Variation of removal efficiency and adsorption amount of cesium adsorption on modified

AC as a function of adsorbent dosage.
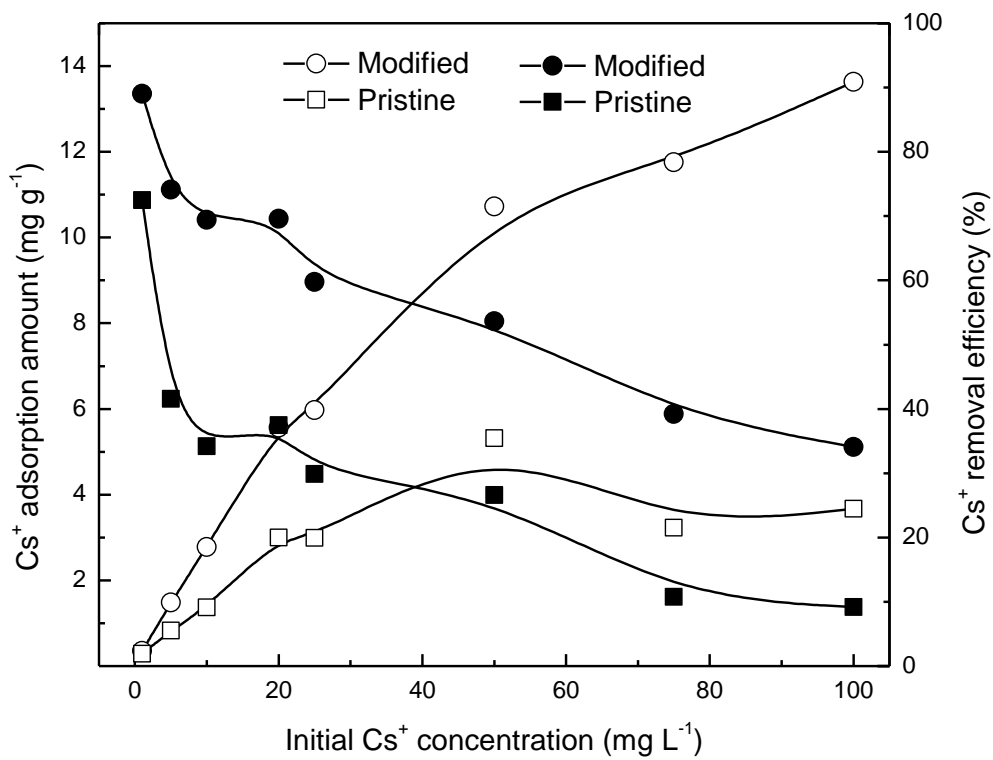
Fig.3-8 Effect of initial concentration on the cesium uptake amount (open symbols) and removal

efficiency (solid symbols) of cesium adsorption on pristine (squares) and modified (circles) AC

$(2.5 \ g \ L^{-1})$.
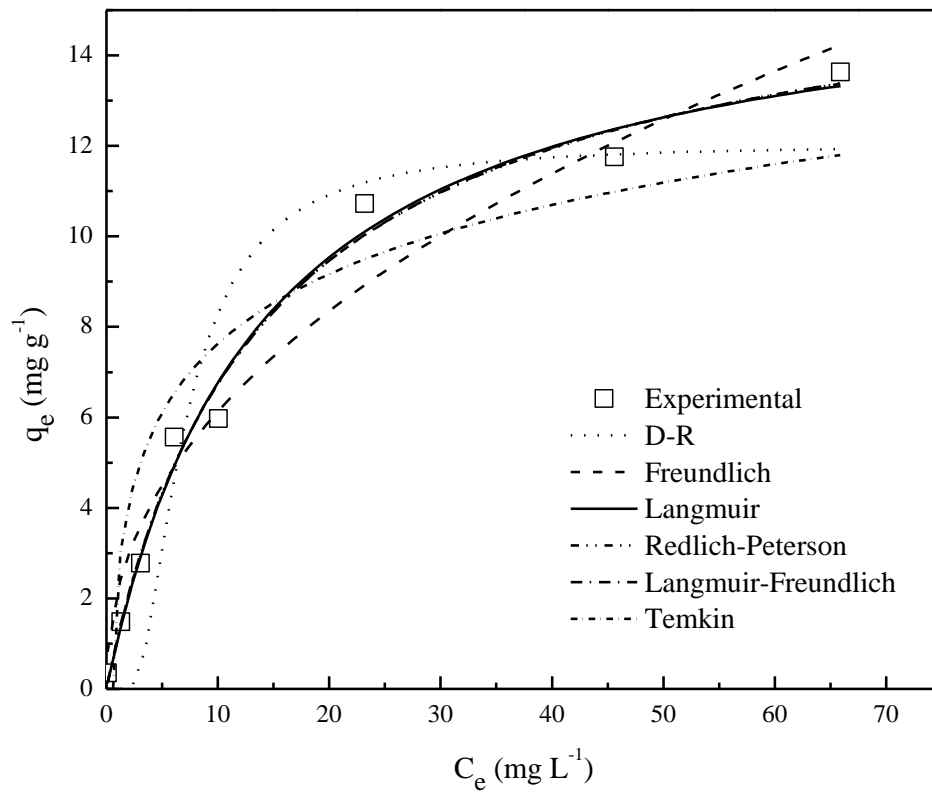
Fig.3-9 Application of adsorption isotherms to cesium adsorption on modified akadama clay (2.5

g L^{-1}).
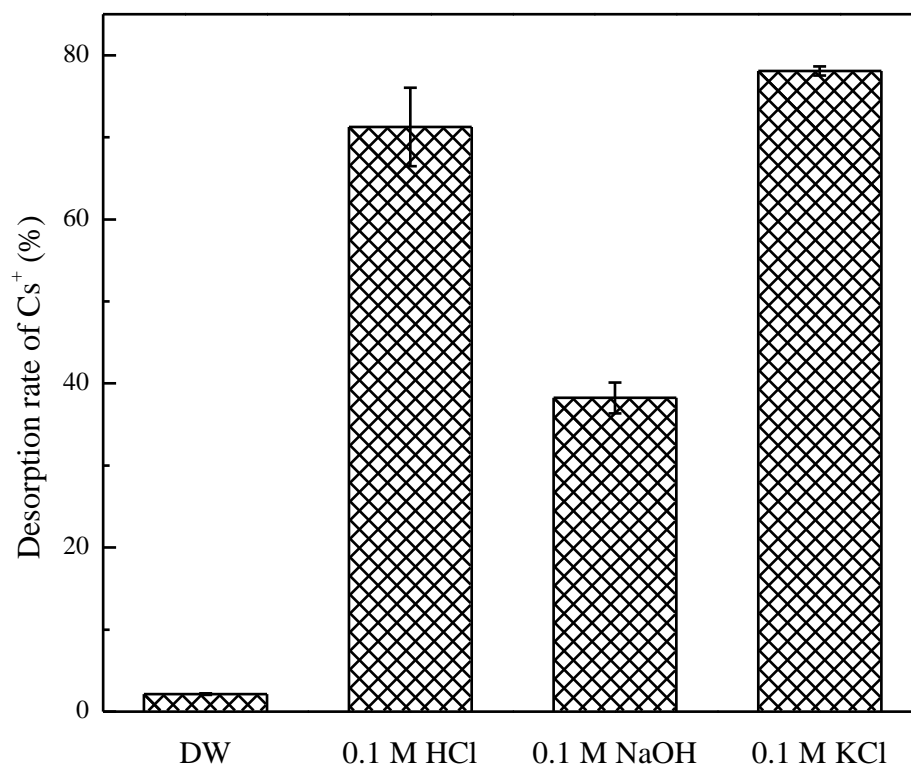
Fig.3-10 Desorption rate of cesium adsorbed modified akadama clay at different solutions.

(Solid/Liquid: 4 g L^{-1})
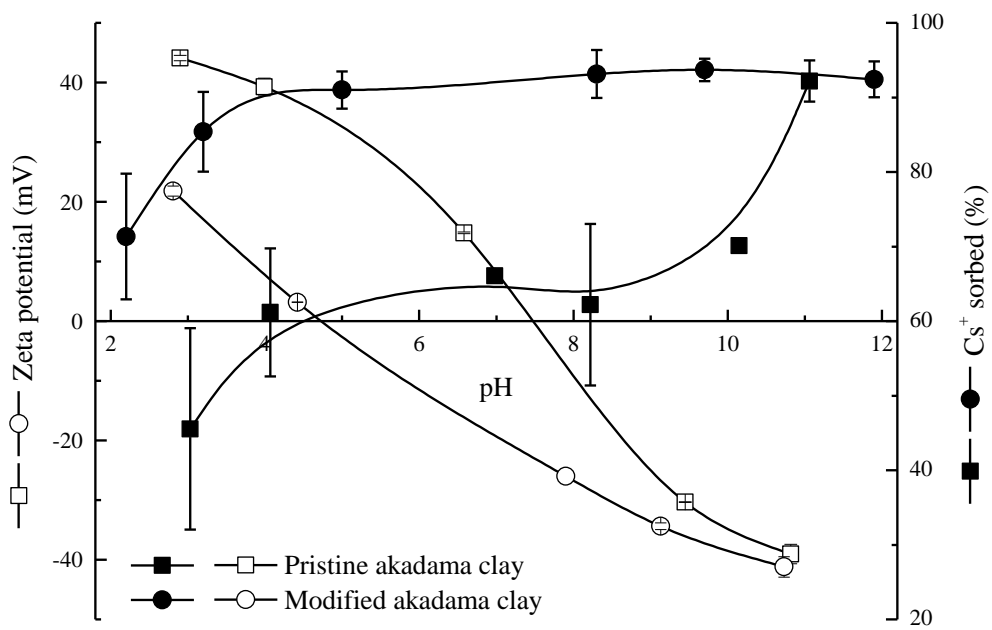
Fig.3-11 Zeta potential of pristine (square) and modified (circle) akadama clay in 1 mM NaNO$_3$

and variation of cesium (1 mg L^{-1}) adsorbed under different pH conditions (5 g L^{-1}).

Chapter 4 Removal of cesium from aqueous solution using ammonium molybdophosphate - polyacrylonitrile (AMP-PAN) beads

4.1 Introduction

Removal of radionuclides attracts much attention of researchers all over the world after the Fukushima nuclear accident caused by the big earthquake in northeast Japan. Before this accident, some related studies have been carried out and many removal processes have been proposed such as adsorption/ion exchange, precipitation, solvent extraction, electrochemical and membrane processes [4, 6-10, 15, 16, 22, 23, 53, 85]. Adsorption/ion exchange process is well known as an efficient and convenient method for radionuclides removal from aqueous solution due to its advantages such as stable, high capacity and low cost [7, 8, 15, 53]. For this process, a general drawback is its capacity loss in high ionic strength wastewater [7]. In other words, a high capacity adsorption material with high selectivity towards target ions is still under investigation. Therefore, developing new adsorption materials and trying to improve their capacities and selectivities become a research hotspot in this field.

Ammonium molybdophosphate, $(NH_4)_3P(Mo_3O_{10})_4\ 3H_2O$ (AMP), is a yellow crystalline inorganic compound which has been demonstrated have the requisite high capacity and selectivity towards Cs^+. As illustrated in previous studies [86, 87], the phosphomolybdate complex ion, $(PMo_{12}O_{40})^{3-}$, consists of a hollow sphere formed by twelve MoO_3 octahedra with the PO_4 group in the center. The ammonium ions with associated water molecules are likely fit in between these spheres of negative ions thus accounting for the cohesion of these ions. According to the special crystal structure of AMP, it exhibits a selectivity sequence for the alkali metals similar to other heteropoly acids of the Keggin structure: $Cs^+ > Rb^+ > K^+ > Na^+ > Li^+$ [86]. The ion exchange mechanism of AMP is reported as an isomorphous exchange of Cs^+ for NH_4^+ in the crystal lattice [88]. The ion exchange process could be expressed as follows [89]:

$$(NH_4)_3PMo_{12}O_{40} + xCs^+_{(aq)} \xrightarrow{\text{irreversible}} Cs_x(NH_4)_{3-x}PMo_{12}O_{40} + x(NH_4)^+_{(aq)} \quad (4\text{-}1)$$

Although the AMP possesses many advantages on Cs^+ removal from liquid wastes, its fine powder size limits its industrial scale practice. A binding agent, substrate, or support that allows it to be used in a packed bed with reasonable flow rate and minimal pressure drop, e.g., acceptable hydrodynamics is necessary [90]. As a result, ammonium molybdophosphate-polyacrylonitrile (AMP-PAN) has been developed and demonstrated as an efficient material for Cs^+ removal through both batch and dynamic column tests [91-93]. The undergoing removal mechanism is the physical adsorption due to weak van der Waals forces and ion exchange between NH_4^+ and Cs^+, where the latter plays a much more important role. Tranter et al. [91] reported that the AMP-PAN maintained high Cs^+ exchange capacity (32 g Cs/kg adsorbent) with high flow rates of heavily salted feed solutions in bench scale column tests. Todd et al. [92] reported batch equilibrium data for AMP-PAN in simulated INEEL (Idaho National Engineering and Environmental Laboratory, USA) composite tank waste solutions. Cesium adsorption followed the classical Langmuir isotherm and the presence of potassium reduced the distribution coefficient (K_d) to the greatest extent. Park et al. [47] reported that the AMP-PAN beads could remove Sr^{2+}, Cs^+ and Co^{2+} from radioactive laundry wastewater.

AMP and PAN play different roles during the adsorption process by using AMP-PAN beads. It is generally believed that AMP is the ion exchanger and therefore plays a much more important role than PAN, which is served as a binder. However, the effect of compositions of AMP-PAN beads including the ratio of AMP/PAN on adsorption capacity is yet unknown up to date. In this study, therefore, AMP-PAN beads with different compositions were synthesized and applied to remove Cs^+ from aqueous solutions. The objective of this study is to determine the best composition of AMP-PAN beads for Cs^+ removal. The thermal stability and its chemical stability in acidic and alkaline solutions were investigated. Effects of experimental conditions on adsorption behavior were conducted with respect to contact time, pH, initial concentration and

competitive ions. Adsorption kinetic and isotherm studies were also investigated through batch adsorption experiments. In addition, desorption tests were carried out to evaluate the recycle capability of as synthesized material.

4.2 Materials and methods

4.2.1 Chemicals

Triammonium 12-molybdo(VI)phosphate trihydrate (AMP, $(NH_4)_3[PO_4Mo_{12} O_{36}]$ $3H_2O$, 98%+, Wako Pure Chemical Industries, Ltd., Japan), dimethyl sulfoxide (DMSO, $(CH_3)_2SO$, 98%+, Wako Pure Chemical Industries, Ltd., Japan) and PAN (polyacrylonitrile, MW=150,000, Polysciences, Inc., USA) were used to synthesize AMP-PAN. Tween 80 was purchased from Kanto Chemical Co. Inc., Japan. Non-radioactive cesium chloride (CsCl) purchased from Tokyo Chemical Industry Co. Ltd., Japan was used as a surrogate for ^{137}Cs because of its same chemical characteristics. Deionized water (DW) generated from a Millipore Elix 3 water purification system (Millipore, USA) equipped with a Progard 2 pre-treatment pack was used throughout the experiments. All the other reagents used in this study were purchased from Wako Pure Chemical Industries Ltd., Japan without further purification.

4.2.2 Preparation of AMP-PAN beads

Four kinds of AMP-PAN beads (named 1#, 2#, 3# and 4#) with different compositions (Table 4-1) were synthesized following the procedure reported by Moon et al. [94]. AMP was used to prepare the inorganic active ion exchangers. AMP and Tween 80 were combined with DMSO. After stirring the solution for 1 h at 50°C and 250 rpm, 8 g of PAN was added to this solution and then stirred using a magnetic stirrer for 5 h at 50°C and 1000 rpm to obtain a homogeneous solution. The composite mixture was fed into a syringe with a needle (0.55$\times$25 mm) manually to obtain the spherical composite beads. The prepared AMP-PAN beads were washed three times

with DW and then dried in an oven for 24 h at $60^{o}C$.

4.2.3 Thermal and chemical stability of AMP-PAN beads

In order to evaluate the thermal and chemical stability of as prepared AMP-PAN beads, thermogravimetric and differential thermal analysis (TG/DTA) and acidic/alkaline solutions were carried out. For the TG/DTA analysis, approximately 7 mg of AMP-PAN beads were prepared into an aluminum pan and heated up to $550^{o}C$ at a constant rate of $10^{o}C$ min^{-1} in normal atmosphere. Carrier gas (air) rate was kept at 200 mL min^{-1}. The TG loss and DTA curves were recorded. For the chemical stability evaluation, 0.01 g of AMP-PAN beads were immersed into 20 mL 0.1 M HCl and NaOH solutions. After a contact time of 24 h, the beads were dried completely and the weight losses were recorded.

4.2.4 Adsorption experiments

1.26 g CsCl was weighed exactly and dissolved into 1 L DW as standard stock Cs^+ solution (~1000 mg L^{-1}), which could be diluted to desired concentrations of Cs^+ solution for further experiments. The solution pH was adjusted by 0.1 M HCl and NaOH solutions and measured by a pH meter (Mettler Toledo SG8, Switzerland). To determine the effect of contact time, amount of AMP-PAN beads was mixed with 200 mL of Cs^+ solution in a 200 mL-glass flask (AS ONE, Japan). Supernatants (about 1 mL for each) were withdrawn at predetermined time intervals along with the initial solution (zero min point). For the dosage effect, different amounts of 4# AMP-PAN beads were mixed with 50 mL of 1 mg L^{-1} Cs^+ solutions. For the effect of initial pH, 0.4 g L^{-1} of AMP-PAN beads was mixed with 20 mL of 1 mg L^{-1} Cs^+ solutions with initial pH value of 2.5, 3.5, 4.5, 5.5 and 7, respectively. To determine the effect of initial Cs^+ concentration, 0.02 g of AMP-PAN beads was mixed with 25 mL of Cs^+ solutions of 5, 10, 20, 50, 80, 100 and 200 mg L^{-1}, respectively. To determine the effect of competitive ions, Na^+, K^+ and Ca^{2+} with concentrations of 10, 50, 100, 200 and 400 mg L^{-1} were added in their hydrochloride salt forms

into the solutions with the initial Cs^+ concentration of 1 mg L^{-1}, respectively.

All the experiments were conducted in 50 mL-polypropylene tubes (Violamo, Japan) vigorously shaken (200 rpm) and at room temperature ($25\pm1^{o}C$) for 24 h (except contact time experiment). All the samples including initial solutions were collected by filtering the supernatants through 0.22 μm mixed cellulose ester membrane (Millipore, Ireland) and diluted with DW to a proper extent (less than 1 mg L^{-1}) into 15 mL-polypropylene tubes (Violamo, Japan) prior to inductively coupled plasma-mass spectrometry (ICP-MS) (Perkin Elmer Elan DRC-e, USA) analysis. Along with the batch adsorption experiments, blank and control tests were also carried out to observe any precipitation and to determine the extent of wall adsorption. The negligible differences between the initial and final concentrations indicated that no precipitation or wall adsorption occurred in this study.

4.2.5 Desorption experiment

0.1 M HCl and NH_4Cl were used as desorption solutions in this study along with DW as reference to evaluate the recycle capability of AMP-PAN beads. The concentrations of Cs^+ desorbed were detected with a similar method as described in adsorption experiments.

4.2.6 Adsorption kinetic and isotherm studies

Nonlinear pseudo-first and pseudo-second order models corresponding to Eqs. (2-1) and (2-2), respectively, are adopted to investigate kinetic behavior of Cs^+ on AMP-PAN beads.

Additionally, the moving boundary model [95, 96] was used to distinguish the relative roles of adsorption steps involved to play. If the adsorption process was controlled by liquid film diffusion, intraparticle diffusion or chemical interaction, the rate constant can be expressed by Eqs. (4-2), (4-3) and (4-4), respectively.

$$k = -\ln(1-F) \qquad\qquad (4-2)$$

$$k = 1 - 3(1-F)^{2/3} + 2(1-F) \qquad (4\text{-}3)$$

$$k = 1 - (1-F)^{1/3} \qquad (4\text{-}4)$$

where F is the adsorption fraction (q_t/q_e), and k is the adsorption rate constant. By plotting a linear relationship of k versus contact time t (min), the regression coefficients (R^2) for three adsorption steps can be obtained, of which the one with the highest R^2 value is assumed to be the rate controlling step.

Langmuir [32] and Freundlich [33] isotherm were adopted to fit the adsorption results in this study. The nonlinear forms of these isotherms are given in Eqs. (2-4) and (2-5), respectively.

4.2.7 Characterization

Video Microscope (VM) observation was performed using a Shimadzu STZ-40TBa type microscope (Shimadzu, Japan). The roundness of the bead samples was determined using a Motic Images Plus 2.3S® (Motic, China) that employs optical imaging with two adaptive full-framematrix cameras. The roundness of the beads was calculated using the following equation:

$$\text{Roundness} = \frac{4\pi A}{P^2} \qquad (4\text{-}5)$$

where A is the area occupied by a single bead image, and P is its perimeter. The two-dimensional image of a sphere has a roundness score of 1. Other shapes have a roundness score less than 1. Scanning electron microscope (SEM) analysis was performed using a JEOL JSM-6330F type microscope (JEOL, Japan) operated at 5.0 kV. The samples were put onto a conductive carbon tape above the metal stub and coated with a thin layer of platinum for charge dissipation during SEM imaging. Fourier transform infrared spectroscopy (FTIR) was recorded in the region of 4000-400 cm^{-1} by a JASCO 300E FT-IR spectrophotometer (JASCO, Japan) using KBr pellet at a resolution of 4 cm^{-1}. As mentioned, TG/DTA was carried out using an Exstar TG/DTA 7300 thermal analyzer (Japan).

4.2.8 Analytical methods

Concentrations of metal ions were analyzed by a fully quantitative analytical method on a Perkin Elmer ELAN DRC-e ICP-MS in standard mode. Each sample was analyzed 5 times and the average was taken. The relative standard deviation (RSD) of multiple measurements was less than 2% and in most cases, less than 1.5%. Concentrations of NH_4^+ in solutions were analyzed by an UV-1800 ultraviolet spectrophotometer (Shimadzu, Japan) according to Nessler reagent colorimetric method.

4.3 Results and discussion

4.3.1 Physicochemical and structural properties of AMP-PAN beads

As shown in Table 4-2, according to different compositions, different physicochemical properties were presented in four kinds of AMP-PAN beads. As for industrial production and application, those beads with consistent size and high roundness were preferred. In this study, the 4# beads presented the largest size, highest roundness and best sphere. 2# and 3# beads had good sphere and roundness. 1# beads presented the worst sphere and roundness. These phenomenon were related with the compositions of AMP-PAN beads, such as the ratio of AMP/PAN, AMP/DMSO, and DMSO/PAN. Because the AMP is the ion exchanger which plays an important role in an ion exchange process, the theoretical ion exchange capacity (IEC) of these AMP-PAN beads follows as: 1#>4#>2#>3# along with the decrease of AMP/(PAN+Tween 80) ratio. It is worth noting that the hypothesis of the calculation of theoretical IEC is that all the NH_4^+ existed in AMP are exchangeable. Also, it is generally considered that the maximum adsorption capacity (q_{max}) is no larger than the theoretical IEC. As a result, as shown in Table 4-1, the q_{max} follows: 2#>3#>4#. It can be seen that though the 2# and 4# AMP-PAN beads have similar theoretical IEC, the q_{max} of them have a remarkable difference. The increase of AMP and PAN while DMSO kept constant in synthesizing 4# AMP-PAN beads results to a larger size and much more compact

internal structure compared with 2# beads. As demonstrated in Table 4-2, 4# beads have larger size and higher roundness, which have much relationship with the mass transfer process during the adsorption process. It is generally believed that large beads size and high roundness lead to a low specific surface area and further a low adsorption capacity. These results also indicate that all the compositions of AMP, DMSO and PAN have effects on adsorption capacity of AMP-PAN beads.

Based on the physicochemical properties of these four kinds of AMP-PAN beads, 1# bead is excluded for its bad sphere and roundness and 3# bead is also removed for its relatively low adsorption capacity. As a result, 2# and 4# beads are selected in this study for the following characterization and adsorption experiments.

Fig.4-1 shows the VM and SEM images of the four kinds of AMP-PAN beads. It can be easily found that all the beads present good sphere except 1# bead. The result can be explained by the low dose of PAN, which provides a highly stable, porous support for the fine AMP particles and allows the sorbent to be formed into larger particles well suited for large-scale application [92]. From the cross section SEM images of 2# and 4# beads, it can be seen that highly porous structure has been developed inside the beads. The magnification SEM images of the walls in 2# and 4# beads indicate their different structures, which are porous in 2# and network in 4# beads.

4.3.2 Thermal stability study

Studies to determine the thermal stability of AMP-PAN beads were performed by TG/DTA and Fig.4-2 shows the thermal analysis results of 2# and 4# AMP-PAN beads. Both of these two samples present two remarkable DTA peaks (exothermic) at temperature of approximately $310^{o}C$ and $430^{o}C$, respectively. And the second one is much more severe. Especially in 4# beads, two typical TG losses were detected at the corresponding temperatures, which are probably caused by the decomposition of PAN and AMP, respectively. The TG losses no larger than 10% before

$310^{\circ}C$ are perhaps due to the loss of water contents in these two kinds of AMP-PAN beads. Because the compositions of AMP and PAN are similar, the TG losses in these two AMP-PAN beads are also similar. The total TG losses of these two samples are approximately 37.8% and 36.7%, respectively. The temperature of the AMP-PAN beads would not be expected to reach temperatures exceeding $310^{\circ}C$, even if loaded with ^{137}Cs, therefore, the thermal stability of the material is adequate for processing radioactive wastes.

4.3.3 FTIR analysis

Functional groups on the surface of AMP-PAN beads are detected through FTIR analysis. As shown in Fig.4-3, the results indicate that the 2# beads present much more intensive peaks than 4# beads, especially at the range of 792, 866 and 1057 cm^{-1}, which are assigned to stretching vibration of P–O, Mo=O, and Mo–O–Mo in AMP, respectively. The peak range of 1390-1500 cm^{-1} is assigned to NH_4^+ [47]. Maximum adsorption at 2234 cm^{-1} is due to the nitrile groups in PAN [97, 98]. The broad absorption peaks observed at the range of 3300-3600 cm^{-1} are assigned to the stretching vibration of hydroxyl groups. The broad band is indicative of hydroxyl group stretching vibrations when the hydroxyl group is hydrogen bonded [67].

4.3.4 Chemical stability study

The results show that the as synthesized AMP-PAN beads are relatively stable in 0.1 M HCl solution rather than NaOH solution (Fig.4-4). In acidic solutions, no larger than 10% of weight loss was detected for all of the AMP-PAN beads. Whereas in alkaline solutions, over 60% of weight losses are observed for all of the beads, which is probably attributed to the reaction between NaOH and AMP. This deduction could be proved by the discoloration of AMP-PAN beads (from yellow to white) after the contact with NaOH solution. As we know, the AMP powder is yellow and PAN powder is white.

4.3.5 Adsorption studies

(1) Effect of contact time and kinetic study

The removal rate is related with the removal mechanism and particle size. As shown in Fig.4-5, the removal process is relatively slow compared with other materials [11, 16, 22], probably due to the ion exchange process and its large size. Same as previous study [47], the contact time of 1 d is determined in this study for the following experiments.

Kinetic model plots and parameters are given in Fig.4-5 and Table 4-3, respectively. Through comparing the R^2 and chi-square analysis, it can be determined that the pseudo second order model fits better with the experimental results than the first order model. The better fitting of second order kinetic model indicates that the Cs^+ adsorption process on AMP-PAN beads is a chemisorption rather than physisorption [22].

As generally viewed, a liquid-solid adsorption process may compose of several successive kinetic steps [99, 100]. Transport in the bulk solution, diffusion across the film surrounding the adsorbents and in the pores of the adsorbents are the initial three steps driven mainly by mass balance and/or Fick diffusion, belonging to physical adsorption processes [101, 102]. Reasonably, they reflect the nature of the first order kinetic order that usually governed by the concept of linear driving force. The hindmost step of an adsorption process is adsorption on the solid surface, which is a chemical reaction as expressed in Formula (4-1) in this study. This step is usually the most important step and would make the whole adsorption process follow the common rate law of chemical reaction, which is well described by the second order kinetic model [100].

As in this case, extra theoretical adsorption models are supplemented to accurately discriminate the adsorption processes. Moving boundary model is designated to identify the controlling adsorption step, by distinguishing the roles of liquid film diffusion, intraparticle diffusion and chemical interaction [96]. The R^2 values of moving boundary models for the adsorption processes, representing their relative importance, are summarized in Table 4-4. The

consistence of the values clearly reveals the liquid film diffusion is the main rate controlling step in adsorption process. This is probably ascribed to poor solvation potential of the surfactant (Tween 80) on the surface of AMP-PAN beads limiting the mass transport of Cs^+ from liquid solutions to AMP-PAN beads. On the other hand, this indicates the well-developed porous structure and nature of loose network, as shown in SEM images, promotes the intraparticle diffusion, making it a relatively rapid process. Meanwhile, the chemical interaction (ion exchange) between adsorbent and adsorbate is also relatively fast and not the rate controlling step.

(2) Effect of pH

As the AMP-PAN beads are not applicable in alkaline solutions, the pH is adjusted to be approximately 2.5, 3.5, 4.5, 5.5 and 7, respectively. As indicated in Fig.4-7, all the pH values were acceptable for Cs^+ adsorption with removal efficiencies higher than 95%. The good Cs^+ uptake is attributed to the ion exchange between NH_4^+ in AMP and Cs^+ and the adsorption of Cs^+ onto the macropores in the AMP-PAN beads [89]. When pH value was as low as 2.5, perhaps inhibited due to the competition between H^+ and Cs^+ for the adsorption sites, the removal efficiency had a small decrease. All the effluent pH values decreased after adsorption and became much more significant with the increase of initial pH value. This is because NH_4^+ was released during the adsorption process and thereafter produced H^+ through hydrolysis. Meanwhile the hydrolysis reaction of NH_4^+ was suppressed when the concentration of H^+ in solution was high. That may be the reason why the decrease was significant at high initial pH solutions and negligible at low initial pH solutions.

(3) Effect of dosage

As shown in Fig.4-8, dosage of 0.1 g L^{-1} was adequate for 1 mg L^{-1} Cs^+ adsorption on AMP-PAN beads and the removal efficiency reached 96.7%. The removal efficiency increased with dosage due to the greater availability of the adsorption sites. However, there is no obvious increase in the removal efficiency when the dosage was larger than 0.2 g L^{-1}, indicating this

dosage was optimal in this experiment.

(4) Effect of initial concentration and adsorption isotherm study

It was found that the 2# beads had the highest adsorption capacity, which well agrees with the highest AMP/PAN ratio. 4# beads had the lowest adsorption capacity, as mentioned above, probably due to the compact internal structure and large size suppressing adsorption process. Furthermore, plot fitting results of Langmuir and Freundlich isotherms are also presented in Fig.4-9 and Table 4-5, respectively. The higher R^2 and lower χ^2/DoF values throughout all the cases indicated that Freundlich isotherm fitted better with Cs^+ adsorption results than Langmuir isotherm in this study. According to the theoretical hypothesis of Freundlich isotherm, the Cs^+ adsorption on AMP-PAN beads was more like a multilayer than a monolayer adsorption process. In addition, the values of Freundlich exponent n were in the range of 1-10, indicating the favorable adsorption [22, 33, 103]. Although the Langmuir isotherm did not give a well fit with the adsorption results, the estimated maximum adsorption capacity could be undertaken for comparison, which was in the order of 2#>3#>4#. Park et al. [47] reported a q_m value of 81 mg g^{-1} for removing Cs^+ from radioactive laundry wastewater by using AMP-PAN beads with a composition of as same as the 4# AMP-PAN beads in this study. Todd and Romanovskiy [90] reported a q_m value of 85 mg g^{-1} for removing Cs^+ from simulated composite INEEL tank waste by using an AMP-PAN beads with a composition of 85.7 wt% AMP and 14.3 wt% PAN.

(5) Effect of competitive ions

As another important factor that could affect the adsorption of target ions on adsorbents, competitive ions are essential to be investigated for a typical adsorption study. Three normal metal ions in natural water bodies including two monovalent ions (Na^+ and K^+) and one divalent ion (Ca^{2+}) were utilized in this study as competitive ions. The concentrations of Cs^+ (1 mg L^{-1}) and competitive ions (0, 10, 50, 100, 200 and 400 mg L^{-1}) were mentioned in the methods part. 4# beads were used for this study and dosage was 0.4 g L^{-1}. Fig.4-10A showed the variations of

removal efficiencies and B showed the variations of distribution coefficients (K_d). It is obvious that the K_d values displayed larger differences than removal efficiencies. This difference could be attributed to the calculations of these two results. There was no obvious change on the removal efficiencies with addition of competitive ions. It decreased from 99.6% without competitive ions to 95.7%, 94.1% and 91.3% with 400 mg L^{-1} of Na$^+$, Ca^{2+} and K$^+$, respectively. Throughout all the cases, the removal efficiencies exceeded 90%, indicating the AMP-PAN beads had selectivity for Cs$^+$ adsorption. However, probably due to the similar radius and hydration energy [81], K$^+$ competed more effectively against Cs$^+$ than other ions, resulting in a lower K_d value (Fig.4-10B). The phenomenon was also observed by other researchers.

(6) Role of ion exchange between Cs$^+$ and NH$_4^+$

It is hypothesized that if adsorption is mainly caused by ion exchange reaction, then the quantity of the released cations (in gram-equivalent) would be close to that of the adsorbed target ions. Fig.4-11 shows the relationship between the Cs$^+$ adsorbed and NH$_4^+$ released during the Cs$^+$ adsorption process using 2# and 4# AMP-PAN beads. Results indicated much more NH$_4^+$ released than Cs$^+$ adsorbed in all the cases, probably attributed to the dissolution of AMP. A close relationship could be observed between Cs$^+$ adsorbed and NH$_4^+$ released at all the contact times except 2 h, indicating the dissolution rate of AMP at 2 h reached highest.

4.3.6 Desorption study

Desorption results indicated the AMP-PAN was relatively stable in these two kinds of desorption solutions. Both of the desorption rates were no larger than 10%. In addition, much more Cs$^+$ could be desorbed in 0.1 M NH$_4$Cl solution than HCl solution (Fig.4-12), probably attributed to the ion exchange between NH$_4^+$ and Cs$^+$. It could be predicted that desorption rate would increase with the concentration of NH$_4^+$.

4.4 Summary

Four kinds of AMP-PAN beads (1#, 2#, 3# and 4#) with different compositions were synthesized in this study for Cs^+ removal from aqueous solution. All of them had well physicochemical and structural properties except 1# beads. Adsorption results indicated the 2# bead had highest ion exchange capacity due to the high ratio of AMP/PAN. Multilayer chemisorption dominated the adsorption process through adsorption kinetic and isotherm studies. The adsorption behavior could not be inhibited at acidic conditions until pH lower than 2.5. A close relationship between adsorbed Cs^+ and NH_4^+ was testified, demonstrating the ion exchange process between them. Three competitive ions (Na^+, K^+ and Ca^{2+}) were utilized in this study to evaluate the selectivity of AMP-PAN beads for Cs^+ removal and positive results were obtained. Finally, spent AMP-PAN beads could be recycled in NH_4Cl solutions.

Table 4-1 Composition of AMP-PAN beads.

No.	AMP (g)	DMSO (mL)	Tween 80 (g)	PAN (g)	Theoretical IEC (meq/g)[a]	q_{max} (meq/g)[b]
1#	2.5	25	0.2	0.5	1.21	-
2#	2.5	25	0.2	1	1.05	1.04
3#	2.5	25	0.2	1.5	0.92	0.69
4#	5	25	0.2	2	1.08	0.54

[a] IEC stands for ion exchange capacity. This capacity is the result of the presence of NH_4^+ which is considered to be exchangeable.

[b] means the maximum adsorption capacity towards Cs^+, which is obtained from the adsorption isotherm studies.

Table 4-2 Physicochemical properties of AMP-PAN beads.

	1#	2#	3#	4#
Beads diameter	<1 mm	1-1.5 mm	1.5-2 mm	1.5-2 mm
Sphere	bad	good	good	perfect
Roundness	0.69±0.03 (8)*	0.85±0.16 (7)	0.94±0.14 (6)	1.0±0.0 (6)

* Numbers in brackets means the amount of beads for this measurement.

Table 4-3 Kinetic model parameters of the Cs^+ adsorption on AMP-PAN beads.

	Pseudo first order model				Pseudo second order model			
	k_1 (min⁻¹)	q_e (mg g⁻¹)	R^2	χ^2/DoF*	k_2 (g mg⁻¹ min⁻¹)	q_e (mg g⁻¹)	R^2	χ^2/DoF
2#10 ppm	0.65±0.2	16.3±1.2	0.932	3.7	0.04±0.01	18.8±1.3	0.962	2.1
4#1 ppm	0.78±0.1	1.8±0.0	0.991	0.005	0.5±0.1	1.99±0.05	0.994	0.003
4#10 ppm	3.1±0.4	9.8±0.3	0.979	0.32	0.5±0.0	10.3±0.1	0.997	0.04

* means chi square/degree of freedom, which is obtained by using nonlinear regression function of Origin software. A smaller χ^2/DoF indicates a better fit.

Table 4-4 Correlation coefficients (R^2) of moving boundary models for the Cs^+ adsorption on

AMP-PAN beads.

Beads	Dose (g L^{-1})	Cs^+ conc. (mg L^{-1})	Liquid film diffusion	Intraparticle diffusion	Chemical interaction
2#	0.5	10 ppm	0.998	0.952	0.939
4#	0.5	1 ppm	0.997	0.999	0.983
			0.954	0.912	0.929
4#	1.0	10 ppm	0.988	0.971	0.943
			0.908	0.866	0.884

Table 4-5 Estimated isotherm parameters for cesium adsorption on AMP-PAN beads.

		2#	3#	4#
Langmuir	q_m (mg g^{-1})	138.9±21.3	95.4±11.7	71.6±8.5
	b (L mg^{-1})	0.11±0.06	0.3±0.2	1.0±0.5
	R^2	0.904	0.896	0.917
	χ^2/DoF	262.7	171.4	72.3
Freundlich	k_f (mg g^{-1} L$^{1/n}$ mg$^{-1/n}$)	36.0±3.0	38.0±3.1	30.6±3.4
	n	3.4±0.3	4.4±0.4	4.0±0.6
	R^2	0.989	0.979	0.940
	χ^2/DoF	29.4	33.9	52.3
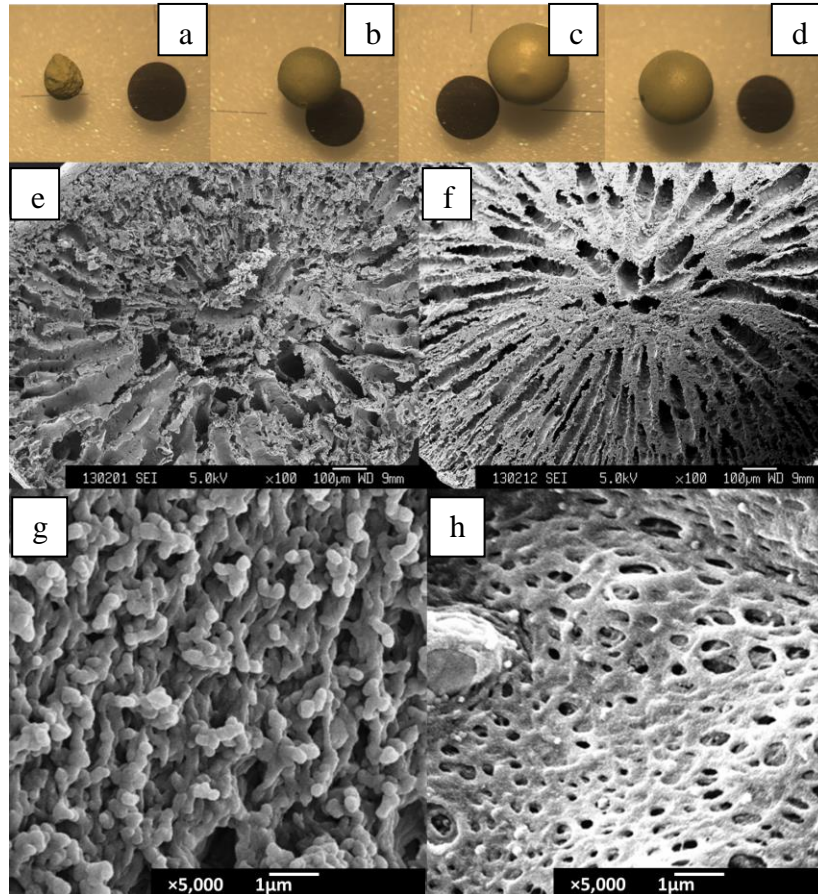
Fig. 4-1 VM images of 1# (a), 2# (b), 3# (c) and 4# (d) AMP-PAN beads and cross section and internal SEM images of 2# (e and g) and 4# (f and h) beads. (Diameter of the calibrate circles in a, b, c and d is 1.5 mm; magnification: 100×(e and f), 5,000×(g and h).)
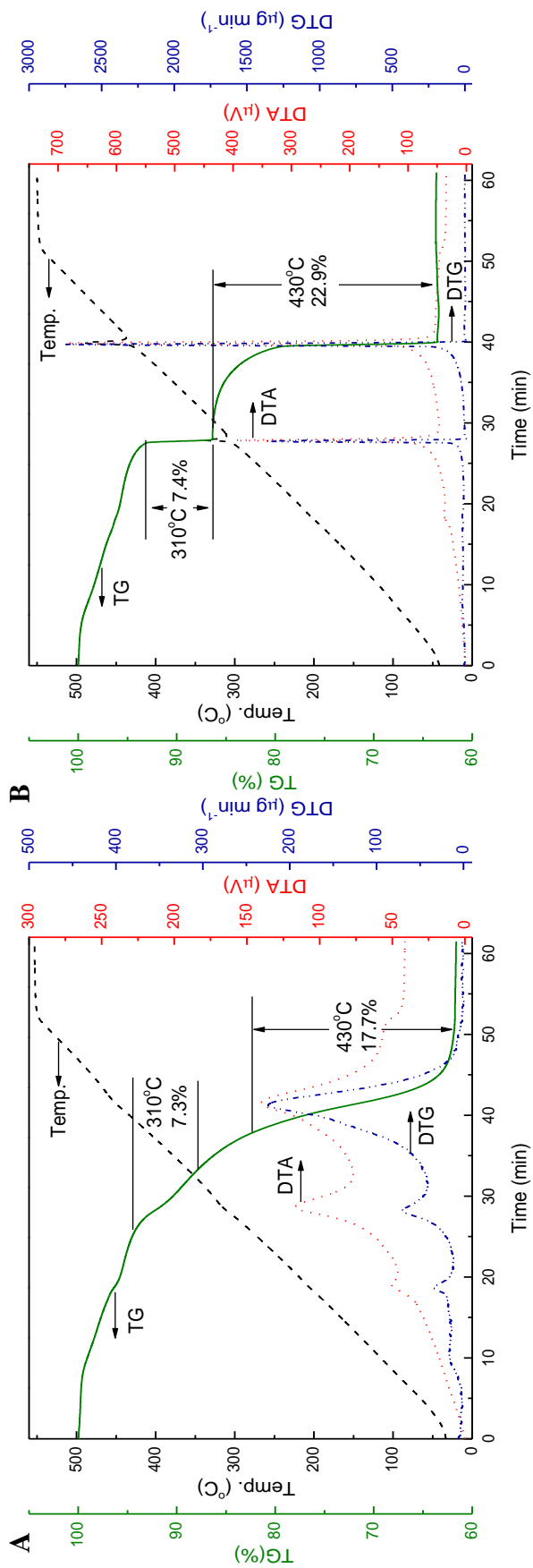
Fig. 4-2 TG/DTA curves of 2# (A) and 4# (B) AMP-PAN beads.
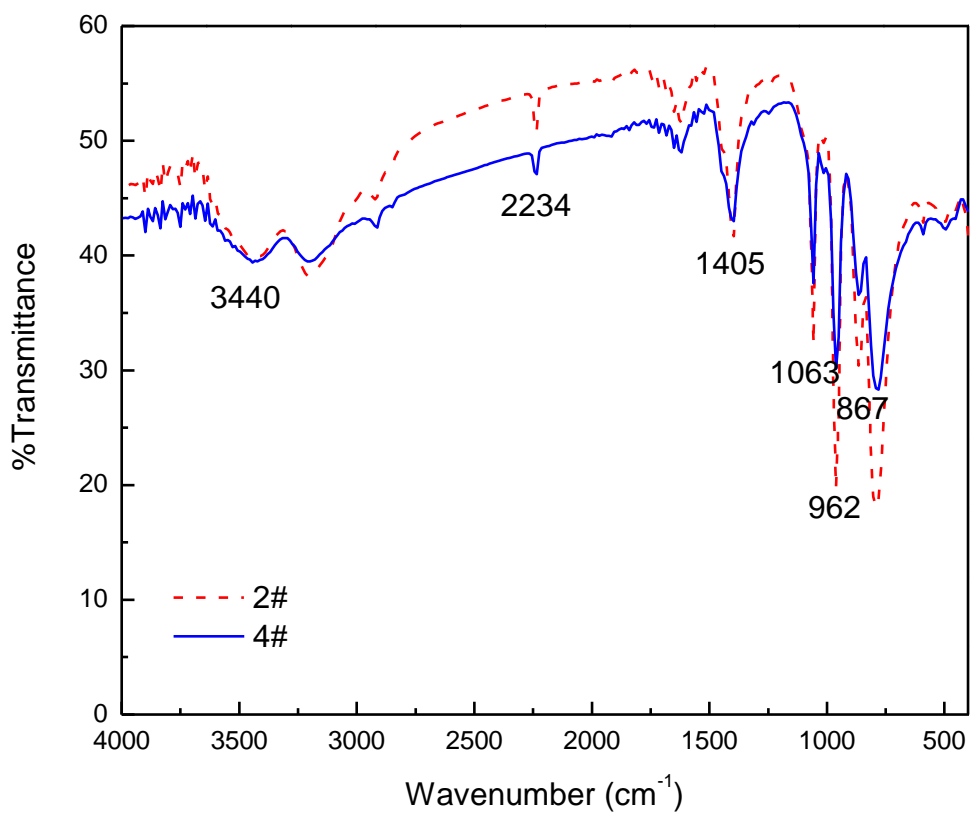
Fig. 4-3 FTIR spectrums of 2# (red) and 4# (blue) AMP-PAN beads.
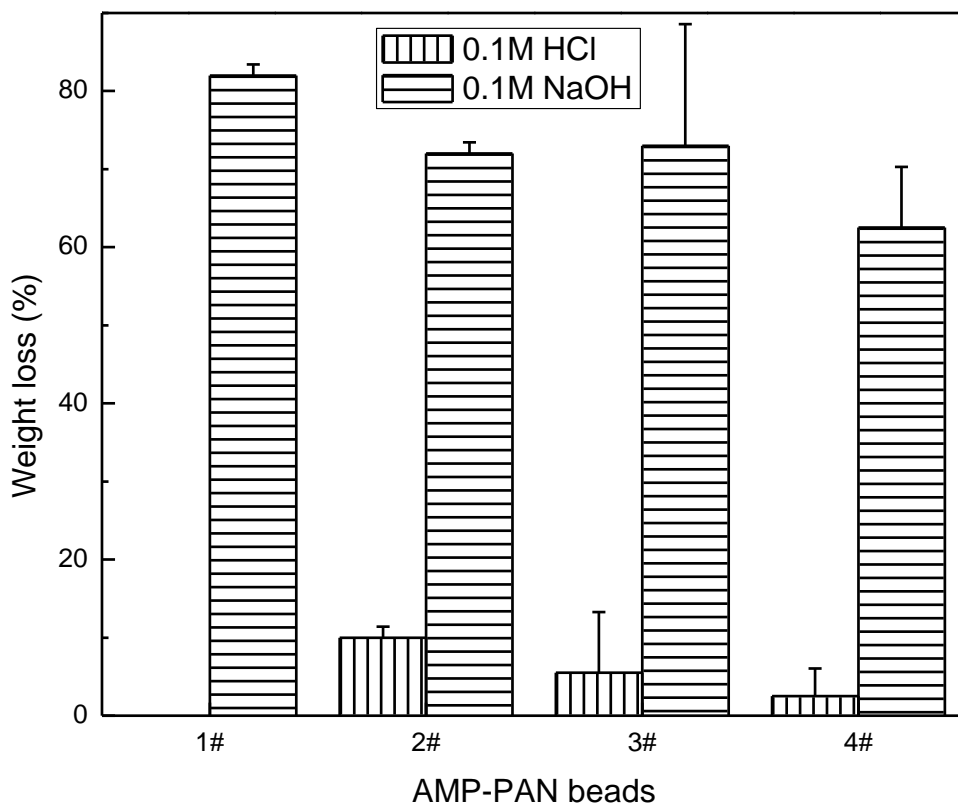
Fig. 4-4 Weight loss of AMP-PAN beads in 0.1 M HCl and NaOH solutions.
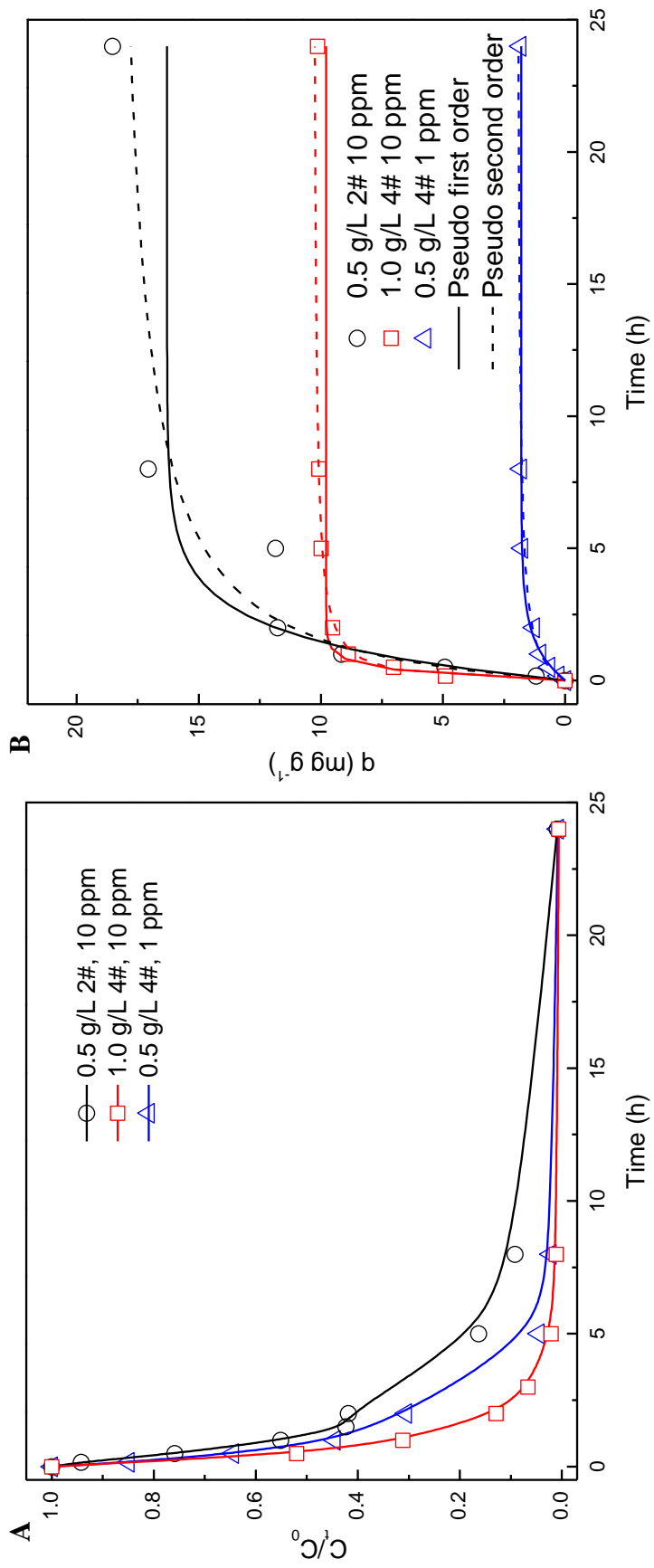
Fig. 4-5 Variation of C_t/C_0 with contact time (A) and the application of pseudo first and second order kinetic model for the

Cs$^+$ adsorption on AMP-PAN beads (B).
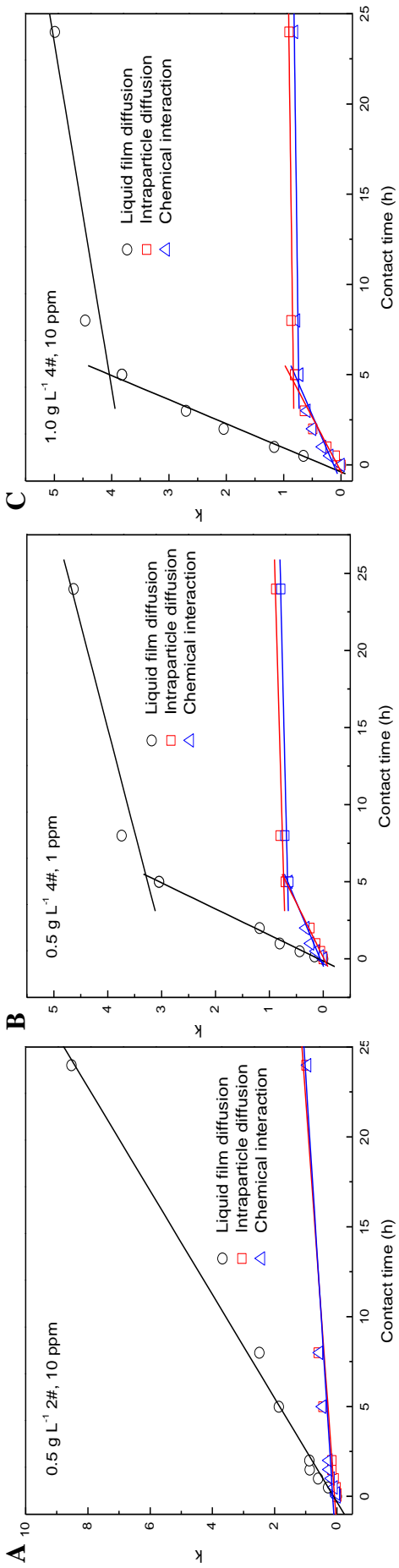
Fig. 4-6 Curve-fitting plot of moving boundary model for Cs$^+$ adsorption on AMP-PAN beads.
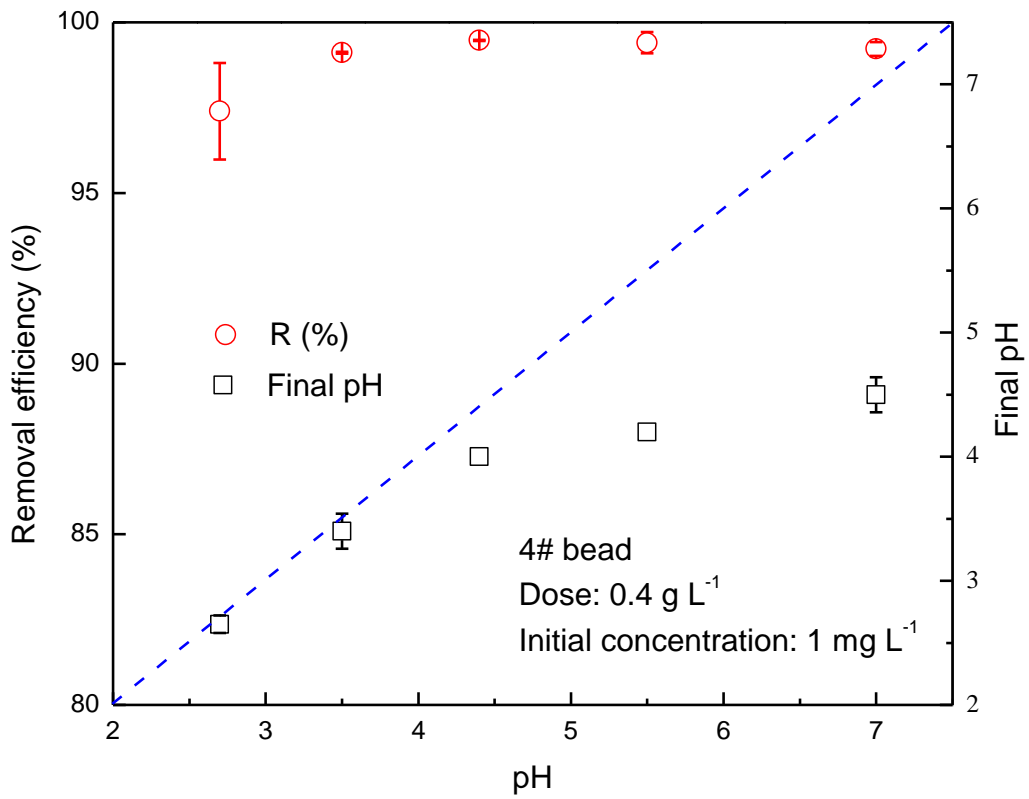
Fig. 4-7 Effect of pH on the Cs$^+$ adsorption on AMP-PAN beads.
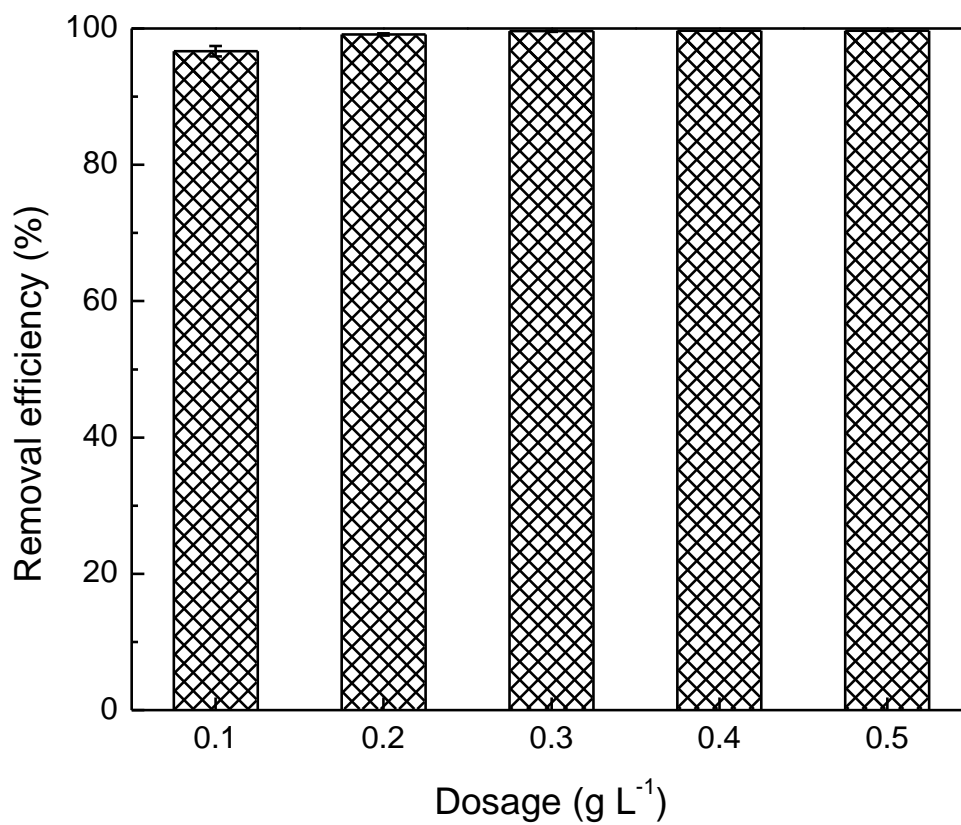
Fig. 4-8 Effect of adsorbent dosage on the Cs^+ (1 ppm) adsorption on 4# AMP-PAN bead.
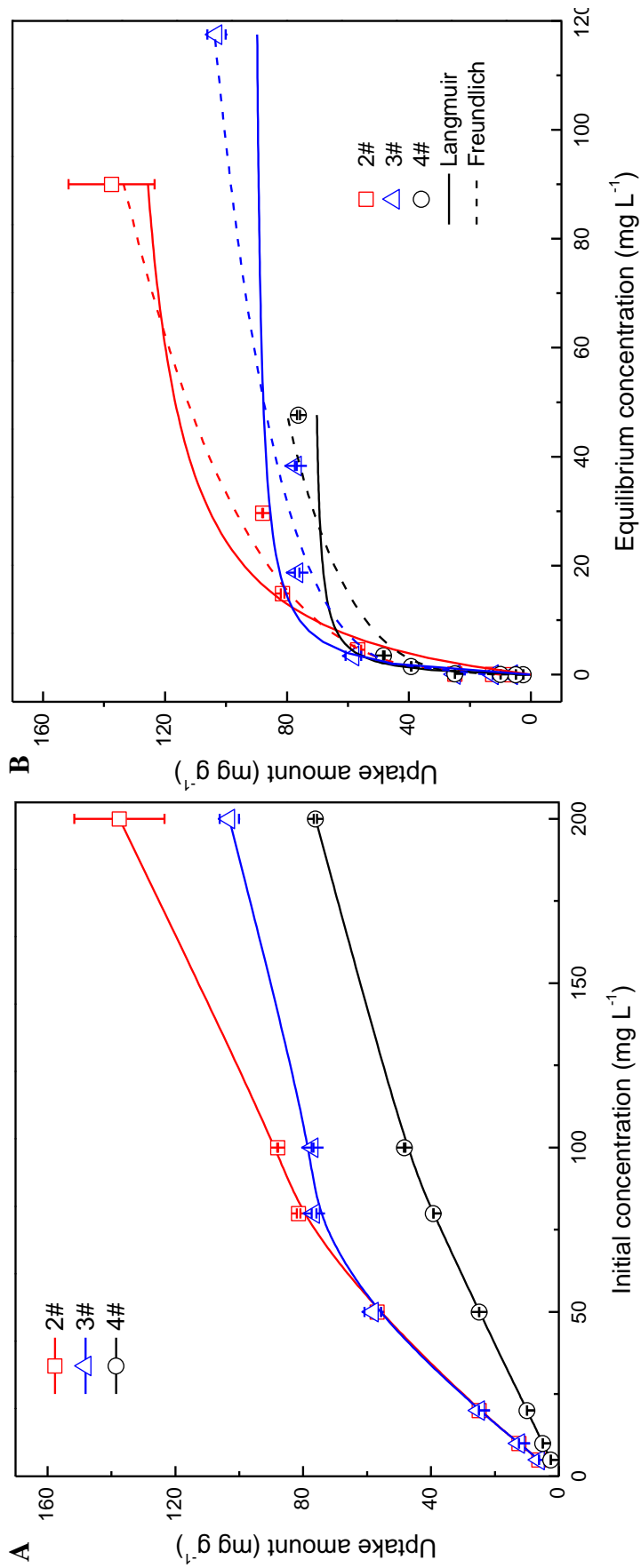
Fig. 4-9 Effect of initial Cs$^+$ concentration on the adsorption process (A) and fitting results with Langmuir and

Freundlich isotherms (B).
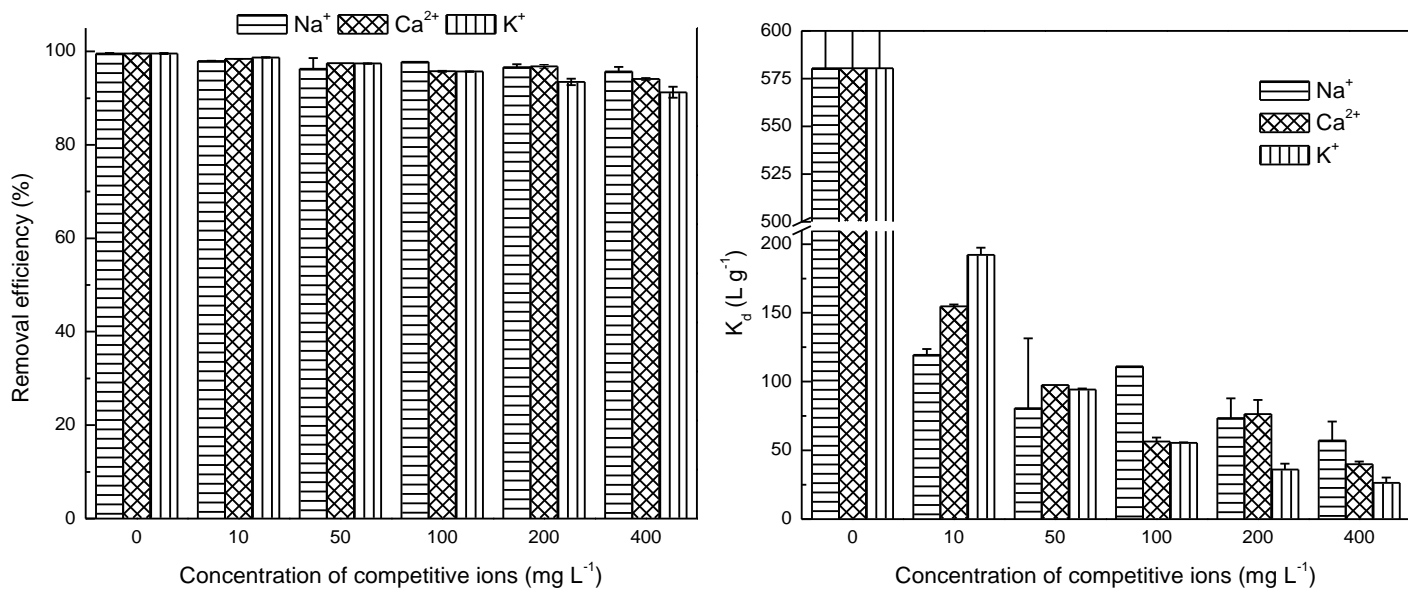
Fig. 4-10 Effect of Na^+, K^+ and Ca^{2+} on Cs^+ removal efficiency (A) and distribution coefficient (B)

on AMP-PAN beads.
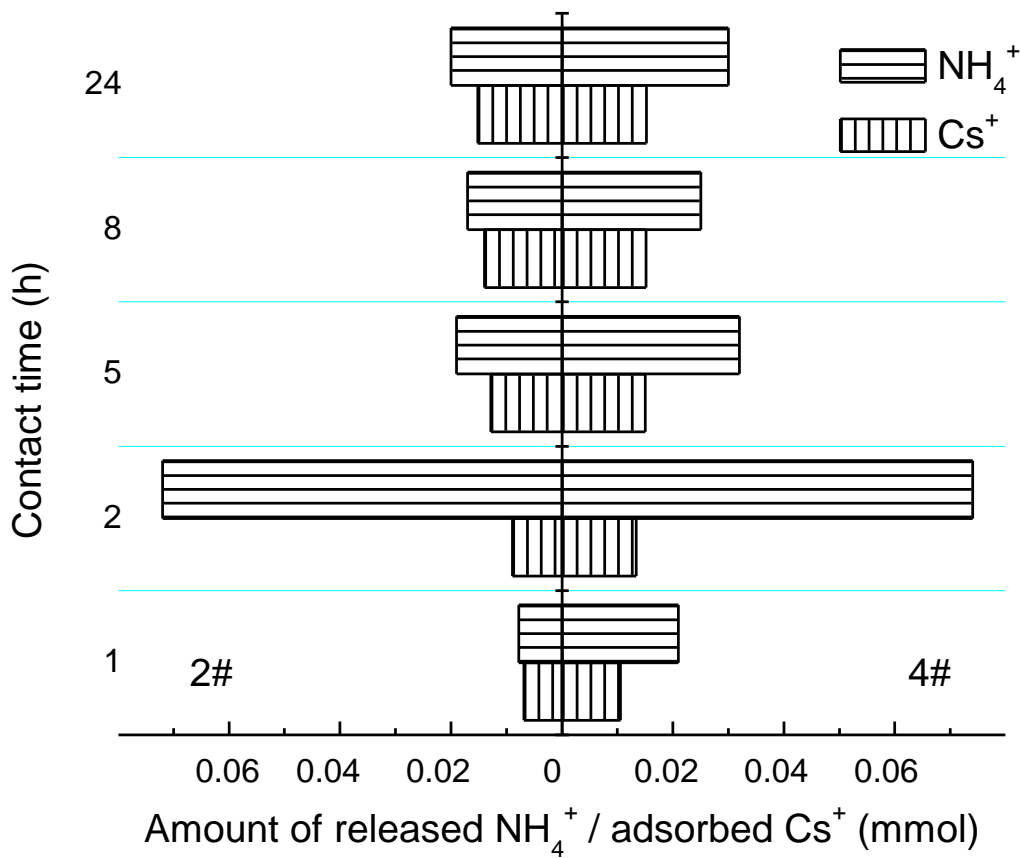
Fig. 4-11 Relationships between released NH_4^+ and adsorbed Cs^+ during the adsorption process.
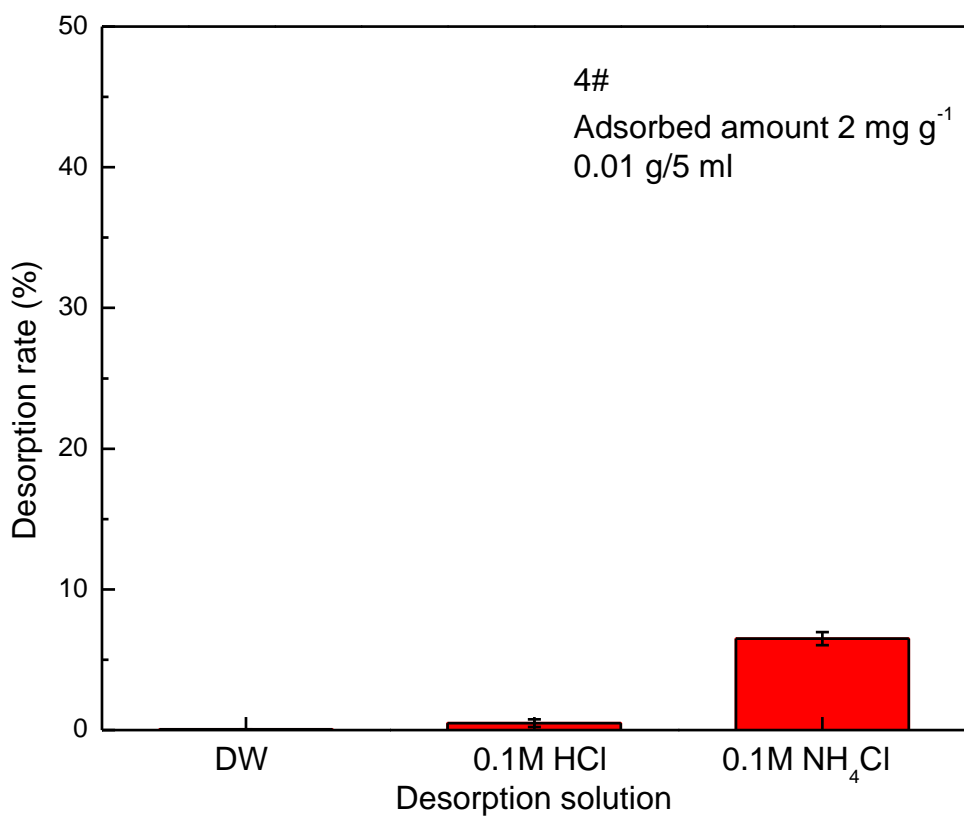
Fig. 4-12 Desorption rate of spent AMP-PAN beads in 0.1 M HCl and NH$_4$Cl solutions.

Chapter 5 Comparative study and conclusions

In this paper, three kinds of material were used for cesium removal from aqueous solutions, which were biomass material (walnut shell), clay material (akadama clay) and synthetic material (AMP-PAN bead).

For the biomass material, NiHCF was incorporated with walnut shell and the equilibrium time was 2 h. The adsorption process well fitted to the pseudo second-order kinetic model, suggesting chemisorption was the main rate-controlling step. Cesium removal by NiHCF-WS was enhanced under acidic and suppressed under alkaline conditions, which makes it especially appropriate in treating acidic radioactive liquid waste. In addition, NiHCF-WS had some selectivity to cesium adsorption and the adsorption was stable. The good correlation coefficient (R^2 = 0.93), low χ^2 and NSD values suggest that cesium adsorption on NiHCF-WS could be best described by the Freundlich adsorption isotherm. Moreover, spent NiHCF-WS could be reduced significantly through incineration at 500°C for 2 h and the total reduction (in volume) from liquid waste to slag residue was up to 99.9%, leading to a considerable space and cost reduction in disposing of the spent adsorption material. This special characteristic makes biomass material appropriate for treating large amount of radioactive liquid wastes. Finally, compared with other adsorption materials, NiHCF-WS is a renewable resource and needs a simple modification process and is low cost, making it a competitive adsorption material in practice.

While for the clay material, akadama clay was transferred into a typical mesoporous material after modification and adsorption performance was greatly enhanced. The newly developed clay material had a much wider applicable pH range (5~12) than the pristine one, indicating the modified AC was applicable for treating weak acidic and alkaline radioactive wastewater. After modification,

the maximum adsorption capacity reached about 16mg g^{-1}, much higher than the pristine one. The distribution coefficient was strongly affected (negatively) by K$^+$ rather than Na$^+$ for both pristine and modified AC. Adsorption isotherms indicate the Cs$^+$ adsorption on modified AC is a monolayer adsorption process. Multiple adsorption interaction mechanisms including electrostatic adsorption and ion exchange are proved during the Cs$^+$ adsorption on modified AC. Finally, above 80% of adsorbed Cs$^+$ could be desorbed in 0.1 M HCl and KCl, while relatively stable in synthetic groundwater, indicating the recyclability of this kind of material.

For the synthetic compound, all the AMP-PAN beads had well physicochemical and structural properties except 1# beads. Adsorption results indicated the 2# bead had highest ion exchange capacity due to the high ratio of AMP/PAN. Multilayer chemisorption was determined through adsorption kinetic and isotherm studies. The adsorption behavior could not be inhibited at acidic conditions until pH lower than 2.5. A close relationship between adsorbed Cs$^+$ and NH$_4^+$ was testified, demonstrating the ion exchange process between them. Finally, spent AMP-PAN beads could be recycled in NH$_4$Cl solutions.

The results of this study would provide useful information for radioactive wastewater treatment. Especially due to the low cost of these materials, it is appropriate for treating large quantity of low level radioactive liquid.

All the experiments were conducted in batch study and laboratory scale in this study. In order to evaluate the real application of these materials, large scale test or column study is needed in the future. For the incineration of cesium loaded walnut shell, due to the experimental conditions, no detection of cesium was carried out. A much more detailed investigation on the transformation of cesium during the incineration process is suggested in the future. For the akadama clay, though the modification is effective in enhancing its adsorption capacity, its performance is still lower than

zeolite and bentonite. Much more effective modification process is recommended in the future study.

For the synthetic process of AMP-PAN beads, the cost reduction is an important topic, which should

be considered in the future work.

Acknowledgements

Time flies. Here comes the end of my doctoral time. Three years is a so short time that we can not think about ourselves carefully. I am proud that I can sit here to write all of these to thank everyone who walks along with me and helps me. First of all, I would like to express my sincere appreciation to my doctor's supervisor, Professor Zhenya Zhang, for his kindly help and guide during my doctor's research. He always gives me valuable suggestions when I am in trouble. His enthusiasm, amicability, and generosity make me feel warm in Japan, and his erudition and encouragement always guide me forward. I would also like to give great appreciation to my co-supervisors, associate professor Yingnan Yang and Zhongfang Lei, for their profound expertise, dedication, and patience during these three years. They always teach me the right way to get along with colleagues, the right way to treat things, and help me correctly view myself.

In addition, I want to give my great thanks to my thesis committee members, Professor Zhenya Zhang, Yingnan Yang, Zhongfang Lei, and Motoo Utsumi for their patient reading and listening, numerous valuable suggestions and comments. All their instructors provided great help for the improvement of my dissertation and future study.

As an EDL member, I want to give great appreciations to all the professors in the EDL program who gave me comprehensive knowledge during the past three years. Dear professor Tsujimura, Wakasugi, Endo, and Sun. Also, always kindly Ms. Takeuchi. I have benefited so much from their courses and constant encouragement. Heartfelt thanks are given to Devena, who spent lots of time for proofreading my manuscripts.

I would also like to thank Professor Chuanping Feng for the recommendation and the support for my abroad study.

References

[1] Y. Masumoto, Y. Miyazawa, D. Tsumune, T. Tsubono, T. Kobayashi, H. Kawamura, C. Estournel, P. Marsaleix, L. Lanerolle, A. Mehra, Z.D. Garraffo, Oceanic dispersion simulations of ^{137}Cs released from the Fukushima Daiichi Nuclear Power Plant, Elements, 8 (2012) 207-212.

[2] D. Parajuli, H. Tanaka, Y. Hakuta, K. Minami, S. Fukuda, K. Umeoka, R. Kamimura, Y. Hayashi, M. Ouchi, T. Kawamoto, Dealing with the aftermath of Fukushima Daiichi Nuclear Accident: Decontamination of radioactive cesium enriched ash, Environ. Sci. Technol., 47 (2013) 3800-3806.

[3] International Atomic Energy Agency (IAEA), Fukushima Daiichi Status Report, 2012, http://www.iaea.org/newscenter/focus/fukushima/statusreports/fukushima28_06_12.htmL.

[4] A. Nilchi, R. Saberi, M. Moradi, H. Azizpour, R. Zarghami, Adsorption of cesium on copper hexacyanoferrate–PAN composite ion exchanger from aqueous solution, Chem. Eng. J., 172 (2011) 572-580.

[5] W. Plazinski, W. Rudzinski, Modeling the effect of surface heterogeneity in equilibrium of heavy metal ion biosorption by using the ion exchange model, Environ. Sci. Technol., 43 (2009) 7465-7471.

[6] R. Chen, H. Tanaka, T. Kawamoto, M. Asai, C. Fukushima, H. Na, M. Kurihara, M. Watanabe, M. Arisaka, T. Nankawa, Selective removal of cesium ions from wastewater using copper hexacyanoferrate nanofilms in an electrochemical system, Electrochim. Acta, 87 (2013) 119-125.

[7] Y. Lin, G.E. Fryxell, H. Wu, M. Engelhard, Selective sorption of cesium using self-assembled monolayers on mesoporous supports, Environ. Sci. Technol., 35 (2001) 3962-3966.

[8] V. Avramenko, S. Bratskaya, V. Zheleznov, I. Sheveleva, O. Voitenko, V. Sergienko, Colloid stable sorbents for cesium removal: Preparation and application of latex particles functionalized with

transition metals ferrocyanides, J. Hazard. Mater., 186 (2011) 1343-1350.

[9] A. Duhart, J.F. Dozol, H. Rouquette, A. Deratani, Selective removal of cesium from model nuclear waste solutions using a solid membrane composed of an unsymmetrical calix[4]arenebiscrown-6 bonded to an immobilized polysiloxane backbone, J. Membrane Sci., 185 (2001) 145-155.

[10] C. Delchet, A. Tokarev, X. Dumail, G. Toquer, Y. Barre, Y. Guari, C. Guerin, J. Larionova, A. Grandjean, Extraction of radioactive cesium using innovative functionalized porous materials, RSC Adv., 2 (2012) 5707-5716.

[11] D. Karamanis, P.A. Assimakopoulos, Efficiency of aluminum-pillared montmorillonite on the removal of cesium and copper from aqueous solutions, Water Res., 41 (2007) 1897-1906.

[12] A. Nilchi, A. Khanchi, M. Ghanadi Maragheh, The importance of cerium substituted phosphates as cation exchanger—some unique properties and related application potentials, Talanta, 56 (2002) 383-393.

[13] J. Lehto, Harjula, R., Separation of cesium from nuclear waste solutions with hexacyanoferrate (II)s and ammonium phosphomolybdate, Solvent Extr. Ion Exch., 5 (1987) 343-352.

[14] S. Goñi, A. Guerrero, M.P. Lorenzo, Efficiency of fly ash belite cement and zeolite matrices for immobilizing cesium, J. Hazard. Mater., 137 (2006) 1608-1617.

[15] E.H. Borai, R. Harjula, L. malinen, A. Paajanen, Efficient removal of cesium from low-level radioactive liquid waste using natural and impregnated zeolite minerals, J. Hazard. Mater., 172 (2009) 416-422.

[16] M.R. El-Naggar, A.M. El-Kamash, M.I. El-Dessouky, A.K. Ghonaim, Two-step method for preparation of NaA-X zeolite blend from fly ash for removal of cesium ions, J. Hazard. Mater., 154 (2008) 963-972.

[17] A. Ararem, O. Bouras, F. Arbaoui, Adsorption of caesium from aqueous solution on binary mixture of iron pillared layered montmorillonite and goethite, Chem. Eng. J., 172 (2011) 230-236.

[18] W.A. Cabrera-Lafaurie, F.R. Román, A.J. Hernández-Maldonado, Transition metal modified and partially calcined inorganic–organic pillared clays for the adsorption of salicylic acid, clofibric acid, carbamazepine, and caffeine from water, J. Colloid Interface Sci., 386 (2012) 381-391.

[19] T.P. R. A. Schoonheydt, Gerhard Lagaly and Nick Gangas, Pillared clays and pillared layered solids, Pure Appl. Chem., 71 (1999) 2367-2371.

[20] E.F. Iliopoulou, S.D. Stefanidis, K.G. Kalogiannis, A. Delimitis, A.A. Lappas, K.S. Triantafyllidis, Catalytic upgrading of biomass pyrolysis vapors using transition metal-modified ZSM-5 zeolite, Appl. Catal. B: Environ., 127 (2012) 281-290.

[21] B. Wang, L. Gu, H. Ma, Electrochemical oxidation of pulp and paper making wastewater assisted by transition metal modified kaolin, J. Hazard. Mater., 143 (2007) 198-205.

[22] H. Parab, M. Sudersanan, Engineering a lignocellulosic biosorbent – Coir pith for removal of cesium from aqueous solutions: Equilibrium and kinetic studies, Water Res., 44 (2010) 854-860.

[23] K. Volchek, M.Y. Miah, W. Kuang, Z. DeMaleki, F.H. Tezel, Adsorption of cesium on cement mortar from aqueous solutions, J. Hazard. Mater., 194 (2011) 331-337.

[24] M. Pyrasch, A. Toutianoush, W.Q. Jin, J. Schnepf, B. Tieke, Self-assembled films of Prussian blue and analogues: Optical and electrochemical properties and application as ion-sieving membranes, Chem. Mater., 15 (2003) 245-254.

[25] M.M. Figueira, B. Volesky, K. Azarian, V.S.T. Ciminelli, Biosorption column performance with a metal mixture, Environ. Sci. Technol., 34 (2000) 4320-4326.

[26] Z. Reddad, C. Gerente, Y. Andres, P. Le Cloirec, Adsorption of several metal ions onto a low-cost biosorbent: Kinetic and equilibrium studies, Environ. Sci. Technol., 36 (2002) 2067-2073.

[27] T. Altun, E. Pehlivan, Removal of Cr(VI) from aqueous solutions by modified walnut shells, Food Chem., 132 (2012) 693-700.

[28] S. Saadat, A. Karimi-Jashni, Optimization of Pb(II) adsorption onto modified walnut shells using factorial design and simplex methodologies, Chem. Eng. J., 173 (2011) 743-749.

[29] M. Zabihi, A. Haghighi Asl, A. Ahmadpour, Studies on adsorption of mercury from aqueous solution on activated carbons prepared from walnut shell, J. Hazard. Mater., 174 (2010) 251-256.

[30] International Atomic Energy Agency (IAEA), Application of thermal technologies for processing of radioactive waste, 2006, http://www-pub.iaea.org/MTCD/publications/ PDF/te_1527_web.pdf.

[31] M.R. Schnobrich, B.P. Chaplin, M.J. Semmens, P.J. Novak, Stimulating hydrogenotrophic denitrification in simulated groundwater containing high dissolved oxygen and nitrate concentrations, Water Res., 41 (2007) 1869-1876.

[32] I. Langmuir, The adsorption of gases on plane surfaces of glass, mica and platinum, J. Am. Chem. Soc., 40 (1918) 1361–1403.

[33] H. Freundlich, Über die adsorption in lösungen, J. Phys. Chem., 57 (1907) 385–470.

[34] M.M. Dubinin, E.D. Zaverina, L.V. Radushkevich, Sorption and structure of active carbons. I. Adsorption of organic vapors., Zh Fiz Khim, 21 (1947) 1351-1362.

[35] D. Mohan, K.P. Singh, Single- and multi-component adsorption of cadmium and zinc using activated carbon derived from bagasse—an agricultural waste, Water Res., 36 (2002) 2304-2318.

[36] P.A. Haas, A review of information on ferrocyanide solids for removal of cesium from solutions, Sep. Sci. Technol., 28 (1993) 2479-2506.

[37] S.-C. Tsai, T.-H. Wang, M.-H. Li, Y.-Y. Wei, S.-P. Teng, Cesium adsorption and distribution onto crushed granite under different physicochemical conditions, J. Hazard. Mater., 161 (2009) 854-861.

[38] I.-H. Yoon, W.-K. Choi, S.-C. Lee, B.-Y. Min, H.-C. Yang, K.-W. Lee, Volatility and leachability

of heavy metals and radionuclides in thermally treated HEPA filter media generated from nuclear facilities, J. Hazard. Mater., 219–220 (2012) 240-246.

[39] T. Damartzis, D. Vamvuka, S. Sfakiotakis, A. Zabaniotou, Thermal degradation studies and kinetic modeling of cardoon (Cynara cardunculus) pyrolysis using thermogravimetric analysis (TGA), Bioresour. Technol., 102 (2011) 6230-6238.

[40] Y. Kar, Co-pyrolysis of walnut shell and tar sand in a fixed-bed reactor, Bioresour. Technol., 102 (2011) 9800-9805.

[41] E. Katsou, S. Malamis, K.J. Haralambous, M. Loizidou, Use of ultrafiltration membranes and aluminosilicate minerals for nickel removal from industrial wastewater, J. Membrane Sci., 360 (2010) 234-249.

[42] L. Zhang, L. Zhao, Y. Yu, C. Chen, Removal of lead from aqueous solution by non-living rhizopus nigricans, Water Res., 32 (1998) 1437-1444.

[43] T. Sangvanich, V. Sukwarotwat, R.J. Wiacek, R.M. Grudzien, G.E. Fryxell, R.S. Addleman, C. Timchalk, W. Yantasee, Selective capture of cesium and thallium from natural waters and simulated wastes with copper ferrocyanide functionalized mesoporous silica, J. Hazard. Mater., 182 (2010) 225-231.

[44] A. Kowal-Fouchard, R. Drot, E. Simoni, J.J. Ehrhardt, Use of spectroscopic techniques for uranium(VI)/montmorillonite interaction modeling, Environ. Sci. Technol., 38 (2004) 1399-1407.

[45] R.T.H. M.A. Lilga, E.V. Alderson, M.O. Hogan, T.L. Hubler, G.L. Jones, Ferrocyanide aging studies final report, PNNL- 11211, Pacific Northwest National Laboratory, Richland, Washington, 1996.

[46] N. Wu, H. Wei, L. Zhang, Efficient removal of heavy metal ions with biopolymer template synthesized mesoporous titania beads of hundreds of micrometers size, Environmental Science &

Technology, 46 (2011) 419-425.

[47] Y. Park, Y.-C. Lee, W.S. Shin, S.-J. Choi, Removal of cobalt, strontium and cesium from radioactive laundry wastewater by ammonium molybdophosphate–polyacrylonitrile (AMP–PAN), Chem. Eng. J., 162 (2010) 685-695.

[48] M. Ramaswamy, Synthesis, sorption and kinetic characteristics of silica-hexacyanoferrate composites, Solvent Extr. Ion Exch., 17 (1999) 1603-1618.

[49] A. Mirmohseni, M.S. Seyed Dorraji, A. Figoli, F. Tasselli, Chitosan hollow fibers as effective biosorbent toward dye: Preparation and modeling, Bioresour. Technol., 121 (2012) 212-220.

[50] C. Loos-Neskovic, S. Ayrault, V. Badillo, B. Jimenez, E. Garnier, M. Fedoroff, D.J. Jones, B. Merinov, Structure of copper-potassium hexacyanoferrate (II) and sorption mechanisms of cesium, J. Solid State Chem., 177 (2004) 1817-1828.

[51] M.Y. Miah, K. Volchek, W. Kuang, F.H. Tezel, Kinetic and equilibrium studies of cesium adsorption on ceiling tiles from aqueous solutions, J. Hazard. Mater., 183 (2010) 712-717.

[52] A.E. Osmanlioglu, Treatment of radioactive liquid waste by sorption on natural zeolite in Turkey, J. Hazard. Mater., 137 (2006) 332-335.

[53] A. Bouzidi, F. Souahi, S. Hanini, Sorption behavior of cesium on Ain Oussera soil under different physicochemical conditions, J. Hazard. Mater., 184 (2010) 640-646.

[54] A.D. L. Al-Attar, R. Harjula, Uptake of radionuclides on antimony silicate, J. Radioanal. Nucl. Chem., 260 (2004) 199-203.

[55] J. Vejsada, E. Jelínek, Z. Řanda, D. Hradil, R. Přikryl, Sorption of cesium on smectite-rich clays from the Bohemian Massif (Czech Republic) and their mixtures with sand, Appl. Radiat. Isot., 62 (2005) 91-96.

[56] T.-H. Wang, M.-H. Li, W.-C. Yeh, Y.-Y. Wei, S.-P. Teng, Removal of cesium ions from aqueous

solution by adsorption onto local Taiwan laterite, J. Hazard. Mater., 160 (2008) 638-642.

[57] T. Melkior, S. Yahiaoui, S. Motellier, D. Thoby, E. Tevissen, Cesium sorption and diffusion in Bure mudrock samples, Appl. Clay Sci., 29 (2005) 172-186.

[58] F. Han, G.-H. Zhang, P. Gu, Removal of cesium from simulated liquid waste with countercurrent two-stage adsorption followed by microfiltration, J. Hazard. Mater., 225–226 (2012) 107-113.

[59] R. Chen, Z. Zhang, C. Feng, Z. Lei, Y. Li, M. Li, K. Shimizu, N. Sugiura, Batch study of arsenate (V) adsorption using Akadama mud: Effect of water mineralization, Appl. Surf. Sci., 256 (2010) 2961-2967.

[60] R. Chen, Z. Zhang, Z. Lei, N. Sugiura, Preparation of iron-impregnated tablet ceramic adsorbent for arsenate removal from aqueous solutions, Desalination, 286 (2012) 56-62.

[61] R. Chen, Q. Xue, Z. Zhang, N. Sugiura, Y. Yang, M. Li, N. Chen, Z. Ying, Z. Lei, Development of long-life-cycle tablet ceramic adsorbent for geosmin removal from water solution, Appl. Surf. Sci., 257 (2011) 2091-2096.

[62] Q. Xue, R. Chen, M.K. Sakharkar, M. Utsumi, M. Li, K. Shimizu, Z. Zhang, N. Sugiura, Development of a ceramic adsorbent for the removal of 2-methylisoborneol from aqueous solution, Desalination, 281 (2011) 293-297.

[63] K. Kosaka, M. Asami, N. Kobashigawa, K. Ohkubo, H. Terada, N. Kishida, M. Akiba, Removal of radioactive iodine and cesium in water purification processes after an explosion at a nuclear power plant due to the Great East Japan Earthquake, Water Res., 46 (2012) 4397-4404.

[64] R.S. Varma, Clay and clay-supported reagents in organic synthesis, Tetrahedron, 58 (2002) 1235-1255.

[65] S. Kawamura, Y. Tanaka, The application of colloid filtration techniques to coagulant dosage control, Water & Sewage Works, 113 (1966) 348.

[66] G. Tiravanti, F. Lore, G. Sonnante, Influence of the charge density of cationic polyelectrolytes on sludge conditioning, Water Res., 19 (1985) 93-97.

[67] Q. Fang, B. Chen, Adsorption of perchlorate onto raw and oxidized carbon nanotubes in aqueous solution, Carbon, 50 (2012) 2209-2219.

[68] V.K. Gupta, S. Agarwal, T.A. Saleh, Chromium removal by combining the magnetic properties of iron oxide with adsorption properties of carbon nanotubes, Water Res., 45 (2011) 2207-2212.

[69] T. Perraki, A. Orfanoudaki, Mineralogical study of zeolites from Pentalofos area, Thrace, Greece, Appl. Clay Sci., 25 (2004) 9-16.

[70] D.A. J. Rouquerol, C. W. Fairbridge, D. H. Everett, J. M. Haynes, N. Pernicone, J. D. F. Ramsay, K. S. W. Sing and K. K. Unger, Recommendations for the characterization of porous solids (Technical Report), Pure Appl. Chem., 66 (1994) 1739-1758.

[71] M. Machida, B. Fotoohi, Y. Amamo, T. Ohba, H. Kanoh, L. Mercier, Cadmium(II) adsorption using functional mesoporous silica and activated carbon, J. Hazard. Mater., 221–222 (2012) 220-227.

[72] H. Sepehrian, S.J. Ahmadi, S. Waqif-Husain, H. Faghihian, H. Alighanbari, Adsorption studies of heavy metal ions on mesoporous aluminosilicate, novel cation exchanger, J. Hazard. Mater., 176 (2010) 252-256.

[73] Y. Tian, X. Wang, Y. Pan, Simple synthesis of Ni-containing ordered mesoporous carbons and their adsorption/desorption of methylene orange, J. Hazard. Mater., 213–214 (2012) 361-368.

[74] D. Park, S.-R. Lim, Y.-S. Yun, J.M. Park, Development of a new Cr(VI)-biosorbent from agricultural biowaste, Bioresour. Technol., 99 (2008) 8810-8818.

[75] K. Ada, A. Ergene, S. Tan, E. Yalçın, Adsorption of remazol Brilliant Blue R using ZnO fine powder: Equilibrium, kinetic and thermodynamic modeling studies, J. Hazard. Mater., 165 (2009) 637-644.

[76] R. Deepthi Rani, P. Sasidhar, Sorption of cesium on clay colloids: Kinetic and thermodynamic studies, Aquat. Geochem., 18 (2012) 281-296.

[77] S. Ali Khan, R. Riaz ur, M. Ali Khan, Sorption of cesium on bentonite, Waste Manage. (Oxford), 14 (1994) 629-642.

[78] T.-H. Wang, C.-L. Chen, L.-Y. Ou, Y.-Y. Wei, F.-L. Chang, S.-P. Teng, Cs sorption to potential host rock of low-level radioactive waste repository in Taiwan: Experiments and numerical fitting study, J. Hazard. Mater., 192 (2011) 1079-1087.

[79] R.C. Marcelo J. Avena, Carlos P. De Pauli, Study of some physicochemical properties of pillared montmorillonites: acid-base potentiometric titrations and electrophoretic measurements, Clay Clay Miner., 38 (1990) 356-362.

[80] Y. Zhang, X.-M. Dou, M. Yang, H. He, C.-Y. Jing, Z.-Y. Wu, Removal of arsenate from water by using an Fe–Ce oxide adsorbent: Effects of coexistent fluoride and phosphate, J. Hazard. Mater., 179 (2010) 208-214.

[81] C. Liu, J.M. Zachara, S.C. Smith, J.P. McKinley, C.C. Ainsworth, Desorption kinetics of radiocesium from subsurface sediments at Hanford Site, USA, Geochim. Cosmochim. Acta, 67 (2003) 2893-2912.

[82] L. Zeng, X. Li, J. Liu, Adsorptive removal of phosphate from aqueous solutions using iron oxide tailings, Water Res., 38 (2004) 1318-1326.

[83] G.S. Gupta, G. Prasad, V.N. Singh, Removal of chrome dye from aqueous solutions by mixed adsorbents: Fly ash and coal, Water Res., 24 (1990) 45-50.

[84] J. Perić, M. Trgo, N. Vukojević Medvidović, Removal of zinc, copper and lead by natural zeolite—a comparison of adsorption isotherms, Water Res., 38 (2004) 1893-1899.

[85] C.-P. Zhang, P. Gu, J. Zhao, D. Zhang, Y. Deng, Research on the treatment of liquid waste

containing cesium by an adsorption–microfiltration process with potassium zinc hexacyanoferrate, J. Hazard. Mater., 167 (2009) 1057-1062.

[86] J.v.R. Smit, Ammonium salts of the heteropolyacids as cation exchangers, Nature 181 (1958) 1530-1531.

[87] J.C.A. Boeyens, G.J. McDougal, J. Van R. Smit, Crystallographic study of the ammonium/potassium 12-molybdophosphate ion-exchange system, J. Solid State Chem., 18 (1976) 191-199.

[88] H. Buchwald, W.P. Thistlethwaite, Some cation exchange properties of ammonium 12-molybdophosphate, J. Inorg. Nucl. Chem., 5 (1957) 341-343.

[89] M. Harrup, M. Jones, L. Polson, B. White, Polymer/silicate composites: new materials for subsurface permeable reactive barriers, J. Sol-Gel Sci. Technol., 47 (2008) 243-251.

[90] T.A. Todd, V.N. Romanovskiy, A comparison of crystalline silicotitanate and ammonium molybdophosphate-oolyacrylonitrile composite sorbent for the separation of cesium from acidic waste, Radiochemistry, 47 (2005) 398-402.

[91] T.J. Tranter, R.S. Herbst, T.A. Todd, A.L. Olson, H.B. Eldredge, Evaluation of ammonium molybdophosphate-polyacrylonitrile (AMP-PAN) as a cesium selective sorbent for the removal of 137Cs from acidic nuclear waste solutions, Adv. Environ. Res., 6 (2002) 107-121.

[92] T. Todd, N. Mann, T. Tranter, F. Šebesta, J. John, A. Motl, Cesium sorption from concentrated acidic tank wastes using ammonium molybdophosphate-polyacrylonitrile composite sorbents, J. Radioanal. Nucl. Chem., 254 (2002) 47-52.

[93] F. Šebesta, J. John, A. Motl, V. Peka, E. Vacková, Composite absorbers consisting of inorganic ion-exchangers and polyacrylonitrile binding matrix, J. Radioanal. Nucl. Chem., 220 (1997) 65-67.

[94] J.-K. Moon, K.-W. Kim, C.-H. Jung, Y.-G. Shul, E.-H. Lee, Preparation of organic-inorganic

composite adsorbent beads for removal of radionuclides and heavy metal ions, J. Radioanal. Nucl. Chem., 246 (2000) 299-307.

[95] G.E. Boyd, L.S. Myers, A.W. Adamson, The exchange adsorption of ions from aqueous solutions by organic zeolites. III. Performance of deep adsorbent beds under non-equilibrium conditions1, J. Am. Chem. Soc., 69 (1947) 2849-2859.

[96] H. Liu, X. Cai, Y. Wang, J. Chen, Adsorption mechanism-based screening of cyclodextrin polymers for adsorption and separation of pesticides from water, Water Res., 45 (2011) 3499-3511.

[97] A. Nilchi, M.R. Hadjmohammadi, S.R. Garmarodi, R. Saberi, Studies on the adsorption behavior of trace amounts of $^{90}Sr^{2+}$, $^{140}La^{3+}$, $^{60}Co^{2+}$, Ni^{2+} and Zr^{4+} cations on synthesized inorganic ion exchangers, J. Hazard. Mater., 167 (2009) 531-535.

[98] M. Alizadeh, H. Eshtiagh-Hosseini, M. Mirzaei, A. Salimi, H. Razavi, Synthesis, X-ray crystallography characterization, vibrational spectroscopy, and DFT theoretical studies of a new organic–inorganic hybrid material, Struct. Chem., 19 (2008) 155-164.

[99] A. Kadous, M. Didi, D. Villemin, A new sorbent for uranium extraction: ethylenediamino tris(methylenephosphonic) acid grafted on polystyrene resin, J. Radioanal. Nucl. Chem., 284 (2010) 431-438.

[100] W. Rudzinski, W. Plazinski, Theoretical description of the kinetics of solute adsorption at heterogeneous solid/solution interfaces: On the possibility of distinguishing between the diffusional and the surface reaction kinetics models, Appl. Surf. Sci., 253 (2007) 5827-5840.

[101] J. Álvarez-Ramírez, G. Fernández-Anaya, F.J. Valdés-Parada, J.A. Ochoa-Tapia, Physical consistency of generalized linear driving force models for adsorption in a particle, Ind. Eng. Chem. Res., 44 (2005) 6776-6783.

[102] Y. Liu, L. Shen, From Langmuir kinetics to first- and second-order rate equations for

adsorption, Langmuir, 24 (2008) 11625-11630.

[103] G. Crini, H.N. Peindy, F. Gimbert, C. Robert, Removal of C.I. Basic Green 4 (Malachite Green) from aqueous solutions by adsorption using cyclodextrin-based adsorbent: Kinetic and equilibrium studies, Sep. Purif. Technol., 53 (2007) 97-110.

Publication List

1. D. Ding, Y. Zhao, S. Yang, W. Shi, Z. Zhang, Z. Lei, Y. Yang, 2013. Adsorption of cesium from aqueous solution using agricultural residue – Walnut shell: Equilibrium, kinetic and thermodynamic modeling studies. **Water Research**, 47, 2563-2571. (**IF: 4.655**)

2. D. Ding, Z. Lei, Y. Yang, C. Feng, Z. Zhang, 2013. Nickel oxide grafted andic soil for efficient cesium removal from aqueous solution: Adsorption behavior and mechanisms. **ACS Applied Materials & Interfaces,** 5, 10151-10158. (**IF: 5.008**)

3. D. Ding, Z. Lei, Y. Yang, Z. Zhang, 2014. Efficiency of transition metal modified akadama clay on cesium removal from aqueous solutions. **Chemical Engineering Journal**, 236, 17-28. (**IF: 3.473**)

4. D. Ding, Z. Lei, Y. Yang, C. Feng, Z. Zhang, 2014. Selective removal of cesium from aqueous solutions with nickel (II) hexacyanoferrate (III) functionalized agricultural residue - walnut shell. **Journal of Hazardous materials**, 270, 187-195. (**IF: 3.925**)

5. S. Yang, D. Ding, Y. Zhao, Z. Zhang, 2013. An electrochemically surface-modified porous granule developed for phosphate removal from aqueous solution. **Chemistry letters,** 42, 307-309. (**IF: 1.594**)

6. S. Yang, D. Ding, Y. Zhao, W. Huang, Z. Zhang, Z. Lei, Y. Yang, 2013. Investigation of phosphate adsorption from aqueous solution using Kanuma mud: Behaviors and mechanisms. **Journal of Environmental Chemical Engineering,** 1, 355-362.

7. Y. Zhao, S. Yang, D. Ding, J. Chen, Y. Yang, Z. Lei, C. Feng, Z. Zhang, 2013. Effective adsorption of Cr (VI) from aqueous solution using natural Akadama clay. **Journal of Colloid and Interface Science**, 395, 198-204. (**IF: 3.172**)

8. S. Yang, Y. Zhao, D. Ding, Y. Wang, C. Feng, Z. Lei, Y. Yang, Z. Zhang, 2013. An electrochemically modified novel tablet porous material developed as adsorbent for phosphate removal from aqueous solution. **Chemical Engineering Journal,** 220, 367-374. (**IF: 3.473**)

9. W. Shi, C. Liu, D. Ding, Z. Lei, Y. Yang, C. Feng, Z. Zhang, 2013. Immobilization of heavy metals in sewage sludge by using subcritical water technology. **Bioresource Technology**, 137, 18-24. (**IF: 4.750**)